

**MOLECULAR ATTEMPTS TO ALTER CARBON PARTITIONING
TOWARDS THE SYNTHESIS OF PHENOLIC COMPOUNDS IN
TRANSGENIC TOBACCO PLANTS**



Dissertation

zur Erlangung des akademischen Grades
Doktor der Naturwissenschaften
-Dr. rer. nat.-

vorgelegt der

Mathematisch-Naturwissenschaftlich-Technischen Fakultät
(mathematisch-naturwissenschaftlicher Bereich)
der Martin-Luther-Universität Halle-Wittenberg

von Herrn Li Ding

geb. am. 03. 08. 1972
in Heilongjiang, Volksrepublik China

1. Gutachter: Prof. Dr. Sonnewald (IPK Gatersleben)
2. Gutachter: Prof. Dr. W. Roos (Universität Halle)
3. Gutachter: Prof. Dr. A. Gierl (TU München)

Halle (Saale), den 18.02.2005

urn:nbn:de:gbv:3-000008055

[<http://nbn-resolving.de/urn/resolver.pl?urn=nbn%3Ade%3Agbv%3A3-000008055>]

1. INTRODUCTION	1
1.1 Phenolic compounds	1
1.2 The shikimate pathway	1
1.2.1 Enzymes of the shikimate pathway.....	2
1.2.1.1 3-deoxy-o-arabino-heptulosonate-7-phosphate synthase.....	2
1.2.1.2 3-dehydroquinate synthase.....	4
1.2.1.3 3-dehydroquinate dehydratase- shikimate dehydrogenase	4
1.2.1.4 Shikimate kinase	5
1.2.1.5 5-enolpyruvyl-shikimate-3-phosphate synthase.....	5
1.2.1.6 Chorismate synthase.....	6
1.2.2 Regulation of the shikimate pathway.....	6
1.2.3 Subcellular localization of the shikimate pathway	7
1.2.4 The shikimate pathway and the quinate pathway.....	8
1.2.5 Carbon resources of the shikimate pathway	9
1.2.5.1 Erythrose-4-phosphate	10
1.2.5.2 Phosphoenolpyruvate.....	11
1.3 Scientific aims of the work	13
2 MATERIALS AND METHODS	15
2.1 Chemicals and enzymes	15
2.2 Plant materials	15
2.3 Bacterial strains, plasmids and oligonucleotides	15
2.4 Tobacco transformation	16
2.5 Molecular cloning techniques	17
2.5.1 RNA preparation and Northern blot analysis	17
2.5.2 Protein extraction and Western blot analysis.....	17
2.5.3 Reverse transcription PCR (RT-PCR)	18
2.5.4 Rapid Amplification of cDNA Ends (RACE).....	18
2.5.5 Production of 6×His-tagged fusion protein in <i>E. coli</i>	18
2.5.6 Activity determination of 6×His-tagged DHD/SHD fusion protein.....	19

2.6 Biochemical methods	19
2.6.1 Plant extracts for enzyme activity assays	19
2.6.2 Enzyme activity measurements	19
2.6.2.1 DHD/SHD activity	19
2.6.2.2 Enolase activity	19
2.6.2.3 PGM activity	20
2.7 Metabolite analysis	20
2.7.1 Trichloroacetic acid (TCA) extraction	20
2.7.2 Ethanol extraction	20
2.7.3 Methanol extraction	21
2.7.4 Determination of metabolites	21
2.7.4.1 Glucose, fructose, and sucrose contents	21
2.7.4.2 Starch	21
2.7.4.3 Chlorophyll	21
2.7.4.4 Total soluble phenolic compound and lignin	21
2.7.4.5 Anthocyanin	22
2.7.4.6 PEP and pyruvate	22
2.7.4.7 3-PGA	22
2.7.4.8 Enzymatic assay of shikimate and dehydroquinone	22
2.7.4.9 IC-MS assay of the shikimate pathway intermediates	23
2.7.4.10 Amino acid	24
2.7.4.11 Chlorogenic acid	24
2.8 Ethanol induction	25
2.9 Floating experiment	25
2.10 Isolation of chloroplasts	25
3 RESULTS	26
3.1 Molecular characterization of tobacco DHD/SHD (Nt-DHD/SHD-1)	26
3.1.1 Cloning a full-length Nt-DHD/SHD-1 cDNA	26
3.1.2 Expressing Nt-DHD/SHD-1 in <i>E. coli</i>	27
3.1.3 Kinetic properties of Nt-DHD/SHD-1	29
3.1.4 A novel enzymatic assay for shikimate and dehydroquinone	30

3.2 Constitutive silencing of Nt-DHD/SHD-1 in transgenic tobacco	31
3.2.1 Plasmid construction and plant transformation	31
3.2.2 Screening the transgenic plants.....	32
3.2.3 Growth characteristics of DHD/SHD RNAi plants.....	33
3.2.4 Transcript analysis.....	35
3.2.5 cDNA macroarray analysis	35
3.2.6 Inhibition of DHD/SHD leads to reduced chlorogenate and lignin content.....	39
3.2.7 Carbohydrates and chlorophyll content in DHD/SHD RNAi plants	40
3.2.8 Silencing of DHD/SHD leads to an accumulation of the pathway intermediates.....	41
3.2.9 Shikimate feeding experiment	42
3.3 Inducible silencing of Nt-DHD/SHD-1 in transgenic tobacco.....	43
3.3.1 Plasmid construction and plant transformation	44
3.3.2 Screening the transgenic plants.....	44
3.3.3 Molecular characterization of <i>Alc</i> -DHD/SHD-RNAi plants	45
3.3.4 Kinetic analysis of the shikimate pathway intermediates	47
3.3.5 Spatial silencing of Nt-DHD/SHD-1 in flowers resulted in male sterility	48
3.4 Cloning a cytosolic DHD/SHD (Nt-DHD/SHD-2) from tobacco.....	52
3.4.1 Cloning a tobacco DHD/SHD isozyme (Nt-DHD/SHD-2)	53
3.4.2 Tissue specific expression of tobacco isoforms	56
3.4.3 Enzymatic properties of Nt-DHD/SHD-2	56
3.4.4 Subcellular localization of tobacco DHD/SHD isoforms	57
3.5 Constitutive silencing of EPSPS in transgenic tobacco.....	59
3.5.1 Plasmid construct and plant transformation	59
3.5.2 Screening the transgenic plants.....	60
3.5.3 Growth characterisation of EPSPS silenced plants	60
3.5.4 Silencing of EPSPS leads to reduced chlorogenate, lignin, and aromatic amino acids content.....	61
3.5.5 Carbohydrates and chlorophyll	62
3.5.6 Silencing of EPSPS resulted in an accumulation of the pathway intermediates.....	63
3.5.7 Shikimate feeding experiment	64
3.6 Introducing a PEP biosynthetic pathway into chloroplasts	64
3.6.1 Chloroplast targeting efficiency of tobacco transketolase transit peptide	65

3.6.2	Introducing <i>E.coli</i> PGM and enolase into tobacco chloroplasts.....	66
3.6.2.1	Plasmid construction and plant transformation.....	66
3.6.2.2	Growth characterization of transgenic plants.....	68
3.6.2.3	PEP and 3-PGA content in transgenic plants.....	70
3.6.2.4	Carbohydrates contents in transgenic plants.....	71
3.6.2.5	Aromatic amino acids and total soluble phenolics in transgenic plants.....	72
3.6.3	Establishment of a plastidic PEP biosynthetic pathway.....	74
3.6.3.1	Plasmid construction and plant transformation.....	74
3.6.3.2	Conversion efficiency of 3-PGA to PEP in transgenic plants.....	75
3.6.3.3	PEP, pyruvate and 3-PGA content in transgenic plants.....	75
3.6.3.4	Carbohydrates content in transgenic plants.....	76
3.6.3.5	Amino acids, chlorogenate and total soluble phenolic compounds.....	77
4	DISCUSSION.....	81
4.1	Constitutive silencing of Nt-DHD/SHD-1 in tobacco.....	81
4.1.1	Silencing of Nt-DHD/SHD-1 led to a reduced biosynthesis of secondary metabolites.....	81
4.1.2	Silencing of Nt-DHD/SHD-1 activated the transcription of DAHPS.....	81
4.1.3	Silencing of Nt-DHD/SHD-1 led to an accumulation of shikimate and dehydroquinate.....	82
4.1.4	Nt-DHD/SHD-1 might be regulated by light.....	83
4.1.5	Nt-DHD/SHD-1 was identified as a potential herbicide target.....	84
4.2	Inducible silencing of Nt-DHD/SHD-1 in tobacco.....	84
4.2.1	Silencing of Nt-DHD/SHD-1 triggered transient changes of the pathway intermediates.....	84
4.2.2	A shuttle to interpret the accumulation of shikimate in DHD/SHD silenced plants.....	85
4.2.3	Spatial silencing of Nt-DHD/SHD-1 led to a reduced biosynthesis of anthocyanins.....	86
4.2.4	Spatial silencing of Nt-DHD/SHD-1 in floral organ led to male sterility.....	88
4.3	Silencing of EPSPS in tobacco plants.....	89
4.3.1	Silencing of EPSPS led to a marked reduction of secondary metabolism.....	89
4.3.2	Differences between DHD/SHD and EPSPS silenced plants.....	89
4.4	Introducing a PEP biosynthetic-pathway into tobacco chloroplasts.....	90

4.4.1 Increase of PEP content did not result in a significant increase of secondary metabolites	91
4.4.2 3-PGA pool in the chloroplast of photosynthetic tissues is not an ideal carbon source for the secondary metabolism	92
5. SUMMARY	93
6. ZUSAMMENFASSUNG	96
7. ABBREVIATIONS	99
8. REFERENCES	100
PUBLICATION LISTS	110
<i>CURRICULUM VITAE</i>	111
ACKNOWLEDGEMENTS	112
ERKLÄRUNG	113

1. Introduction

1.1 Phenolic compounds

Plants produce a large variety of secondary compounds containing a phenol group. These phenolic compounds are synthesized via two different routes: the shikimate pathway and the acetate-malonate pathway, and thus represent a heterogeneous group. The shikimate pathway participates in the synthesis of most plant phenolics, whereas the malonate pathway is of less significance in higher plants, although it is an important source of phenolic products in fungi and bacteria (Taiz and Zeiger, 2002).

Phenolic compounds are classified into several groups, including anthocyanins, the pigments that attract animals; flavonoids, the compounds to serve as ultraviolet light protectants; isoflavonoids (phytoalexins), the compounds that act as antifungal and antibacterial defences; lignin, the phenolic macromolecule which is involved in mechanical support and protection; and tannins, polymeric phenolic compounds that function as feeding deterrents to herbivores.

Most classes of phenolic compounds in plants are derived from phenylalanine and tyrosine, and in most plant species the key step of the biosyntheses is the conversion of phenylalanine to cinnamic acid by the elimination of an ammonia molecule. The reaction is catalyzed by phenylalanine ammonia lyase (PAL), an important regulatory enzyme of secondary metabolism (Yao et al., 1995). Evidences suggest that phenylpropanoid pathway intermediates can regulate the expression of the pathway at the transcriptional and posttranslational levels. For an example, the biosyntheses of phenylpropanoids increase in cultured pine and soybean cells after treatment with a fungal elicitor and have been correlated with increase of PAL activity (Campbell and Ellis, 1992). In contrast, the inhibition of PAL activity by the mechanism of co-suppression reduced the accumulation of chlorogenic acid in transgenic tobacco plants (Elkind et al., 1990; Bate et al., 1994).

1.2 The shikimate pathway

The shikimate pathway is defined as seven metabolic steps beginning with the condensation of phosphoenolpyruvate (PEP) and erythrose 4-phosphate (Ery4P) and ending with the synthesis of chorismate. It is the common route leading to the production of three aromatic amino acids: phenylalanine (Phe), tyrosine (Tyr) and tryptophan (Trp). Higher plants use these amino acids

not only as protein building blocks, but also as precursors for a large number of secondary metabolites, among them plant pigments, flavonoids, auxins, phytoalexins, lignin and tannins (Herrmann, 1995). All pathway intermediates can also be considered as branch point compounds that may serve as substrates for other metabolic pathways (Herrmann and Weaver, 1999). Under normal growth conditions, 20% of the carbon fixed by plants is directed towards the shikimate pathway (Haslam, 1993). The shikimate pathway is restricted to plants, fungi and bacteria, making aromatic amino acids essential in the diets of animal. On the other hand, the pathway is an important target for herbicides (Kishore and Shah, 1988), antibiotics and live vaccines (O'Callaghan et al., 1988), because chemicals that interfere with any enzyme activity in this pathway are safe for humans when handled in reasonable concentration (Herrmann, 1995).

1.2.1 Enzymes of the shikimate pathway

The seven enzymes of the shikimate pathway were originally discovered through studies on bacteria, mainly *Escherichia coli* (*E.coli*). Although the substrates, intermediates and products of these enzymes are identical for prokaryotic and eukaryotic organisms, big differences are found in the primary structure and properties of the prokaryotic and eukaryotic enzymes sometimes. In addition, the regulation mechanism is well understood in some microorganisms but is now under investigation in higher plants. Figure 1 gives the names of the seven enzymes and intermediates of the shikimate pathway.

1.2.1.1 3-deoxy-o-arabino-heptulosonate-7-phosphate synthase

3-deoxy-o-arabino-heptulosonate-7-phosphate synthase (DAHPS) is the first enzyme of the shikimate pathway. It catalyzes the condensation of phosphoenolpyruvate (PEP) and erythrose-4-phosphate (Ery4P) to yield DAHP. The most intensively investigated DAHP synthase is the enzyme from *E.coli*.

Wild type *E.coli* produces three feedback inhibitor-sensitive DAHP synthase isoenzymes: a Tyr-sensitive, a Phe-sensitive and a Trp-sensitive enzyme. This multi-isoenzyme system apparently ensures a sufficient supply of chorismate for the biosynthesis of other aromatic compounds when Tyr, Phe and Trp are present in excess in the growth medium (Stephens and Bauerle, 1992).

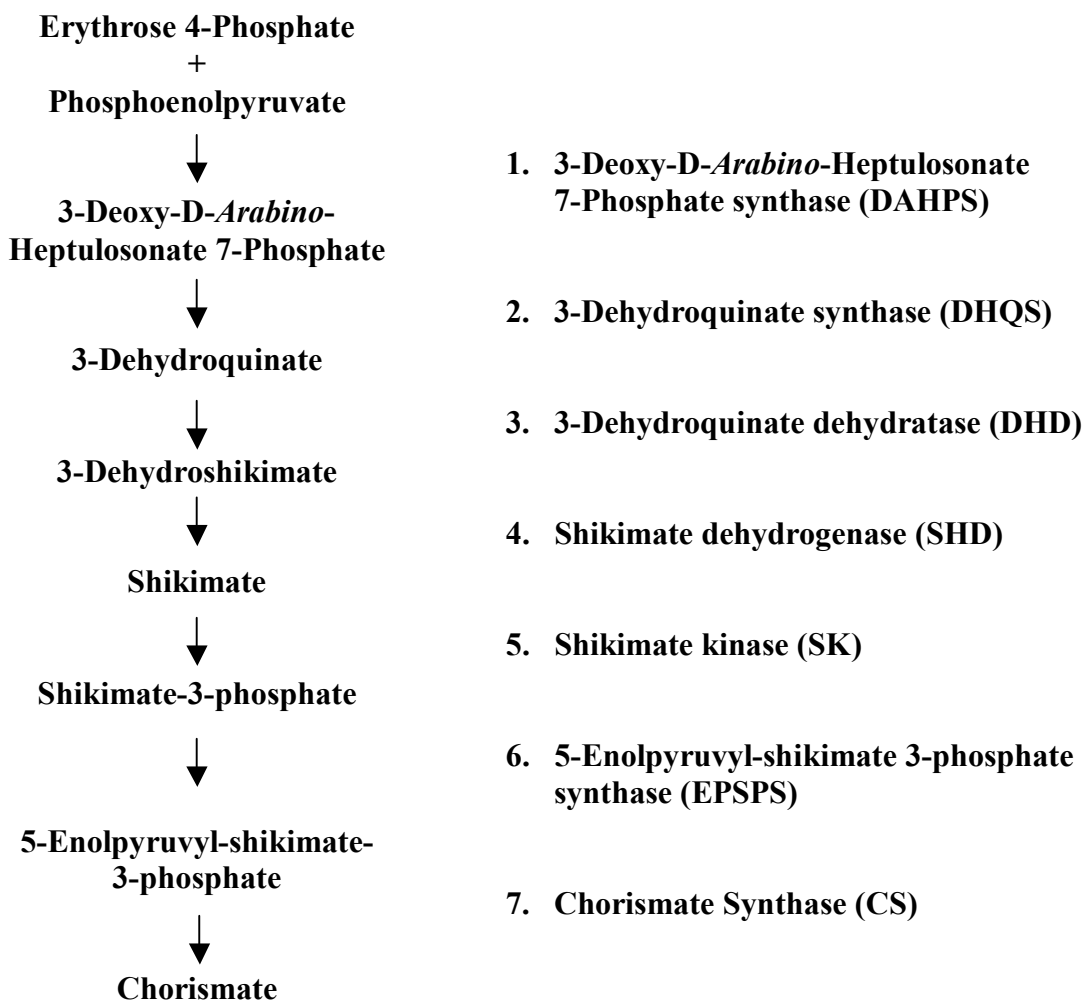


Figure 1. Reactions, pathway intermediates and enzymes of the shikimate pathway

In contrast to the microbial enzymes, none of plant DAHP synthases is inhibited by any of these three aromatic amino acids. In plants, metabolic regulation of DAHP synthase appears to occur preferentially at the transcriptional level. DAHP synthase mRNA and activity are induced by abiotic stresses such as mechanical wounding (Dyer et al., 1989) and glyphosate (Pinto et al., 1988). The induction of DAHP synthase gene expression in response to several of these environmental stimuli parallels a similar induction of PAL mRNA (Dyer et al., 1989; Henstrand et al., 1992), suggesting that the synthesis of aromatic amino acids and secondary aromatic compounds might be regulated in concert at the transcriptional level. In addition, several isoenzymes were described for plant DAHP synthase (Hartmann et al., 2001), suggesting that distinct regulation mechanism for the biosynthesis of aromatic compounds may exist within the chloroplasts.

1.2.1.2 3-dehydroquinase synthase

3-dehydroquinase synthase is the second enzyme of the shikimate pathway. It catalyzes the elimination of phosphate from DAHP to generate 3-dehydroquinase (DHQ). The enzyme from *E.coli* requires divalent cations for activity. DHQ synthase from *E.coli* is activated by inorganic phosphate, and it also requires catalytic amounts of NAD for activity, although the enzyme catalyses a redox neutral reaction (Bender et al., 1989). Unlike DAHPS, potato DHQ synthase activity does not change when cells are exposed to glyphosate (Pinto et al., 1988).

1.2.1.3 3-dehydroquinase dehydratase- shikimate dehydrogenase

The third step of the shikimate pathway, the dehydration of DHQ to form 3-dehydroshikimate (DHS), is catalysed by DHQ dehydrogenase (DHD). There are two types of DHD in bacteria. The type I enzyme is heat labile, catalyses a *syn* elimination and has K_m values in the lower micromolar range. The type II enzyme is heat stable, and catalyses a *trans* elimination (Harris et al., 1993). The K_m of the type II enzyme is one or two orders of magnitude higher as compared to the type I enzyme. There is no sequence similarity between these two types of isoenzymes. Most bacteria and plants only have the type I enzyme of DHD, whereas fungi have both (Deka et al., 1994). In general, the type I enzyme participates in the anabolic reaction of the shikimate pathway, and the type II enzyme participates in the catabolic reaction of the quinate pathway (Giles et al., 1985). The fourth step of the shikimate pathway is the reduction of DHS to shikimate. In *E.coli*, the reaction is catalyzed by an NADP-dependent shikimate dehydrogenase (SHD) with a molecular weight of 29 KD (Anton and Coggins, 1988). In plants, step three and four of the shikimate pathway are catalysed by a bifunctional enzyme 3-dehydroquinase dehydratase (EC 4.2.1.10) – shikimate dehydrogenase (EC 1.1.1.25) (DHD/SHD), which catalyzes the conversion of dehydroquinase to dehydroshikimate and dehydroshikimate to shikimate, respectively (Fiedler and Schultz, 1985). The turnover number of 3-dehydroquinase dehydratase is approximately one-tenth of shikimate dehydrogenase; therefore, dehydroquinase is readily converted to shikimate without accumulation of dehydroshikimate (Fiedler and Schultz, 1985). cDNAs encoding DHD/SHD of pea (Deka et al. 1994), tobacco (Bonner and Jensen, 1994) and tomato (Bischoff et al., 2001) have been isolated.

In 1994, Bonner and Jensen isolated a partial cDNA encoding tobacco DHD/SHD by screening a *Nicotiana tabacum* cDNA expression library with a DHD/SHD specific polyclonal antibody. This cDNA comprised the entire coding region for the mature enzyme plus 69 upstream

nucleotides, which was speculated to encode part of transit peptide for plastidic targeting. The mature sequence translates into a protein with both enzymatic activities: the dehydratase in the amino-terminal and the dehydrogenase in the carboxyl-terminal part. The putative transit peptide is rich in hydroxylated amino acid residues but has a net negative charge, a feature not seen for any other known chloroplast transit peptide (Gavel and von Heijne, 1990). In 2001, Bischoff et al. cloned a full-length cDNA encoding tomato DHD/SHD. The deduced amino acid sequence revealed that the DHD/SHD is most likely synthesized as a precursor with a very short (13 amino acids) plastid-specific transit peptide, which was highly similar to the tobacco counterpart.

1.2.1.4 Shikimate kinase

In the fifth step of the pathway, shikimate kinase catalyzes the phosphorylation of shikimate to yield shikimate 3-phosphate. *E.coli* has two isoenzymes of shikimate kinase, and both can function *in vitro* for aromatic amino acid biosynthesis. Isoenzyme II has a K_m of 200 μM for shikimate, while the K_m for enzyme I is more than 100 times higher. Thus, *in vivo*, isoenzyme I might not be an enzyme of the shikimate pathway. Plant shikimate kinase has been described for spinach (Schmidt et al., 1990) and tomato (Schmid et al., 1992). The shikimate kinase gene is expressed in an organ-specific manner similar to the expression of EPSP synthase and chorismate synthase. The abundance of shikimate kinase transcripts was highest in flowers, lower in roots and even lower in stems, cotyledons and leaves (Gorlach et al., 1994)

1.2.1.5 5-enolpyruvyl-shikimate-3-phosphate synthase

5-enolpyruvyl-shikimate-3-phosphate synthase (EPSPS) (EC 2.5.1.19) is the sixth enzyme of the shikimate pathway. It catalyzes the reversible formation of 5-enolpyruvyl-shikimate-3-phosphate (EPSP) from shikimate 3-phosphate and PEP. Plant cDNAs encoding EPSPS have been isolated from petunia (Shah et al., 1986), *Arabidopsis* (Klee et al., 1987), tomato (Gasser et al., 1988), and tobacco (Wang et al., 1991). All cDNAs encode precursor proteins with N-terminal transit sequences for plastid import. *In vivo* uptake experiments have shown that the petunia transit sequence directs proteins into plastids (Della-Cioppa et al., 1986). This enzyme has been deeply analysed because it is the target of a broad-spectrum herbicide, glyphosate (N-[phosphonomethyl]-glycine) (Steinrucken and Amrhein, 1980). When challenged with glyphosate, plant cells would accumulate or excrete shikimate (Amrhein et al., 1980). High-level accumulation of shikimate in the glyphosate-treated plants may be the result of a

deficiency of feedback control of the shikimate pathway (Jensen, 1985). The immediate precursor for EPSPS enzyme is shikimate 3-phosphate, but this compound is likely to be cleaved in the tonoplast or vacuole by a phosphatase, yielding shikimate (Hollaender-Czytko and Amrhein, 1983). Measurement of shikimate accumulation in response to glyphosate inhibition of EPSPS is a rapid and accurate assay to quantify glyphosate-induced damage in sensitive plants (Pline et al., 2002).

1.2.1.6 Chorismate synthase

Chorismate synthase (EC 4.6.1.4) is the last enzyme of the shikimate pathway. It catalyzes the trans-1, 4 elimination of phosphate from EPSPS to yield chorismate. In this reaction, the second of three double bonds of the benzene ring is introduced. Chorismate synthase requires a reduced flavin nucleotide (FMNH₂) as a cofactor, even though the overall reaction is redox neutral. In this aspect, the enzyme is similar to DHQ synthase, the second enzyme in the shikimate pathway. Like other shikimate pathway enzymes, the cDNA of chorismate synthase encodes a precursor protein with N-terminal transit sequences for plastidic targeting. Chorismate synthase activity requires cleavage of the transit peptide (Henstrand et al., 1995). In contrast, other shikimate pathway enzymes (shikimate kinase, DHD/SHD and EPSP synthase) have been shown to be active in both immature and mature forms.

1.2.2 Regulation of the shikimate pathway

The demand for phenolic metabolites varies during plant development and during periods of environmental stress such as wounding or pathogen attack. Therefore, mechanisms that control carbon flow into the shikimate pathway must perceive and respond accordingly. For both plants and bacteria, at least two of the shikimate pathway enzymes, DAHP synthase and shikimate kinase can be regulated.

The prokaryotic DAHP synthase is regulated by feedback inhibition. The genes encoding the Tyr- and Trp-sensitive isoenzymes are regulated by Tyr and Trp, respectively (Garner and Herrmann, 1985; Klig et al., 1988), whereas the Trp-sensitive isoenzyme is regulated by both amino acids (Muday et al., 1991).

In contrast to bacterial DAHPS, plant DAHP synthases are not subject to feedback inhibition by the aromatic amino acids. Unexpectedly, the purified enzymes from carrot and potato are

activated by Trp and to a less degree by Tyr in a hysteretic fashion (Suzich et al., 1985). Thus, the aromatic amino acids cannot be considered to be feedback inhibitors of plant DAHP synthase. Rubin and Jensen (1985) observed that 0.15 mM arogenate led to 50% inhibition of the bean enzyme. Based on this fact, they proposed a model for sequential feedback inhibition of the aromatic compounds biosynthesis. This model predicted a cessation of carbon flow into the shikimate pathway under a high concentration of arogenate, a rather unstable shikimate pathway derivative.

The first evidence of metabolic regulation of a plant DAHP synthase came from experiments with suspension-cultured potato cells which has been exposed to glyphosate (Pinto et al., 1988). Glyphosate activated DAHPS by increasing the amount of this enzyme *in vivo*. This activation was specific, because other shikimate pathway enzymes were not affected. The herbicide has no effect on DAHP synthase *in vitro*, indicating that inhibition of chorismate synthesis results in the production of a signal that presumably affects transcription and/or translation of the gene encoding DAHP synthase.

Both mechanical wounding and fungal elicitation induce DAHP synthase mRNA accumulation. The induction of DAHP synthase gene expression parallels a similar induction of PAL mRNA (Dyer et al., 1989; Henstrand et al., 1992), suggesting that the synthesis of aromatic amino acids and secondary aromatic compounds might be regulated in concert at the transcriptional level.

Shikimate kinase represents a second control step in the shikimate pathway. This enzyme is subject to control by energy charge (Schmidt et al., 1990). Such a control indicates that in plants, under energetically favourable conditions, carbon of shikimate is diverted from the main trunk of the pathway into secondary products or stored in the form of quinate and its derivatives.

1.2.3 Subcellular localization of the shikimate pathway

In plants, proteins are synthesized in three different compartments: in the cytoplasm, in the plastids and in the mitochondria. Therefore the aromatic amino acids must either be synthesized *in situ* in the respective protein-synthesizing compartments or synthesized outside the compartments and have to be imported.

Early work revealed that the isolated chloroplasts from spinach were able to synthesize aromatic amino acids from CO₂ or shikimate (Bickel et al., 1978). This indicates the existence of an

aromatic biosynthetic pathway in chloroplasts. Moreover, the localization of the shikimate pathway in the plastids is supported by molecular analysis. In higher plants, the shikimate pathway enzymes are normally synthesized as precursors with a N-terminal extension, presumably a plastid-specific transit peptide. In addition, *in vitro* experiments demonstrated that some shikimate pathway enzymes (e.g. shikimate kinase and EPSPS) can be imported into chloroplasts (Della-Cioppa, et al. 1986, Schmid, et al. 1992). Thus, the shikimate pathway appears to be firmly established in plastids. However, it has been proposed that the chloroplast-localized biosynthetic activity does not count for 100% of the observed aromatic amino acid biosynthesis. Hence, a spatially separated pathway in the cytosol might exist (Buchholz et al., 1979). The dual pathway hypothesis proposed a plastid-located shikimate pathway responsible for the production of aromatic amino acids and a cytosolic pathway responsible for the production of secondary metabolites, because enzymes of phenylpropanoid and flavonoid biosynthesis are not present in plastids. The evidence for a dual shikimate pathway is further supported by isozyme analysis in subcellular fractions. Putative cytosolic isozymes have been described for DAHP synthase (Ganson et al., 1986), DHD/SHD (Mousdale et al., 1987), EPSP synthase (Mousdale and Coggins, 1985) and chorismate mutase (d'Amato, 1984). Moreover, since shikimate kinase (Schmid et al., 1992) and EPSPS (Della-Cioppa et al., 1986) are active with their transit peptides, these enzymes could also be a part of cytosolic shikimate pathway.

1.2.4 The shikimate pathway and the quinate pathway

As summarized by Bentley (1990), the shikimate pathway has many branches. The intermediates of the shikimate pathway are potential branch points leading to other metabolic pathways. For instance, the shikimate pathway inter-crosses with the quinate pathway, and they share at least two pathway intermediates 3-dehydroquininate and 3-dehydroshikimate (Figure 2). Quinate could be synthesized in one step from dehydroquininate by quinate dehydrogenase or from shikimate by quinate hydrolyase. Plants can also use quinate as a carbon source for aromatic amino acid synthesis (Leuschner and Schultz, 1991). In higher plants, quinate is a precursor for chlorogenate (Beaudoin-Eagan and Thorpe, 1984). Although the accumulation of quinate appears to be restricted to specific plants, the occurrence of chlorogenate and its derivatives, the major soluble phenylpropanoids in tobacco and preformed protectants against fungal attack, are more widespread, (Maher et al. 1994).

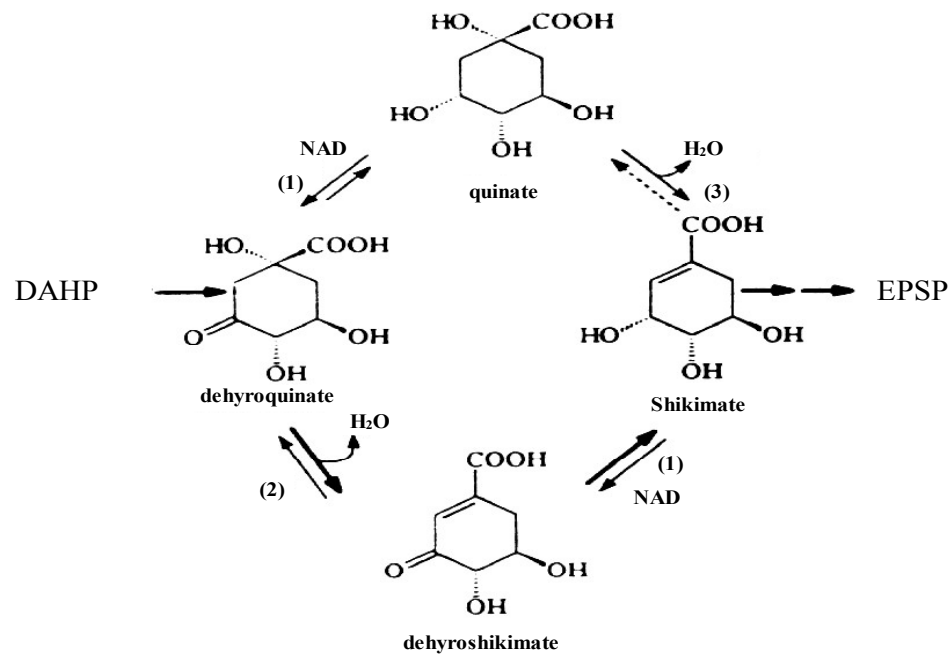


Figure 2. Metabolic intermediates and enzymes of the shikimate pathway and the quinate pathway. The shikimate pathway and the quinate pathway share dehydroquinate and dehydroshikimate as common intermediates. Enzymes of the quinate pathway are indicated. (1) quinate (shikimate) dehydrogenase, (2) 3-dehydroquinate dehydratase and (3) quinate hydrolyase. Bold arrows indicate reactions of the main trunk of the shikimate pathway.

1.2.5 Carbon resources of the shikimate pathway

The immediate substrates for the shikimate pathway are erythrose 4-phosphate (Ery4P) and phosphoenolpyruvate (PEP) (Mousdale and Coggins, 1985; Schmid and Amrhein, 1995). Ery4P is an intermediate of both the oxidative and the reductive pentose phosphate pathway of plastids. It is provided by transketolase, which converts glyceraldehyde-3-phosphate and fructose-6-phosphate to xylulose-5-phosphate and Ery4P. Unlike Ery4P, PEP cannot be generated in chloroplasts. Because most plastids have little or no PGM and enolase activity, glycolysis cannot proceed further than 3-phosphoglycerate (Bagge and Larsson, 1986; Stitt, 1997). Plastids therefore rely on the supply of cytosolic PEP. The transport of PEP from the cytosol into plastids is mediated by a specific PEP/phosphate translocator (PPT), which imports cytosolic PEP into the plastids in exchange with inorganic phosphate. Fischer et al. (1997a) isolated a plastidic PEP/phosphate translocator from maize endosperm membranes and subsequently cloned the corresponding cDNAs from maize root, cauliflower buds, tobacco and *Arabidopsis* leaves. All above proteins hold N-terminal targeting sequences, indicating that PPTs are located at the plastid membrane. Compared with the chloroplast triose phosphate / phosphate translocator (cTPT), which exports fixed photosynthetic carbon in the form of triose phosphate

and 3-phosphoglycerate, PPT exhibits a higher affinity and specificity for the transport of inorganic phosphate and PEP (Flügge et al., 1989).

The availability of mutants defective in particular gene functions opens the way to analyze the impact of a specific gene on plant performance. It has been demonstrated that the *Arabidopsis chlorophyll a/b binding protein under-expressed 1* mutant (*cue1*) is deficient in the plastidic PPT protein (Voll et al., 2003). These plants are characterized by a reticulate phenotype and a reduced growth. Biochemical analysis revealed that they are suppressed in their capability to produce aromatic amino acids and derived metabolites. Interestingly, the reticulate phenotype could be rescued by feeding a combination of aromatic amino acids to the mutant, indicating that flux into the shikimate pathway was diminished in *cue1* mutants (Streatfield et al. 1999). The mutant phenotype could also be rescued by the overexpression of a PPT gene or a plastidic pyruvate phosphate dikinase (PPDK), which led to the generation of PEP inside the plastids (Voll et al., 2003). Both findings support the proposed function of the PPT in supplying PEP for the shikimate pathway.

However, the levels of aromatic amino acids were only slightly affected in *cue1* mutant, suggesting that not a general, but a specific lack of phenylpropanoids caused the *cue1* mutant phenotype. Knappe et al. (2003) isolated a second PPT gene (AtPPT2) from *Arabidopsis*. Both isoforms of PPT were located in chloroplasts with similar substrate specificities and were able to import PEP into plastids. The *cue1* phenotype could partially be complemented by overexpression of AtPPT2. The first isoform AtPPT1 was mainly expressed in the vasculature of leaves and roots, especially in xylem parenchyma cells, but not in leaf mesophyll cells, whereas the second isoform AtPPT2 was exclusively expressed in leaves. Accordingly, it has been proposed that AtPPT1 is involved in the generation of phenylpropanoid metabolism-derived signal molecules that trigger development in interveinal leaf regions.

1.2.5.1 Erythrose-4-phosphate

Transketolase (TK) catalyzes reactions in the Calvin cycle and the oxidative pentose phosphate pathway (OPPP) and produces Ery4P, which is a precursor for the shikimate pathway. Henkes et al. (2001) observed that a 60% to 80% reduction of TK activity led to decreased levels of aromatic amino acids, chlorogenate and lignin. A simple explanation for these changes was that carbon flux towards the shikimate pathway and phenylpropanoid metabolism has been restricted by the supply of Ery4P. Henkes et al. (2001) estimated the flux control coefficient of

TK for the shikimate pathway and indicated that TK has a remarkably high flux control coefficient of 0.7 for the phenylpropanoid biosynthesis. This value was similar to or larger than the effects of the decreased expression of phenylalanine ammonia-lyase, 4-coumarate:CoA lyase, and cinnamate-4-hydroxylase, suggesting that secondary metabolism might be limited by precursor supply, and major changes in secondary metabolism would require appropriate reprogramming of primary metabolism.

1.2.5.2 Phosphoenolpyruvate

As described above, chloroplasts from C3 plants depend on the import of PEP from the cytosol as a substrate for the shikimate pathway. Fischer et al. (1997a) proposed a shuttle model to explain the supply of PEP to chloroplasts. According to this model, triose phosphate (TP), an intermediate of photosynthesis, would be exported into the cytosol by triose phosphate translocator (TPT), and converted to PEP by the catalysis of cytosolic PGM and enolase. Afterwards, PEP is imported into chloroplasts by PPT to join the shikimate pathway. Thus a total of two trans-membrane actions are required.

The supply of PEP in plastids might be a limiting factor determining the biosynthesis of secondary metabolites. To improve the plastidic PEP level, three strategies could be followed: (i) Increase the uptake efficiency of cytosolic PEP by over-expressing a PPT translocator in chloroplasts. (ii) Convert pyruvate to PEP by expressing a C4 type PPDK in chloroplasts, which catalyzes the ATP-dependent conversion of pyruvate and Pi to PEP, AMP and pyrophosphate. (iii) Create a plastidic PEP biosynthetic pathway by expressing heterologous plastid targeted enolase and phosphoglycerate mutase (PGM) genes.

Voll et al. (2003) introduced a PPT and a PPDK into the *Arabidopsis* mutant *cue1*, respectively. In both transformations, the mutant phenotype is rescued by the elevation of plastidic PEP, suggesting that PEP deficiency within the plastids triggered developmental constraints in *cue1*. In the *cue1*/PPT line, the PEP-specific transport rates increased fivefold above wild-type level, and 24-fold above the *cue1* mutant, whereas total PEP production was not considerably altered compared to the wild type. In contrast, the *cue1*/PPDK lines accumulated substantial amount of PEP (6-fold higher than wild-type plants and mutant) during the photoperiod, indicating that PPDK was active in chloroplasts. The increase of PEP rescued the synthesis of phenylpropanoids and aromatic amino acids in transgenic plants. In *cue1* mutant,

phenylpropanoids decreased to 25% of wild type level. Phenylpropanoids were almost restored to wild-type level in *cue1*/PPDK and *cue1*/PPT plants.

As the initial product of the Calvin cycle, there is a large 3-PGA pool in chloroplasts, making it possible to create a 3-PGA: PEP pathway in the plastids. To achieve this goal, PGM and enolase would have to be over-expressed in chloroplasts, and thus the plastidic 3-PGA would be catalyzed to 2-PGA, and further to PEP.

Phosphoglycerate mutase (EC 5.4.2.1) (PGM) catalyzes the conversion of 2-phosphoglycerate (2-PGA) and 3-phosphoglycerate (3-PGA). Two apparently evolutionarily unrelated enzymes with PGM activity have been characterised. One enzyme (dPGM) requires the cofactor 2,3-bisphosphoglycerate (2,3- BPGA) for activity, while the other (iPGM) does not. Vertebrates, budding yeast, and various eubacterial species only have dPGM, whilst nematodes, archaea, higher plants and various other eubacteria only possess iPGM. In addition, a small number of eubacteria appear to encode both enzymes (Fothergill-Gilmore and Watson, 1989). Comparison of kinetic properties and expression levels of the two PGM of *E.coli* has allowed assessing the metabolic roles of each. Both PGM isoforms catalyze the interconversion of 2-phosphoglycerate and 3-phosphoglycerate in the glycolytic and gluconeogenic directions, but dPGM has at least a 10-fold higher specific activity for both reactions (Fraser et al., 1999).

Enolase (2-phospho-glycerate hydrolase, EC 4.2.1.1) catalyzes the formation of phosphoenolpyruvate from 2-phosphoglycerate (2-PGA). The reaction involves dehydration, the removal of a water molecule, to form the *enol* structure of PEP. The enzyme has been purified and the genes have been cloned from diverse sources: *E.coli* (Weng et al., 1986), yeast (Chin et al., 1981), spinach (Sinha and Brewer, 1984), tomato and *Arabidopsis* (Van der Straeten et al., 1991). Although octameric enzymes have been described, in all eukaryotes and many prokaryotes, enolase is biologically active as a dimer, with subunits having a molecular weight of approximately 45,000 dalton (Hannaert et al., 2000)

Like PGM, enolase is also a cytosolic enzyme. Van der Straeten et al (1991) demonstrated the absence of enolase in *Arabidopsis* chloroplasts by enzyme activity and immunoblot analysis. They also found that N-terminal region of enolase was highly conserved between yeast and *Arabidopsis*, and moreover, had no homology to the consensus of chloroplast target sequence. When 11 N-terminal amino acids from tomato enolase were replaced by 9 amino acids encoded by the polylinker of pT7-7 vector, enolase was completely deactivated. In chloroplasts,

glycolytic enzymes fulfil functions in photosynthetic carbon fixation (dark reaction). Enolase is one of the few enzymes that are not involved in the Calvin cycle and, therefore, there is no essential need for it in chloroplasts.

1.3 Scientific aims of the work

The shikimate pathway provides precursors for a large number of the phenolic compounds. In addition to protect plants from UV light and pathogen attack, these compounds are widely accepted as protective agents against cardiovascular diseases and some forms of cancers. Thus, the elevation of phenolic compounds in plants by increasing carbon flux through the shikimate pathway is of biotechnological interest. On the other hand, this pathway is an important target for herbicides, antibiotics and vaccines, because it is restricted to plants, fungi, and bacteria. Chemicals that interfere with any enzyme activity of this pathway are considered safe for humans.

The first aim of this work was the identification of some herbicide targets, and to investigate regulating mechanisms of the shikimate pathway. To this end, activity of shikimate pathway genes has been silenced in the transgenic plants by either antisense or RNAi technologies. Silencing of corresponding enzyme has been evaluated by characterizing the molecular, physiological and metabolic changes in transgenic plants. The regulation of the pathway has been investigated by analyzing transcripts encoding shikimate pathway enzymes. In addition, feeding experiments may provide indispensable information for understanding of the regulation mechanism of the pathway on enzymatic level.

The second aim was to characterize candidate enzymes, and to produce functional proteins for the screening of enzyme inhibitors. Thus, corresponding proteins has been expressed and purified in *E.coli* expression systems. Enzymatic properties have been investigated *in vivo*, which may help to understand the reaction kinetics, and to identify enzyme inhibitors.

The third aim was to increase carbon flux into secondary metabolism in plants. To this end, a plastidic PEP biosynthetic pathway was created by over-producing PGM and enolase in tobacco chloroplasts. As a result, conversion of plastidic 3-PGA to PEP, and a higher level of carbon into secondary metabolism through the shikimate pathway was expected. Pathway intermediates (3-PGA, PEP and pyruvate) and end products (aromatic amino acids, chlorogenate, and lignin)

have been determined in the transgenic plants to evaluate the feasibility and consequence of this strategy.

2 Materials and methods

2.1 Chemicals and enzymes

The chemicals and enzymes were purchased from the following companies: Biogenes (Berlin, Germany), Bio-Rad (Richmond, USA), Boehringer (Mannheim, Germany), Clontech (Heidelberg, Germany), GibcoBRL (Paisley, England), Invitrogen (Carlsbad, USA), Macherey-Nagel (Düren, Germany), Merck (Darmstadt, Germany), NEB (England), Promega (Madison, USA), Qiagen, (Valencia, USA), Roth (Karlsruhe, Germany), Serva (Heidelberg, Germany), and Sigma (München, Germany).

2.2 Plant materials

Tobacco plants (*Nicotiana tabacum* cv. Samsun NN) were obtained from Vereinigte Saatzuchten AG (Ebstorf, Germany) and grown in tissue culture under a 16-h light/8 h dark regime (irradiance $150 \mu\text{mol quanta m}^{-2} \text{s}^{-1}$) at 50% humidity on Murashige Skoog medium (Sigma, St. Louis, MO, USA) containing 2% (w/v) sucrose. Plants for biochemical analysis were kept in soil in the greenhouse with 16 h supplementary light ($200 \pm 300 \mu\text{mol quanta m}^{-2} \text{s}^{-1}$) and 8 h darkness. Relative humidity varied between 60 and 70% and temperatures were adjusted to 22 and 15°C during the light and dark period, respectively.

2.3 Bacterial strains, plasmids and oligonucleotides

Escherichia coli strain XL-1 Blue (Stratagen) was used for plasmid amplification. The bacteria was cultivated and transformed using standard techniques (Sambrook et al., 1989). *Escherichia coli* strain M15:pREP4 (Qiagen) was used as hosts for expressing fusion proteins. *Agrobacterium tumefaciens* strain C58C1 carrying the virulence plasmid pGV2260 was cultivated and used for all plants transformation (Rosahl et al., 1987).

The vector pCRBlunt (Invitrogen) was used for the cloning of PCR products. The vector pQE (Qiagen) was used for the expression of 6×His-tagged fusion proteins. The binary vector pBin19 and its derivatives were used for plants transformation. The vector pUC-RNAi (Chen et al. 2003) was used for dsRNA constructions.

Oligonucleotides used for PCR, RT-PCR and RACE amplifications are listed in Table 1. All oligonucleotides were synthesized by Metabion AG (Martinsried, Germany).

Table 1. Oligonucleotides used for PCR, RT-PCR and RACE amplifications. The created restriction sites are underlined.

Number	Sequence	Name
1	5'- <u>GGATCC</u> GTTGGGACCAGATAACCAGAATA-3'	5'-primer, Nt-DHD/SHD-1 for RNAi construct
2	5'- <u>GTCGAC</u> GCTAAGCTCGTCAAGAGACAAAG-3'	3'-primer, Nt-DHD/SHD-1 for RNAi construct
3	5'- <u>GGATCC</u> GCAATGGCACAGATTAGC-3'	5' primer, EPSPS for co-suppression construct
4	5'- <u>GGATCC</u> GTGACACTGTTCTCTCTGTCC-3'	3' primer, EPSPS for co-suppression construct
5	5'- <u>GGATCC</u> ATGTCCAAAATCGTAAAAATCA-3'	5' primer, <i>E.coli</i> enolase coding sequence for TK-TP-pBin 9
6	5'- <u>GTCGAC</u> TTATGCCTGGCCTTTGATCTCT-3'	3' primer <i>E.coli</i> enolase coding sequence for TK-TP-pBin 9
7	5'- <u>GGATCC</u> ATGGCTGTAACCTAAGCTGGTTC-3'	5' primer, <i>E.coli</i> PGM coding sequence for TK-TP-pBin 9
8	5'- <u>GTCGAC</u> TTACTTCGCTTTACCCTGGTTT-3'	3' primer, <i>E.coli</i> PGM (BPG dependent) for TK-TP-pBin 9
9	5'- <u>AAGCTT</u> CCATGGAGTCAAAGATTCAAATAG-3'	5' primer, 35S promoter
10	5'- <u>AAGCTT</u> GGACAATCAGTAAATTGAACGGAG-3'	3' primer, <i>ocs</i> terminator
11	5'-TTCATCACCAGCATACTGACCCCCTTCCC-3'	5' primer, Nt-DHD/SHD-1 for RACE
12	5'-GCGTCTTTCACGCAGAGTAGTCTTTCTA-3'	5' primer, Nt-DHD/SHD-2 for RACE
13	5'-TCGAAGAGCAGGAGAGCTGAAATTGTGA-3'	3' primer, Nt-DHD/SHD-2 for RACE
14	5'-GTTTTCCAGTCACGACGTT-3'	M13 Forward primer
15	5'-AGGAAACAGCTATGACCATG-3'	M13 Reverse primer
16	5'- <u>GGATCC</u> GGGGAGGCAATGACGAGGAAC-3'	5' Primer, Nt-DHD/SHD-1 mature protein for pQE9
17	5'- <u>CTGCAG</u> TTAATTCCTCCGAAGCACAAATGG-3'	3' Primer, Nt-DHD/SHD-1 mature protein for pQE9
18	5'- <u>GTCGAC</u> ATGGGTAGTGTGGATTGTTG-3'	5' primer, Nt-DHD/SHD-2 coding sequece for pQE9
19	5'- <u>GTCGAC</u> TTAGAATTTTGCCATAACGATGT-3'	3' primer, Nt-DHD/SHD-1 coding sequece for pQE9
20	5'- <u>GGATCC</u> GCAATGGCACAGATTAGC-3'	5' primer, Tobacco EPSPS fragment for pQE9
21	5'- <u>GGATCC</u> GTGACACTGTTCTCTCTGTCC-3'	3' primer, Tobacco EPSPS fragment for pQE9

Restriction sites are underlined.

2.4 Tobacco transformation

The binary vectors containing target inserts were introduced into *Agrobacterium tumefaciens* via electroporation. Tobacco plants (*Nicotiana tabacum* cv. Samsun NN) were transformed by

Agrobacterium-mediated leaf disc technique as described (Rosahl et al., 1987). After regeneration on selective medium, the primary transformants were transferred to soil and screened by Northern blot hybridization.

2.5 Molecular cloning techniques

2.5.1 RNA preparation and Northern blot analysis

Total RNA was prepared as described (Logemann et al., 1987). Following a standard extraction with phenol/chloroform/isopropanol, RNA was ethanol-precipitated and washed with 3 M sodium acetate, pH 5.2. Afterwards, pellets were washed by 80% ethanol. RNA was dissolved in diethylpyrocarbonate (DEPC) treated H₂O, and incubated at 65°C for 10 minutes with shaking. Northern blot hybridization was performed according to Amasino (1986). 30 µg RNA was separated on a 1.5% (w/v) agarose gel in the presence of formaldehyde, and blotted on Hybond-N membrane with 20 X SSC. The filters were then fixed by UV cross-linking. Radioactive labelling of cDNA fragments was performed using the High Prime-kit (Boeringer Mannheim, Germany) and [³²P]-dCTP. Hybridization was carried out as described (Hajirezaei et al., 2002). Hybridization signals were quantified by BAS 2000 Bio-Imaging Analyser (Fujifilm).

2.5.2 Protein extraction and Western blot analysis

Protein extracts were prepared by grinding leaf materials in an ice-cold extraction buffer (50 mM Tris-HCl pH 6.8, 5 mM MgCl₂, 5 mM mercaptoethanol, 15% (v/v) glycerol, 1 mM EDTA, and 1 mM EGTA). The homogenate was centrifuged at 15000 rpm at 4°C for 10 minutes, and the supernatant was used for further analysis. Protein concentrations were determined according to the method of Bradford (1976).

Western blot was performed as described by Hajirezaei et al. (2002). Soluble protein was adjusted to 1 mg protein ml⁻¹. 20 µg protein aliquots were separated on 12.5 % SDS-polyacrylamid gels and electro-transferred onto a nitrocellulose membrane (Porablot; Macherey-Nagel, Düren, Germany) in the presence of transfer buffer (39 mM glycine, 48 mM Tris-base, 0.01 % (w/v) SDS and 20% methanol). The membrane was blocked for 1 hour in buffer (TBS/T: 20 mM Tris, 500 mM NaCl, 0.1% (v/v) Tween20 containing 5% (w/v) non-fat milk powder and incubated for a minimum of 1 hour with the rabbit anti-DHD/SHD or anti-EPSPS primary antibody (1: 2000) in TBS/T supplemented with 1% (w/v) milk powder.

Development of the immunoblots was performed with the Supersignal® West Pico Chemiluminescent Substrate system (Pierce, Rockford, USA) after incubation (1 hour) with an anti-rabbit horseradish peroxidase (HRP) conjugated secondary antibody (1: 100000) (Pierce, Rockford, USA). The blots were exposed to X-ray films (Sigma) and quantified by BAS 2000 Bio-Imaging Analyser (Fujifilm).

2.5.3 Reverse transcription PCR (RT-PCR)

About 2-10 µg total RNA from tobacco tissues was reverse transcribed in a total volume of 50 µl with Promega™ M-MLV reverse transcriptase. The transcription was performed at 37°C for 1 hour. 2 µl of the reverse transcription product was used for PCR amplification with appropriate primers (Table 1) and cycling parameters.

2.5.4 Rapid Amplification of cDNA Ends (RACE)

The first-strand cDNA was synthesized from 1 µg of tobacco total RNA with SMART™ RACE cDNA Amplification Kit (Clontech laboratories, Inc), in a total volume of 10 µl. 5'-RACE and / or 3'-RACE was performed with appropriate primers (Table 1) according to the manufacture's instruction. Amplified PCR products were blunted with pfu polymerase (Promega), and cloned into the vector pCRblunt. Positive clones were sequenced by MegaBace 1000 system, and analyzed by the software Vector NTI (Informax Inc., USA)

2.5.5 Production of 6×His-tagged fusion protein in *E. coli*

To over-express 6×His-tagged fusion protein in *E. coli*, the coding regions of protein was amplified by RT-PCR from plant materials with gene specific primers (Table 1). PCR product was sub-cloned into corresponding restriction site of a pQE vector. Expression of the recombinant 6×His-tagged protein was induced by 0.05 mM IPTG at room temperature. Sonication and purification with metal affinity resin Ni-NTA agarose were operated on ice according to manufacturer's instruction (Qiagen, Valencia, USA). The purified His-tagged fusion protein was used for antibody production and for determination of the shikimate pathway intermediates in tobacco plants.

2.5.6 Activity determination of 6×His-tagged DHD/SHD fusion protein

The enzyme activity of 6×His-tagged DHD/SHD fusion protein was determined spectrophotometrically at 334 nm by measuring the production of NADPH. 1 µl of purified protein was incubated in 800µl reaction buffer (200µM NADP, 100 mM glycine-NaOH, pH9.0) at room temperature for 3 minutes. The reaction was started by 2 µl of 100 mM shikimate solution. DHD/SHD activity was determined by calculating the production rate of NADPH ($\mu\text{mol}^{-1} \text{min}^{-1}$).

2.6 Biochemical methods

2.6.1 Plant extracts for enzyme activity assays

Protein extract was prepared by grinding leaf material in an ice-cold extraction buffer (50 mM Tris-HCl pH 6.8, 5 mM MgCl_2 , 5 mM mercaptoethanol, 15% (v/v) glycerol, 1 mM EDTA, and 1 mM EGTA). The homogenate was centrifuged at 15000 rpm at 4°C for 10 minutes, and the supernatant was used for further analysis. Protein concentration was determined according to the method of Bradford (1976).

2.6.2 Enzyme activity measurements

2.6.2.1 DHD/SHD activity

20 µl of plant extract was incubated in 780 µl reaction buffer (1mM NADP in 100 mM Glycine-NaOH buffer, pH9.0). The mixture was kept at room temperature for 5 minutes, and measured by photometer (Uvikon 922, Kontron instruments, Germany). The measurement was started by adding 2 µl of shikimate solution (100 mM). The DHD/SHD activity was determined by calculating the production rate of NADPH ($\mu\text{mol min}^{-1} \text{g}^{-1} \text{FW}$).

2.6.2.2 Enolase activity

Enolase activity was determined from tobacco leaf materials according to Mujer et al. (1995). 20 µl of plant extract was incubated in 780 µl reaction buffer containing 50 mM MOPS-KOH, pH7.0, 5 mM MgSO_4 , 50 mM KCl, 0.2 mM NADH, 1 mM ADP, 1 unit Lactate dehydrogenase and 2 units Pyruvate kinase. The mixture was kept at room temperature for 5 minutes and measured by photometer (Uvikon 922, Kontron instruments, Germany). The measurement was

started by adding 2 μl of 2-phosphoglycerate solution (100 mM). Enolase activity was determined by calculating the production rate of NAD ($\mu\text{mol min}^{-1} \text{g}^{-1} \text{FW}$).

2.6.2.3 PGM activity

PGM activity was determined according to Fraser et al. (1999) with slight modifications. 20 μl of plant extract was incubated in 780 μl reaction buffer containing 30 mM Tris-HCl, pH7.0, 5 mM MgSO_4 , 20 mM KCl, 0.15 mM NADH, 0.2 mM ATP, 0.1 mM 2,3-bisphosphoglycerate, and 0.5 units phosphoglycerate kinase. The mixture was kept at room temperature for 5 minutes and measured by photometer (Uvikon 922, Kontron instruments, Germany). The measurement was started by adding a mixture of 2 μl of 2-phosphoglycerate solution (100 mM) and 1 unit of glyceraldehyde 3-phosphate dehydrogenase (GAPDH). Enolase activity was determined by calculating the production rate of NAD ($\mu\text{mol min}^{-1} \text{g}^{-1} \text{FW}$).

2.7 Metabolite analysis

2.7.1 Trichloroacetic acid (TCA) extraction

Phosphorylated intermediates and shikimate pathway intermediates were extracted in TCA, according to Jelitto et al. (1992). Plant material was ground to a fine powder in liquid nitrogen. 1.5 ml of 16% (w/v) TCA in diethylether was added to the homogenate. The mixture was kept on dry ice for 15 minutes. Afterwards, 0.8 ml of 16% TCA solution in water with 5 mM EGTA was added to above mixtures. The mixture was further homogenized, and centrifuged for 5 minute at 4°C. The upper phase (water) was transferred to a new tube, and washed 3 times with water-saturated ether. A small volume of 5 M KOH/ 1 M triethanolamine mixture was added to neutralize the TCA extract. The TCA extract was frozen in liquid nitrogen for further assay.

2.7.2 Ethanol extraction

Soluble sugars were determined in an ethanol-water extract, according to Sonnewald et al. (1991). The plants material was incubated in 80% ethanol containing 20 mM HEPES/KOH, pH7.0. After centrifugation, the supernatant was used for the measurement of soluble sugars; the pellet was used for the measurement of starch.

2.7.3 Methanol extraction

Total soluble phenolics and chlorogenate were determined in methanol extract. Leaf material was homogenized in methanol. After centrifugation, the supernatant was transferred to a new reaction tube, and used for the measurement of total soluble phenolic compounds and chlorogenate. After two washes with methanol, the pellet was used for lignin measurement.

2.7.4 Determination of metabolites

2.7.4.1 Glucose, fructose, and sucrose contents

Glucose, fructose, and sucrose were determined according to Sonnewald et al. (1991). 5- 10 μ l of extract was incubated in 300 μ l of 100mM imidazol buffer (pH6.9), containing 5 mM MgCl, 2 mM NAD, 1 mM ATP, 1 unit glucose 6-phosphate dehydrogenase, at room temperature for 5 minutes. Mixture was measured by an Elisa Reader (Tecan Spectra, Germany). 1 unit hexokinase, phosphoglucose isomerase, and fructosidase were added subsequently for glucose, fructose, and sucrose measurements.

2.7.4.2 Starch

After two washes with 80% ethanol, the insoluble debris of ethanol extraction was homogenized in 400 μ l 0.2 N KOH. The homogenate was incubated at 95°C for 1 hour, and neutralized with 70 μ l 1 N acetic acid. Afterwards, 50 μ l supernatant were incubated at 55°C with 50 μ l of amyloglucosidase solution (2 mg ml⁻¹ in 50mM sodium acetate, pH5.2) for 2 hours. Starch content was calculated by measuring the glucose in the mixtures.

2.7.4.3 Chlorophyll

Chlorophyll was measured in ethanol extracts and the concentration was determined as described in Lichtenthaler (1987).

2.7.4.4 Total soluble phenolic compound and lignin

Total soluble phenolic compound was extracted and determined using the Folin-Ciocalteu reagent according published method (Díaz and Merino, 1998). Standard curve was obtained by measuring different concentrations of chlorogenic acid, which is one of the most abundant

phenolic compounds in tobacco. Lignin was extracted and determined according to Campbell and Ellis (1992). Lignin phloroglucinol-HCl staining was carried out according to Redman et al. (1999).

2.7.4.5 Anthocyanin

Anthocyanin content was determined as described in Martin et al. (2002). Plant material was homogenized in liquid nitrogen. Anthocyanin was extracted by 300 μ l methanol containing of 7 % (v/v) hydrochloric acid. Relative anthocyanin concentration was calculated as absorbency (530 nm) minus absorbency (657 nm).

2.7.4.6 PEP and pyruvate

PEP and pyruvate were determined in TCA extracts by using an enzymatic assay. 50 μ l TCA (16%) extract was incubated in 550 μ l reaction buffer containing 50 mM HEPES, pH7.0, 5 mM $MgCl_2$, 0.2 mM NADH and 0.7 mM ADP. The mixture was incubated at room temperature for 5 minutes, and then measured by ZWS-II photometer (Sigma, Germany) with 20 times multiplication. When OD_{334} was stable, start measurement with 1 unit of lactate dehydrogenase and 1 unit of pyruvate kinase to determine pyruvate and PEP, respectively.

2.7.4.7 3-PGA

3-PGA was quantified in TCA extracts by using an enzymatic assay. 50 μ l TCA (16%) extract was incubated in 550 μ l reaction buffer containing 100 mM Tris-HCl, pH8.1, 5 mM $MgCl_2$, 0.2 mM NADH, 1 mM ATP. The mixture was incubated at room temperature for 5 minutes, and then measured by ZWS-II photometer (Sigma, Germany) with 20 times multiplication. The measurement was started by adding 1 unit of phosphoglycerate kinase and 1 unit of glyceraldehyde 3-phosphate dehydrogenase (GAPDH).

2.7.4.8 Enzymatic assay of shikimate and dehydroquininate

Under the catalysis of DHD/SHD enzyme, shikimate and dehydroquininate were determined spectrophotometrically in TCA extract. 50 μ l TCA (16%) extract was incubated in 550 μ l reaction buffer 1 (100 μ M NADP in 100 mM glycine-NaOH buffer, pH9.0), and then measured by ZWS-II photometer (Sigma, Germany) with 20 times multiplication. When OD_{334} was stable, start measurement with 1 μ l DHD/SHD enzyme. Dehydroquininate could also be

measured when the reaction catalyzed by DHD/SHD proceeds in reverse direction. 10 μ l TCA extract was incubated in 590 μ l reaction buffer 2 (100 μ M NADPH in 100 mM HEPES-KOH buffer, pH7.2) at room temperature for 5 minutes, and then measured by ZWS-II photometer, with 10 times multiplication. When OD_{334} was stable, start measurement with 1 μ l of DHD/SHD enzyme. The amount of shikimate or dehydroquinone was determined by calibrating the conversions between NADPH and NADP. The reliability of the extraction and assay of shikimate was checked by adding different amounts of pure shikimate to the plant material (Jelitto et al., 1992)

2.7.4.9 IC-MS assay of the shikimate pathway intermediates

Metabolite profiling was carried out by ion chromatography coupled with mass spectrometry (IC-MS). To measure the concentrations of anions, a Dionex (Idstein, Germany) system was used including a gradient pump, a degasser module, an autosampler and a conductivity detector. Separation of the anionic compounds was carried out using a high capacity ion exchange column (AS11-HC, 250 x 2 mm) connected to a guard column of the same material (AG 11-HC, 10 x 2 mm) and an ATC-1 anion trap column which was placed between the eluents and separation columns to remove the anions present in the solutions. The Gradient was accomplished with purest water (buffer A, Millipore) and 100 mM sodiumhydroxide (Baker, 50 % solution, buffer B). The column was equilibrated with a mixture of buffer A (96 %) and buffer B (4 %) at a flow rate of 0.5 ml per minute and heated at 30°C during the whole measurement. The gradient was produced by changes of the buffer B as follows: 0-8 min at 4 %, 8-28 min at 30 %, 28-38 min at 60 %, 38-51 min at 100 %, 51-54 at 4 % and 54-64 at 4 %. The duration of the run is 64 minutes.

MS analysis was performed using a single quadrupole (MSQ, Dionex) with enhanced low mass option. The following parameters were employed: probe temperature 400 °C, sheath gas nitrogen, capillary voltage 3.5 kV, detection in negative ion mode using cone voltage of 50 V and dwell time of 1 second. Deprotonated ions $[M-H]^-$ were monitored with a span of 1 amu. Single SIM's were performed in small time windows of about 5 min during total run time (64 min), i.e. up to five SIM's are run in parallel at maximum. This allows to minimize parallel monitoring and to enhance sensitivity. The standard of dehydroquinone and dehydroshikimate were kindly provided by Dr. Maro Oldiges, Forschungszentrum, Jülich.

2.7.4.10 Amino acid

Samples were prepared in 80 % ethanol, 20 mM Hepes-KOH, pH 7.5. After incubation for 90 minutes at 80°C and centrifugation at 14000 rpm, supernatant were evaporated to dryness, resuspended in purest water and used for HPLC analysis. Prior to the measurement, primary and secondary amino acids were derivatized using 6-aminoquinolyl-N-hydroxy succinidyl carbonate as a fluorescing substance. Using a reversed phase HPLC system (Fa. Waters) concentrations of various amino acids were determined. The HPLC consists of a gradient pump (600), a degasing module, an autosampler (717) and a fluorescence detector (474). Chromatograms were recorded using the software program Millennium 32. The gradient was accomplished with a buffer A containing 140 mM sodium acetate, pH 5.8 (Suprapur, Merck) and 7 mM triethanolamine (Sigma, Germany). Acetonitril (Roti C Solv HPLC, Roth) and purest HPLC water (Baker) were used as eluents B and C. To separate amino acids, a reversed phase column (AccQ Tag, 3.9 mm x 150 mm) was used which consists of silica as matrix modified by an apolar C18 group. The column was equilibrated with buffer A at a flow rate of 1 ml per minute and heated at 37°C during the whole measurement.

2.7.4.11 Chlorogenic acid

100 mg leaf tissue were homogenized and dissolved in 500 µl of methanol (gradient grade, Sigma-Aldrich, Germany). Subsequently, the sample was mixed and centrifuged at 14000 rpm for 5 minutes. The supernatant was transferred into a new Eppendorf tube. The remaining residue was resuspended in 300 µl of methanol and centrifuged as described above. The washing step was repeated using 200 µl of methanol. The supernatants were pooled and used for the analysis. Prior to the measurement the methanol concentration of the sample was brought up to 20 % using the eluent A (9.5% acetonitrile and 1% acetic acid in water). Using a reversed phase HPLC system (Fa. Waters) the concentration of chlorogenic acid was determined. Chromatograms were recorded using the software program Millennium 32. The gradient was accomplished with a buffer A and a buffer B (100 % acetonitrile). To separate the chlorogenic acid a reversed phase column (Luna 5µ C18(2), 250 x 4.6 mm, Phenomenex Germany) was used. The column was equilibrated with buffer A at a flow rate of 1 ml per minute. Chlorogenic acid was recorded by UV detector at 280 nm.

2.8 Ethanol induction

Plants (42 days old) cultivated in the greenhouse were induced with 100 ml 1% (v/v) ethanol solution via root drenching. Normal watering was resumed after application. Samples for RNA, chlorophyll and protein analysis were taken at various time points. If not otherwise stated, young leaves, being approximately 10 cm at the time point of induction, were followed over the time course of the experiment. For spatial induction, floral organ was enclosed in a 25 cm x 20 cm transparent plastic bag with 3 ml of 4% (v/v) ethanol as described previously by Sweetman et al. (2002). The bag was removed 24 h later and phenotype development was followed daily.

2.9 Floating experiment

Tobacco leaf discs (about 40 mg) were floated on 50 mM HEPES solution (pH7.0) containing 20 mM shikimate at room temperature for 16 hours. As a control, leaf discs were floated on 50 mM HEPES solution without shikimate under the same conditions. Afterwards, leaf discs were washed 3 times with milipore water, dried with filter paper and frozen in liquid nitrogen for further analysis.

2.10 Isolation of chloroplasts

Chloroplasts were isolated from tobacco leaves according to Hajirezaei et al. (2002) with minor modification. All isolation procedures were carried out at 4 °C. Tobacco leaves (5 g) were cut into small pieces and homogenized three times (5 seconds each) in a Waring blender in 40 ml buffer A (25 mM Hepes-NaOH pH 6.8, 330 mM mannitol, 5 mM ascorbate, 1 mM MgCl₂, 1 mM MnCl₂, 5 mM EDTA, 4mM DTT, 25 mM MES and 0.2% (w/v) bovine serum albumin). The homogenate was filtered through four layers of Miracloth. The filtrate was centrifuged for 2 min at 2000 g in a Sorvall SLA 1500 rotor. The supernatant was frozen in liquid nitrogen as soluble proteins from cytoplasm fraction. The pellet was resuspended in 1 ml buffer A. Chloroplasts suspension was mixed with 100 ml buffer A containing 35% (w/v) percoll, and centrifuged for 25 min at 50 000 g in a Beckman L7-55 ultracentrifuge. The chloroplast band was carefully removed from the tube with a pasteur pipette and diluted with 50 ml of buffer A. The suspension was centrifuged for two minutes at 3500 g. The resulting pellet was finally resuspended in 1 ml of buffer B (25 mM Hepes-NaOH pH 6.8, 330 mM mannitol, 25 mM MES) and frozen in liquid nitrogen until further analysis.

3 Results

3.1 Molecular characterization of tobacco DHD/SHD (Nt-DHD/SHD-1)

3.1.1 Cloning a full-length Nt-DHD/SHD-1 cDNA

Bonner and Jensen (1994) isolated a cDNA encoding tobacco DHD/SHD by screening a *Nicotiana tabacum* cDNA expression library with a DHD/SHD specific polyclonal antibody. However, because no translation start codon was identified, this sequence was judged to be incomplete, although the cDNA included the entire coding region for the mature enzyme and 69 upstream nucleotides, which were speculated to encode part of the transit peptide for plastidic targeting. To clone the full-length cDNA encoding tobacco DHD/SHD, a 5'-RACE experiment was performed with the universal primer and DHD/SHD 5'-RACE primer listed in Table 1 (primer 11), based on the published sequence (Genbank: L32794). An approximately 500 bp fragment was amplified, cloned, and sequenced. As far as they overlapped, the sequence of the RACE product was identical to the published sequence. The full-length cDNA was assembled by the software VectorNTI (InforMax, Inc., USA), as shown in Figure 3. This sequence was designated as Nt-DHD/SHD-1 and submitted to Genbank (accession No.: AY578144).

```

1  GGGGGGACTTTTTCAAGCTGGCTGCTGAGCCTACATTTCTGCTGTTTACCCATTTTTGTG
      M E L V V D S G V R K M E G
61  CTCTAAAGTTGGTTGCTAATGGAGTTGGTAGTGGATTTCAGGGGTGAGGAAGATGGAGGGG
      E A M T R N E T L I C A P I M A D T V D
121 GAGGCAATGACGAGGAACGAAACACTAATTTGTGCACCAATCATGGCAGACACAGTGGAT
      Q M L N L M Q K A K I S G A D L V E V R
181 CAAATGTTGAATCTAATGCAAAAGGCTAAAATTAGTGGTGCTGATCTTGTGGAAGTTCGA
      L D S L K S F N P Q S D I D T I I K Q S
241 TTGGATAGCTTGAAAAGCTTTAATCCTCAATCAGATATCGATACTATTATCAAACAGTCC
      P L P T L F T Y R P T W E G G Q Y A G D
301 CCTTTGCCTACCCTTTTCACTTACAGGCCCACTTGGGAAGGGGGTCAGTATGCTGGTGAT
      E V S R L D A L R V A M E L G A D Y I D
361 GAAGTGAGTCGACTGGATGCACTTCGAGTAGCAATGGAGTTGGGAGCTGATTACATTGAT
      V E L K A I D E F N T A L H G N K S A K
421 GTTGAGCTAAAGGCTATTGACGAGTTCAATACTGCTCTACATGGAAATAAATCAGCAAAA
      C K V I V S S H N Y D N T P S S E E L G
481 TGCAAAGTTATTGTTTCTTCTCACAACATGATAATACACCATCATCTGAGGAGCTCGGC
      N L V A R I Q A S G A D I V K F A T T A
541 AATCTAGTAGCAAGAATACAGGCATCTGGAGCTGACATTGTGAAGTTTGCAACAACCTGCA
      L D I M D V A R V F Q I T V H S Q V P I
601 CTGGATATCATGGATGTTGCACGTGTATTCCAAATTACTGTACATTCTCAAGTACCAATA
      I A M V M G E K G L M S R I L C P K F G
661 ATAGCCATGGTCATGGGAGAGAAGGGTTTTGATGTCTCGAATACTTTGTCCAAAATTTGGT
      G Y L T F G T L E V G K V S A P G Q P T
721 GGATACCTCACATTTGGTACTCTTGAAGTGGGAAAGGTTTCGGCTCCTGGGCAACCAACA
      I K D L L N I Y N F R Q L G P D T R I F
781 ATTAAAGATCTTTTGAATATATACAATTTTCAGACAGTTGGGACCAGATACCAGAATATTT

```

```

      G I I G K P V S H S K S P L L Y N E A F
841  GGCATTATCGGGAAGCCTGTTAGCCATAGCAAATCACCTTTATTGTATAATGAAGCTTTC
      R S V G F N G V Y M P L L V D D V A N F
901  AGATCAGTTGGGTTTAATGGTGTTTATATGCCTTTGCTGGTTGATGATGTTGCAAATTTTC
      F R T Y S S L D F A G S A V T I P H K E
961  TTTCCGACTTACTCATCTTTAGATTTTGGCTGGCTCAGCTGTAACAATTCTCACAAGGAA
      A I V D C C D E L N P T A K V I G A V N
1021 GCCATTGTTGACTGCTGTGATGAGTTGAATCCTACCGCTAAAGTAATAGGGGCTGTCAAT
      C V V S R L D G K L F G C N T D Y V G A
1081 TGTGCTGTAAGCCGACTCGATGGGAAGTTGTTGGTTGCAATACAGACTATGTGGGTGCA
      I S A I E E A L Q G S Q P S M S G S P L
1141 ATCTCCGCCATTGAAGAAGCGTTGCAAGGCTCACAGCCTAGTATGTCTGGGTCTCCCTTA
      A G K L F V V I G A G G A G K A L A Y G
1201 GCTGGTAAATTATTTGTGGTCATTGGTGCTGGTGCGCTGGCAAGGCCTTGCTTATGGT
      A K E K G A R V V I A N R T Y E R A R E
1261 GCAAAGGAAAAGGGGGCTCGGGTGGTGATTGCTAACCGTACCTATGAACGAGCGAGAGAA
      L A D V V G G Q A L S L D E L S N F H P
1321 CTTGCTGATGTAGTTGGAGGTCAGGCTTTGTCTCTTGACGAGCTTAGCAATTTCCATCCA
      E N D M I L A N T T S I G M Q P K V D D
1381 GAAAATGACATGATTCTTGCAAATACCACCTCCATTGGCATGCAACCAAAGGTTGATGAT
      T P I F K E A L R Y Y S L V F D A V Y T
1441 ACACCAATCTTTAAGGAAGCTTTGAGGTACTACTCACTTGTATTTGATGCTGTTTATACG
      P K I T R L L R E A H E S G V K I V T G
1501 CCCAAAATCACTAGACTCTTGCGGGAAGCTCACGAGAGTGGAGTAAAAAATTGTAACAGGA
      V E M F I G Q A Y E Q Y E R F T G L A S
1561 GTTGAAATGTTTATCGGCCAGGCATATGAACAATATGAGAGATTTACAGGGCTTGCCAGC
      S K G T F Q E N Y G W I L R A R S L S L
1621 TCCAAAGGAACTTTTCAAGAAAATTATGGCTGGATATTGAGAGCAAGGCTCTTTCCCTT
      F N A A L L V T F P P K S L H S C V I A
1681 TTCAATGCGGCCCTGCTAGTTACTTTTCTCCTAAATCCCTACATAGTTGTGTGATAGCA
      M V L D S S A L P F V L R R N *
1741 ATGGTCTTAGATTCCTCTGCCCTACCATTTGTGCTTCGGAGGAATTAATTCGTTCCAGGT
1801 AAATCGTGATTTTCACCAAAACAAATTCCTTGAGGATGTTTCAGGAAGGCAGTCAGACATAC
1861 CAGTGGACAATCGCCGTCATTCTGGCTTATATTAGACTCTTGTAGCACTTCATTCTTTGA
1921 CAACTATGGTATCTCTAATTGTGCTTTTCATTAAACACAGATGTATCAGTGTTCCTCATTG
1981 TGACCCCATACTTGAATTCCTCTTGATTATCATTATTATTAAATCTTGTACATTATTG
2041 TATGATTTGTATCAAAAAAAAAA

```

Figure 3. Nucleotide and deduced amino acid sequence of Nt-DHD/SHD-1 from *Nicotiana tabacum*. The translation start codon is underlined.

The first full-length DHD/SHD cDNA was isolated from tomato by Bischoff et al (2001). The deduced amino acid sequence revealed that tomato DHD/SHD is most likely synthesized as a precursor with a very short (13 amino acids) plastid-specific transit peptide. Although the N terminus of the deduced amino acid sequence of tomato DHD/SHD did not exhibit the typical feature of transit peptides (Keegstra et al., 1989), sub-cellular localization studies indicated that DHD/SHD was localized in plastids.

3.1.2 Expressing Nt-DHD/SHD-1 in *E. coli*

For biochemical characterization of the Nt-DHD/SHD-1 protein, the cDNA encoding the predicted mature protein was PCR amplified and cloned into the *E. coli* expression vector pQE

(see materials and methods). Expression of the 6xHis tagged Nt-DHD/SHD-1 mature protein (60 kDa) was induced and purified under native conditions by a metal-chelated affinity chromatography (Ni-NTA, Qiagen). This procedure allowed the preparation of large amounts of soluble protein with high purity (>90%), as shown in Figure 4A.

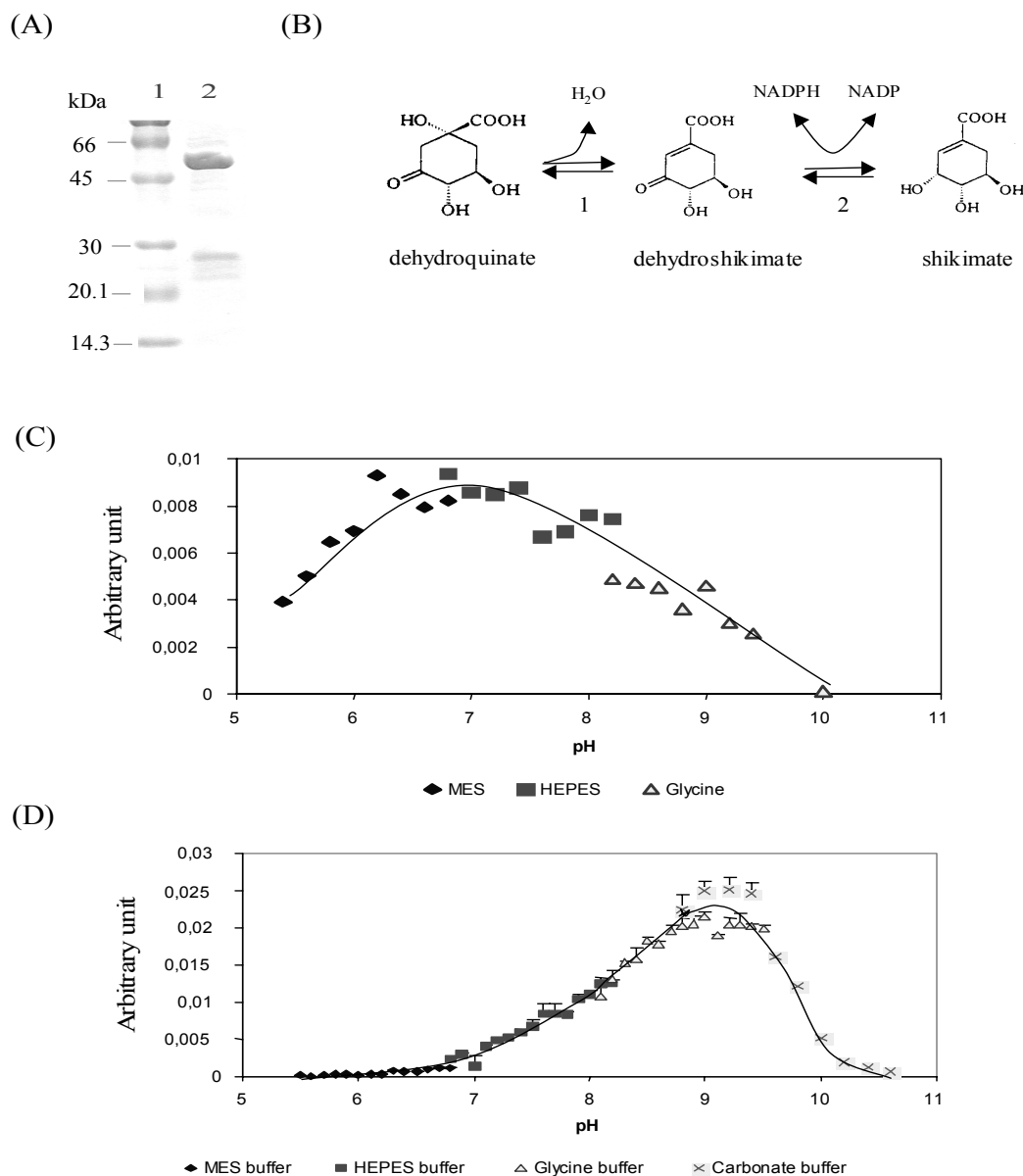


Figure 4. Overproduction of the Nt-DHD/SHD-1 mature protein in *E.coli* and characterization of enzyme properties. (A), Nt-DHD/SHD-1 mature protein was induced and purified with metal affinity resin Ni-NTA, under native conditions. Lane 1: molecular weight marker; lane 2: purified DHD/SHD mature protein (60 kDa). (B), Reactions catalyzed by 3-dehydroquininate dehydratase (DHD) domain (1) and shikimate dehydrogenase (SHD) domain (2). (C), Optimum reaction buffer and pH of anabolic reaction catalyzed by Nt-DHD/SHD-1 were evaluated by plotting reaction velocity under different reaction buffers and pH (100 mM MES buffer, pH 5.4-6.8; 100 mM HEPEPS buffer, pH 6.8-8.2; and 100 mM glycine buffer, pH 8.2-10.0). (D), Optimum reaction buffer and

pH of catabolic reactions catalyzed by DHD/SHD were investigated by plotting reaction velocity under different reaction buffers and pH (100 mM MES buffer, pH 5.4-6.8; 100 mM HEPEPS buffer, pH 6.8-8.2; 100 mM glycine buffer, pH 8.2-10.0; and 100 mM carbonate buffer, pH8.8-10.6).

3.1.3 Kinetic properties of Nt-DHD/SHD-1

To investigate enzymatic properties of Nt-DHD/SHD-1, several analyses have been performed. Enzyme pH preference was determined in both the forward and reverse reaction (Figure 4C, 5D) in different buffer systems. The optimum pH for the anabolic reaction (from dehydroquininate to shikimate) was between 6.8 and 7.2. For the catabolic reaction, a higher pH optimum was determined. The reaction velocity reached a maximum at pH 9-9.4. This indicates that under normal physiological pH conditions (pH6.8 to pH8.2) (Hauser et al., 1995), the anabolic reaction is most likely predominant.

The effect of temperature on the DHD/SHD-catalyzed reaction was determined for both the forward and reverse reactions. The velocity of DHD/SHD catalyzed reaction rose linearly from 5°C to 30°C, reached maximum value at 30°C, and kept this value up to 45°C. Afterwards, the reaction velocity dropped rapidly as a result of the deactivation of the protein (data not shown). Thus the optimum temperature for DHD/SHD was determined to be 30°C.

DHD/SHD catalyzes two neighbouring reversible reactions. Limited by the detection of dehydroshikimate, only the shikimate-NADP and dehydroquininate-NADPH pairs could be employed to determine the kinetic properties of Nt-DHD/SHD-1. The SHD domain, which catalyzed the oxidation of shikimate to dehydroshikimate, exhibited typical Michaelis-Menten kinetics. The K_m value for shikimate was $130 \pm 15 \mu\text{M}$ (Figure 5A). This value was determined from a reciprocal $1/v-1/S$ curve, when NADP served as constant and shikimate served as variable substrate in glycine-NaOH, pH 9 buffer. The K_m value for NADP was determined to be $31 \pm 7 \mu\text{M}$, when NADP served as constant and shikimate served as variable substrate in the same reaction buffer (Figure 5B).

When dehydroquininate and NADPH was applied to the reaction, dehydroquininate was first dehydrated to dehydroshikimate, and then reduced to shikimate. Only the second step of the reaction can be monitored to predict the reaction velocity. The ratio of the turnover number for DHD to SHD is about 1:10 (Fiedler and Schultz, 1985), suggesting that the overall velocity was limited by the first reaction.

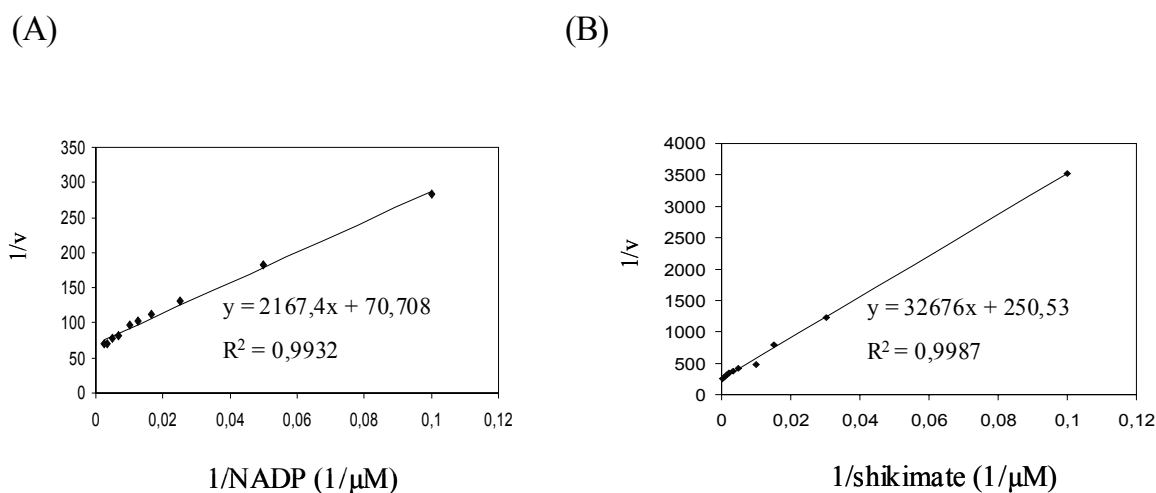


Figure 5. Determination of the apparent K_m value for SHD of DHD/SHD enzyme to its substrates. Apparent K_m values were obtained by double reciprocal plots of the initial velocities of SHD with NADP (A) and shikimate (B) as the variable substrate. These experiments were replicated three times.

Moreover, dehydroquinate is a substrate of the first reaction, whereas NADPH is a product of the second reaction. For both reasons, the reciprocal $1/v-1/S$ curves to dehydroquinate-NADPH pair did not exhibit Michaelis-Menten kinetics.

3.1.4 A novel enzymatic assay for shikimate and dehydroquinate

Shikimate is an important intermediate of the shikimate pathway. In glyphosate-treated plants, high levels of shikimate accumulate. The abundance of shikimate is a measure for the inhibition of EPSPS in plants (Pline et al., 2002). A novel enzymatic assay to measure the shikimate content in plants (see the materials and methods section) was developed by measuring the conversion of NADP to NADPH in the presence of DHD/SHD. To evaluate the accuracy of the enzymatic assay, the standard curve with known concentrations of shikimate was plotted (Figure 6). Linear equation for enzymatic assay was $y = 1.0504 x + 0,1974$ ($R^2 = 0,9993$), whereas the predicted equation was $y = 1 x$. The slope of the supplemented *vs.* observed shikimate $\mu\text{g ml}^{-1}$ from samples was 1.0504, indicating a high correlation between the expected and the measured shikimate. The detection limit was 1 nmol ml^{-1} shikimate. Because DHD/SHD enzyme catalyzes a reversible reaction, dehydroquinate / dehydroshikimate can also be quantified in the same samples when the reaction proceeds in the reverse direction. However, the bi-functional nature of the plant enzyme does not allow separating dehydroshikimate from dehydroquinate.

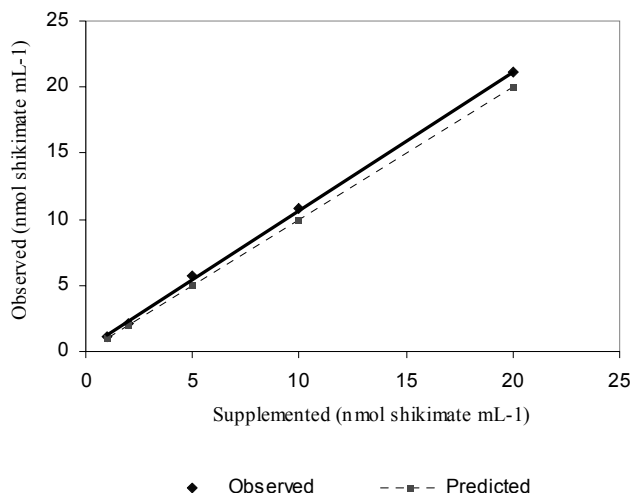


Figure 6. Reliability of the enzymatic assay. The reliability of the enzymatic assay was evaluated by the recovery efficiency of known amounts of shikimate. Predicted vs. observed recovery of shikimate (nmol shikimate mL⁻¹) is plotted. Linear equation for enzyme method is as follows: $y = 1,0504x + 0,1974$, ($R^2 = 0,9993$), predicted: $y=x$.

3.2 Constitutive silencing of Nt-DHD/SHD-1 in transgenic tobacco

3.2.1 Plasmid construction and plant transformation

RNA interference (RNAi) is a powerful tool for the investigation of gene function by silencing the expression of endogenous genes (Fire et al., 1998). To achieve an efficient silencing of DHD/SHD, a double stranded RNA (dsRNA) cassette was constructed. The partial coding region of the tobacco Nt-DHD/SHD-1, ranging from 768 nt to 1320 nt (GenBank: AY578144) was amplified by PCR, using the gene specific primers in Table 1 (primer 1, 2). PCR product was cloned into the vector pUC-RNAi, in sense and antisense orientation separated by the first intron of the GA20 oxidase gene from *Solanum tuberosum* (Chen et al. 2003). Subsequently, the hairpin cassette was inserted into the vector pBinAR, between the CaMV 35S promoter and the *ocs* terminator, yielding pBin-DHD/SHD-RNAi (Figure 7). The binary vector was transformed into *Agrobacterium tumefaciens* strain C58C1 (pGV2260). Following *Agrobacterium* mediated gene transfer, 80 kanamycin-resistant tobacco plantlets were selected for further analysis and transferred to the greenhouse.

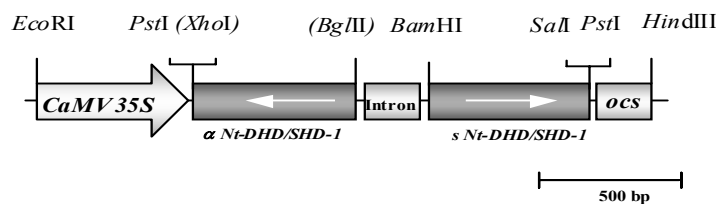


Figure 7. Schematic drawing of pBin-DHD/SHD-RNAi. pBin-DHD/SHD-RNAi was created by inserting the fragment DHD/SHD-RNAi, which comprises the reversed replication of DHD/SHD fragments (553 bp, nts 768 to 1320 of Nt-DHD/SHD-1 cDNA; accession no. AY578144) and the spacer GA20, into binary vector pBinAR between 35S promoter and *ocs* terminator.

3.2.2 Screening the transgenic plants

DHD/SHD-RNAi primary transformants were screened by Northern blot hybridization. 14 out of 80 transformants showed decreased levels of transcripts (data not shown). Depletion of DHD/SHD was further confirmed by enzyme activity measurements. 6 independent transgenic lines with 16 – 87 % remaining DHD/SHD activity was selected for detailed analysis in the T1 generation (Figure 8).

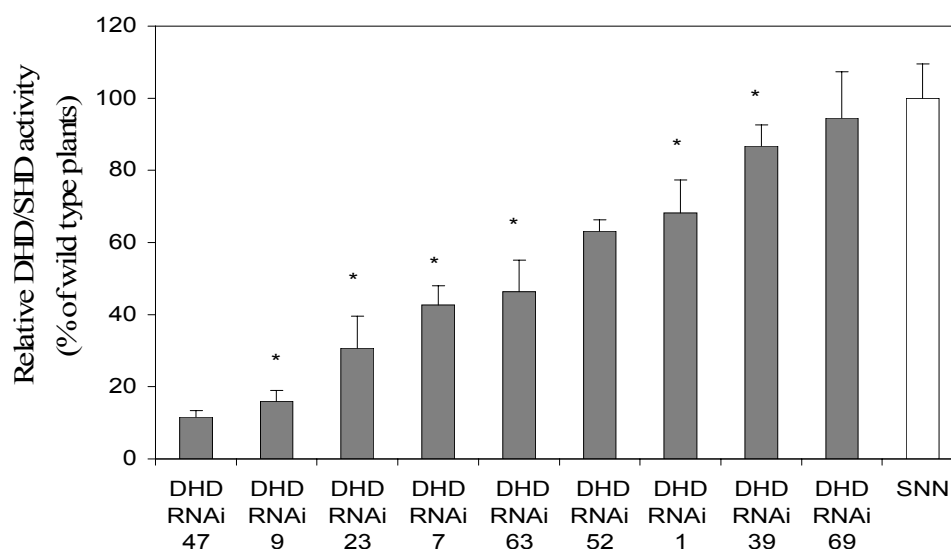


Figure 8. DHD/SHD activity in DHD/SHD-RNAi plants from the T0 generation. DHD/SHD activity in each of the T0 transgenic lines was related to the activity of wild type plants (SNN). DHD/SHD activity in wild type plants was calculated to be $46 \pm 5.6 \mu\text{mol shikimate m}^{-2} \text{ *min}^{-1}$. Transgenic plants marked with an asterisk were selected to produce progenies. Enzyme activity was measured in leaf materials of 6-week old plants. Data are given as the mean of 4 replicates of each independent transgenic plants \pm SE.

Based on enzyme activity, DHD/SHD RNAi plants from the T1 generation were classified into 4 groups, high (H, DHD/SHD activity 85-60%); middle (M, DHD/SHD activity 60-40%); low (L, DHD/SHD activity 40-20%) and very low (VL, DHD/SHD activity 20-5 %) (Figure 9).

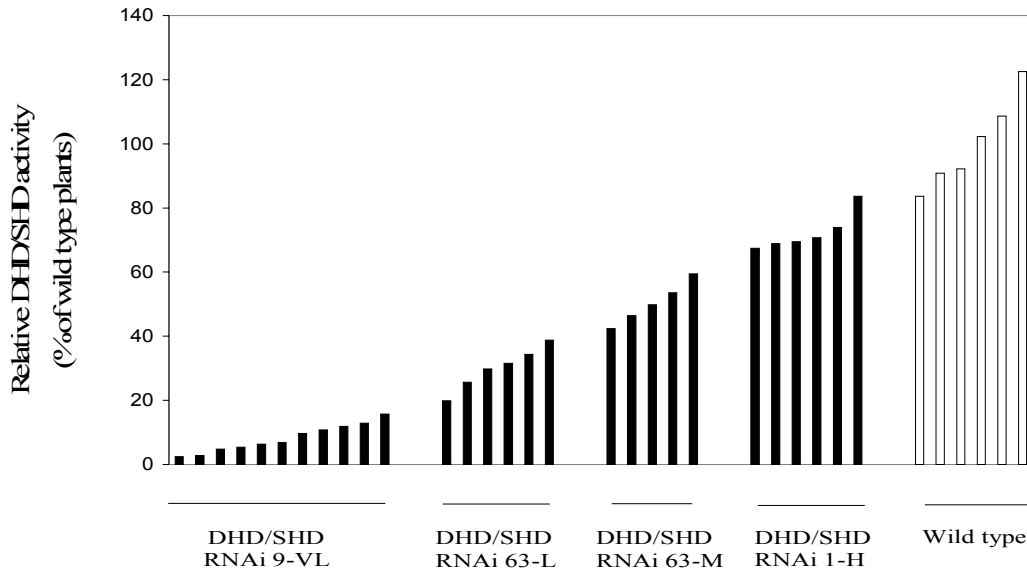


Figure 9. DHD/SHD activity in T1 offspring of DHD/SHD RNAi plants. Based on enzyme activity, T1 progenies of selected transgenic plants were categorized into 4 ranks: high (H), medium (M), low (L) and very low (VL). Enzyme activity was measured in leaf materials of the 6-week old plants in the greenhouse.

3.2.3 Growth characteristics of DHD/SHD RNAi plants

Silencing of DHD/SHD led to dramatic phenotypical changes of the transgenic plants. A 40-60% reduction of DHD/SHD activity (DHD/SHD-RNAi-M plants) led to chlorotic leaves. Bleached areas developed in intercostal regions of mature leaves. A further reduction (60-80%) resulted in a dwarfed phenotype. When DHD/SHD activity dropped below 20% of wild type, transgenic plants (DHD/SHD RNAi-VL series) stopped growth and frequently died in one to two weeks after transfer from tissue culture to the greenhouse (Figure 10).

To correlate the reduction of DHD/SHD activity with the biomass production, DHD/SHD-RNAi plants (T1 generation) were germinated in sand and fertilised with nutrient solution, as described in Geiger et al. (1999). Growth parameters were acquired by measuring the fresh weight (FW), the dry weight (DW) and the plant height.

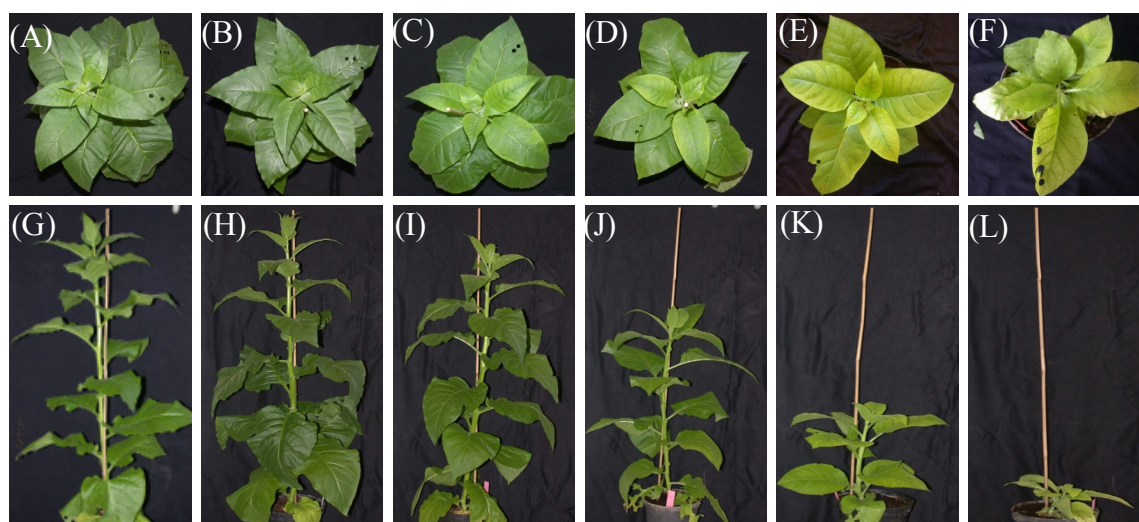


Figure 10. Impact of reduced DHD/SHD expression on plant growth and leaf morphology. (A), (B), (G) and (H) are wild type plants; (C) and (I) are DHD/SHD RNAi 1-H. (D) and (J) are DHD/SHD RNAi 63-M; (E) and (K) are DHD/SHD RNAi 63-L; (f) and (l) are DHD/SHD RNAi 9-VL.

An up to 40% reduction of DHD/SHD (DHD/SHD 1-H) did not result in growth retardation. Whereas 40% to 60% reduction of enzyme activity (DHD/SHD 63-M) led to 33% reduction of fresh weight, 42% reduction of dry weight, and 37% reduction of plant height, respectively. In plants with 20% or lower DHD/SHD activity (DHD/SHD 9-VL), the growth parameters dropped even further, to 7% (fresh weight and dry weight), and 36% (plant height) as compared to wild type plants (Table 2). These results indicated that the loss of DHD/SHD activity led to a paralleled reduction in biomass of transgenic plants.

Table 2. Growth parameters of DHD/SHD RNAi plants

	Plant height (cm)	Shoot FW (g)	Shoot DW (g)	FW/DW
DHD/SHD 1-H	12.9±2.3	6.32±1.46	0.34±0.10	18.59
DHD/SHD 63-M	8.6±2.1	4.83±0.67	0.24±0.07	20.13
DHD/SHD 63-L	7.2±1.7	1.79±0.19	0.10±0.05	17.9
DHD/SHD 9-VL	4.9±1.2	0.50±0.083	0.03±0.01	16.67
Wild type	13.5±2.6	7.13±1.24	0.41±0.18	17.39

Growth parameters were determined in 6-week old plants in greenhouse Results are mean of 6 wild type plants and 6 T1 progenies of each independent transgenic lines ± SE.

3.2.4 Transcript analysis

To study whether the reduction of DHD/SHD would influence the expression of other shikimate pathway genes, the transcripts of DAHPS, dehydroquinase synthase, shikimate kinase, EPSPS and chorismate synthase were probed by Northern blot hybridization in both transgenic and control plants as demonstrated in Figure 11. Silencing of DHD/SHD did not affect expression of downstream genes and the adjacent upstream gene, dehydroquinase synthase. DAHPS was the only gene to be regulated on the transcriptional level. The transcripts of DAHPS increased up to 4 times in DHD/SHD-VL plants.

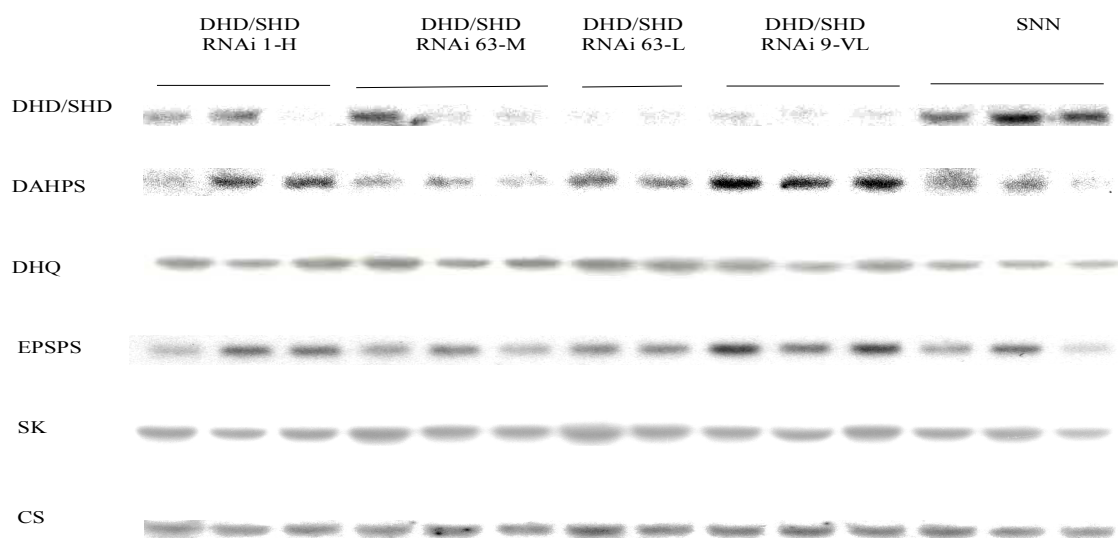


Figure 11. Influence of reduced DHD/SHD on transcription level of genes involved in the shikimate pathway. 30 μ g total RNA was prepared from tobacco source leaves, which was cultivated in greenhouse for 6 weeks. RNA was separated on a 1.5% agarose gel, blotted and hybridized using the indicated shikimate pathway probes, which were labelled with 32 P-dCTP. DAHPS: 3-deoxy-D-arabino-heptulosonate-7-phosphate synthase; DHQS: dehydroquinase synthase, SK: shikimate kinase, CS: chorismate synthase.

3.2.5 cDNA macroarray analysis

Macroarray technology provides a means of measuring the expression of hundreds of genes simultaneously. This technique brings new perspectives for the study of expression networks and their regulation, potentially providing valuable insights into the molecular mechanisms underlying the regulation of metabolism (Schulze and Downward, 2001). The shikimate pathway links primary metabolism and secondary metabolism. To investigate whether the silencing of DHD/SHD would influence the expression of other genes involved in primary and

secondary metabolism, a cDNA macroarray analysis was performed on DHD/SHD-RNAi plants. All cDNA probes were PCR amplified from our construct collections, using M13 forward and reverse sequencing primers (Table 1, primer 14,15) for pUC 8/9, pBluescript, pCRscript and pCRblunt cloning vectors. PCR products were purified by gel extraction kit (Qiagen), and quantified by measuring the absorbance at 260nm. A total of 94 cDNA probes (50 nanogram each) of primary metabolism (photosynthesis, the Calvin cycle, glycolysis and sugar biosynthesis), secondary metabolism (shikimate pathway and phenylpropanoids pathway), nitrogen metabolism and phosphate metabolism were blotted onto nylon membranes with two duplicates, according to the published procedures (Domachowske et al., 2001) (Table 3). Hybridization signals were quantified and analyzed by the software BioArray Software Environment (BASE), as shown in Figure 12.

Table 3. cDNA probes used for cDNA macroarray analysis

Probes	Genes	Function	Probe	Genes	Function
1	CAB SNN	Photosynthesis	48	Flavonol synthase	Phenylpropanoids
2	FNR Tobacco	Photosynthesis	49	Cinnamyl alcohol dehydrogenase	Phenylpropanoids
3	PSJ-G homolog	Photosynthesis	50	PAL	Phenylpropanoids
4	PSJ-D homolog	Photosynthesis	51	PFP beta SU	Glycolysis
5	33 KDA(49)	Photosynthesis	52	PFP alpha SU	Glycolysis
6	Chl. FBpase	The Calvin cycle	53	cy aldolase	Glycolysis
7	PPT	The Calvin cycle	54	GAP-8	Glycolysis
8	GAP-A	The Calvin cycle	55	TPI-7	Glycolysis
9	TPT	The Calvin cycle	56	M1-1	Energy
10	TPI-7	The Calvin cycle	57	ANT	Energy
11	Rubisco	The Calvin cycle	58	ATPase B	Energy
12	Rcase	The Calvin cycle	59	Lipid oxylase	Lipid
13	ppT8.3	The Calvin cycle	60	Potato ppase	Phosphate metabolism
14	PPT10.1	The Calvin cycle	61	STPT-1	Phosphate metabolism
15	INV-19	Sugar	62	STPT-2	Phosphate metabolism
16	cy FBP1	Sugar	63	Nitrat-transporter	Nitrogen assimilation
17	apo Inv potato	Sugar	64	22 KD protein	storage & breakdown
18	pl-GTP	Sugar	65	Ubiquitin-c-terminal hydrolase	storage & breakdown
19	PGI	Sugar	66	CYSP homolog	storage & breakdown

20	Malat-dehydrogenase	Sugar	67	ACC oxidase	Plant hormon
21	cyt INV INH	Sugar	68	ACC synthase	Plant hormon
22	apo INV INH	Sugar	69	Alcohol DH	Alcohol
23	HK10	Sugar	70	Klon 247 EF hand	Signal transduction
24	M.t sugar transporter	Sugar	71	ntcdpk 19	Signal transduction
25	NAD-MDH	Sugar	72	proline phosphatase 2c	Signal transduction
26	AGPase S9-D	Starch	73	TVP-5 3' spezifisch	Tonoplast
27	GBSS	Starch	74	TVP-9 3' spezifisch	Tonoplast
28	Alpha-amylase	Starch	75	TVP-31 3' spezifisch	Tonoplast
29	Beta-amylase	Starch	76	TIP 31	Tonoplast
30	Atase 1	Nucleotide	77	EA synthase	Defense
31	CAR B 6/2	Nucleotide	78	SAR 8.2	Defense
32	GMP6	Nucleotide	79	sr. Chitinase(PRQ)	Defense
33	ASL 3	Nucleotide	80	PR 1b	Defense
34	PRPP-synthetase	Nucleotide	81	B2 (PCR-pto)	Defense
35	DAHPS-1	Shikimate pathway	82	XGT 1/1 xyloglucan-transferase	Cell wall
36	DAHPS-2	Shikimate pathway	83	pGRP 10	Others
37	DAHPS-3	Shikimate pathway	84	Klon 118	Others
38	DHD/SHD	Shikimate pathway	85	Klon 130	Others
39	EPSPs	Shikimate pathway	86	Klon 139	Others
40	Shikimate Kinase	Shikimate pathway	87	1310b	Others
41	Chorismate synthase	Shikimate pathway	88	2547a	Others
42	Chorismate synthase	Shikimate pathway	89	OR	Others
43	Chorismate mutase	Shikimate pathway	90	ENPL	Others
44	DHQ synthase	Shikimate pathway	91	Metallothioein like protein	Others
45	Chalcone synthase	Phenylpropanoids	92	NADH ubichinon	Others
46	4-Coumarate: CoA ligase	Phenylpropanoids	93	33KDA(49)	Others
47	Dihydroflavonol-4-reductase	Phenylpropanoids	94	SNT	Others

50 micrograms of total RNA from DHD/SHD RNAi-VL plants and wild-type plants was labelled with trace amounts of ^{33}P -dCTP in a cDNA synthesis reaction, using an oligo d(T)₂₅ as primer. The labelled cDNA were hybridized to the membranes overnight at 65°C. Following stringent washing, signals were scanned by BAS 2000 Bio-Imaging Analyser (Fujifilm) (Figure 12)

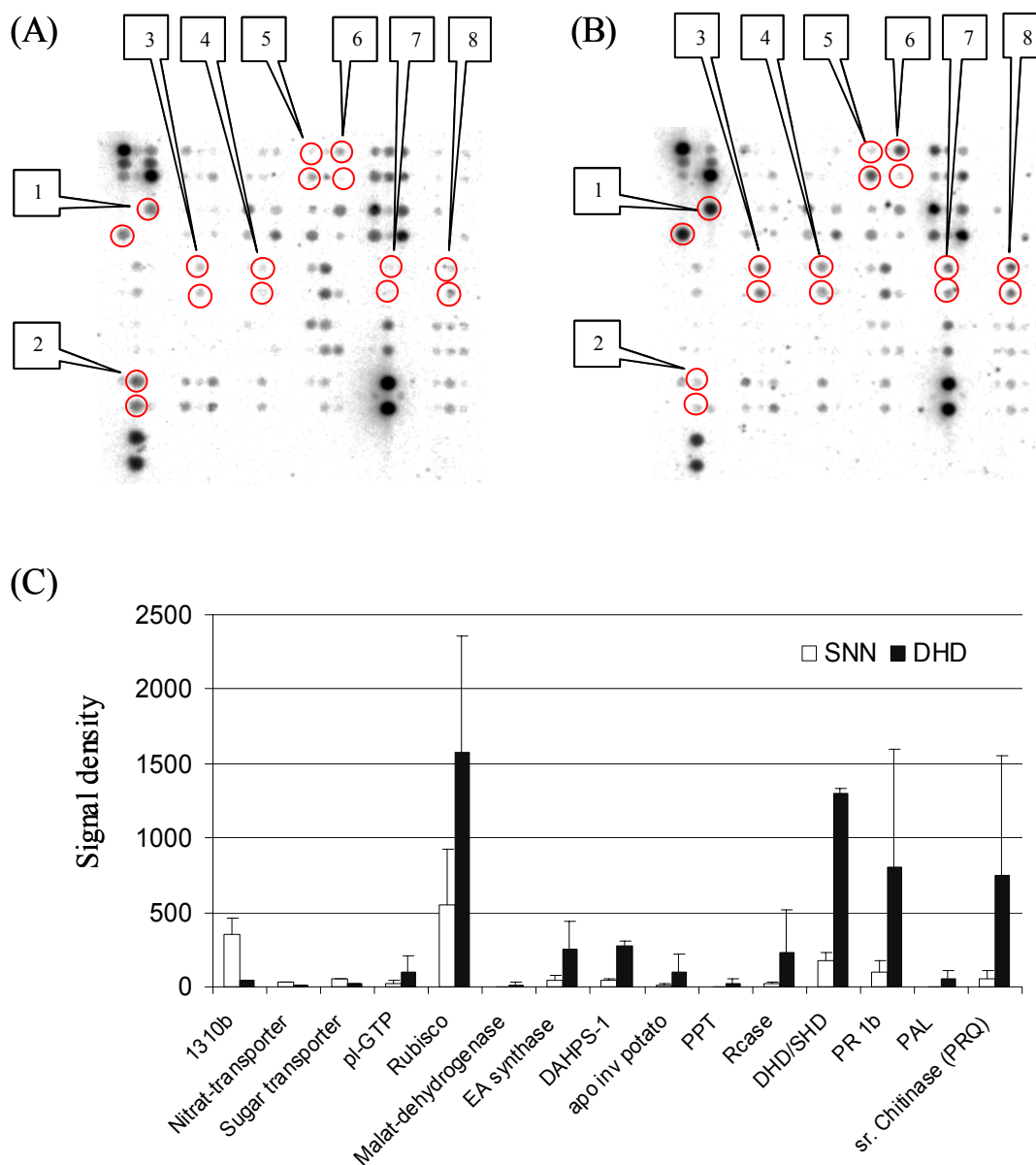


Figure 12. Hybridization signals and quantification of signal density of cDNA macroarray analysis. Probe 1, DHD/SHD; probe 2, 1310b; probe 3, apo invertase; probe 4, EA synthase; probe 5, PAL; probe 6, DAHPS; probe 7, Rubisco; probe 8, sr. Chitinase (PRQ). (A), Hybridization signals of the wild type plants. (B), Hybridization signals of DHD/SHD RNAi plants. (C), Signal density of cDNA macroarray. Hybridization signals were scanned and analyzed by the software BASE. Total RNA was prepared from leaf material of 6-week old plants in the greenhouse. Data are given by the mean of 4 replicates \pm SE.

Silencing of DHD/SHD activated genes involved in secondary metabolism, such as PAL and PPT, and genes involved in defence reactions, such as pathogenesis-related protein (PR1b) and chitinase (PRQ). The silencing of DHD/SHD did not affect expression of other shikimate pathway genes except DAHPS, whose transcripts increased by 3.56 times compared to wild

type plants. This result is in good agreement with the results obtained by Northern blot hybridization (Figure 11).

3.2.6 Inhibition of DHD/SHD leads to reduced chlorogenate and lignin content

To determine the effect of DHD/SHD silencing on secondary metabolism, chlorogenate and lignin were determined in transgenic plants. In plants with more than 60% DHD/SHD activity (DHD/SHD 1-H), a slight decrease of chlorogenate and lignin was measured with values of 96% and 93% of wild type plants, respectively.

A 40% to 60% reduction of DHD/SHD activity led to a remarkable reduction of the aromatic compounds, in which the lignin dropped 37%. More than 80% reduction of DHD/SHD activity led to 57% reduction of chlorogenate and 63% reduction of lignin (Figure 13).

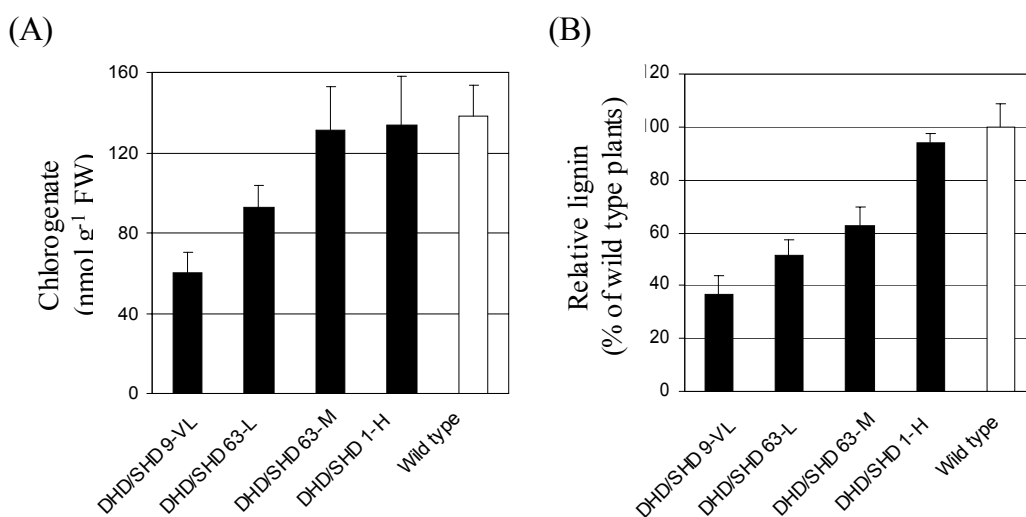


Figure 13. Chlorogenate, and lignin content in DHD/SHD RNAi plants. (A), Chlorogenate content. (B), Relative content of lignin. Metabolites were measured in leaf materials of 6-week old plants. Data are given as the mean of 4 replicates of each independent transgenic plants \pm SE.

To visualize lignin in transgenic plants, leaf material was stained by the phloroglucinol-HCl method (Redman et al., 1999). Tobacco petioles (6 weeks old) were decolorized in 70% (v/v) ethanol for 6 to 8 h, washed with distilled water, and sliced by scalpel. The slices were stained in 1% (w/v) phloroglucinol (Sigma) for 1 to 2 hours. Afterwards, the slices were then exposed to 6 M HCl until a red colour developed. Vascular tissues in petioles of wild type plants were stained to brilliant red, indicating high concentrations of phenolic compounds and lignin; whereas in DHD/SHD silenced plants, vascular tissue in petioles was only slightly stained to

pale red, suggesting that less amounts of phenolic compounds and lignin accumulates in the transgenic plants (Figure 14). The measurement of chlorogenate and lignin indicated that the inhibition of the shikimate pathway led to a strong decrease in phenolic compounds production.

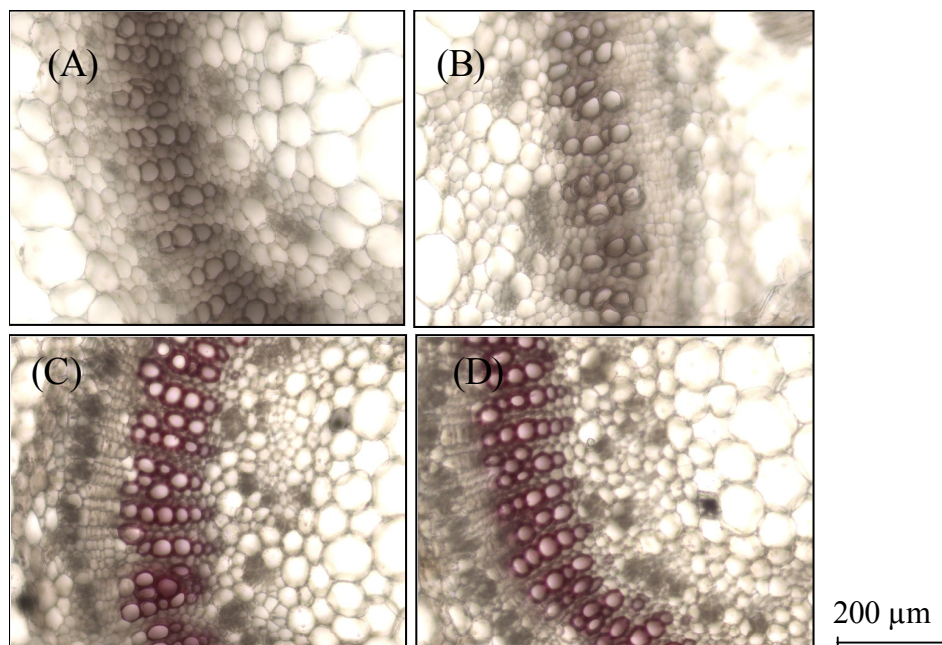


Figure 14. Histochemical detection of lignin in petiole cross-section of tobacco plants with reduced activity of DHD/SHD. (A), (B), Cross-section of petioles of DHD/SHD RNAi 63-L and DHD/SHD RNAi 9-VL mature leaves, respectively. (C), (D), Cross-section of petioles of wild type plants.

3.2.7 Carbohydrates and chlorophyll content in DHD/SHD RNAi plants

The shikimate pathway links primary and secondary metabolisms. Under normal growth conditions about 20% of fixed carbon is directed towards the shikimate pathway, which subsequently leads to the accumulation of secondary metabolites (Haslam, 1993). To determine the effect of blockage of the shikimate pathway on primary metabolism, carbohydrate and chlorophyll contents in DHD/SHD inhibited plants were measured. Similar amounts of carbohydrates were detected in all DHD/SHD RNAi plants when compared to wild type (Table 4). This result suggests that the inhibition of DHD/SHD had no effect on primary metabolism. As mentioned above, leaves of DHD/SHD RNAi plants exhibited a bleached phenotype. Therefore the chlorophyll content was investigated in leaves of transgenic plants. As shown in Table 4, progressive decreases of chlorophyll content were observed in DHD/SHD RNAi plants.

Table 4. Influence of decreased DHD/SHD activity on the content of carbohydrates and chlorophyll in tobacco plants

	Glucose ($\mu\text{mol g}^{-1}$ FW)	Fructose ($\mu\text{mol g}^{-1}$ FW)	Sucrose ($\mu\text{mol g}^{-1}$ FW)	Chlorophyll (mg m^{-2})
DHD/SHD 9-VL	4.51 \pm 1.10	2.05 \pm 0.47	13.28 \pm 4.13	95.62 \pm 24.10
DHD/SHD 63-L	4.61 \pm 0.91	2.42 \pm 1.08	13.06 \pm 2.23	179.24 \pm 45.81
DHD/SHD 63-M	3.79 \pm 1.24	1.93 \pm 0.40	13.66 \pm 2.05	212.09 \pm 38.69
DHD/SHD 1-H	4.66 \pm 1.05	2.20 \pm 0.75	14.21 \pm 3.17	252.30 \pm 15.00
SNN	4.55 \pm 0.79	2.22 \pm 0.36	14.17 \pm 2.11	262.26 \pm 17.49

Carbohydrates and chlorophyll were measured in leaf materials of 6-week old plants. Each value represents the mean of 6 different plants \pm SE.

3.2.8 Silencing of DHD/SHD leads to an accumulation of the pathway intermediates

It can be expected that silencing of DHD/SHD enzyme might disturb the balance between the substrate and product of this enzyme in transgenic plants. Therefore, dehydroquinate and shikimate contents were determined in leaf extract using an enzymatic assay. In plants with less than 50% of DHD/SHD activity, considerable amount of dehydroquinate accumulated (Figure 15A). In wild type plants and DHD/SHD RNAi plants with more than 50 % DHD/SHD activity, no dehydroquinate could be detected. Whereas in plants with less than 50% residual DHD/SHD activity, 2 to 10 μmol of dehydroquinate were measured in 1 gram leaf material (fresh weight). The accumulation of dehydroquinate in these plants correlated with the reduction of DHD/SHD activity. In transgenic line DHD/SHD 9-VL, the accumulation of dehydroquinate was as high as 9 $\mu\text{mol g}^{-1}$ FW. This level of accumulation is comparable to that of total sugars.

Unexpectedly, shikimate, the product of DHD/SHD was also accumulated in DHD/SHD silenced plants with 60% or less DHD/SHD residual activities. The accumulations of this pathway intermediate were paralleled with the accumulation of dehydroquinate in the transgenic plants. In plants with more than 60% DHD/SHD activity, neither dehydroquinate nor shikimate accumulated. In plants with less than 50% residual DHD/SHD activity, 3.5 to 8 times higher shikimate were detected (Figure 15B).

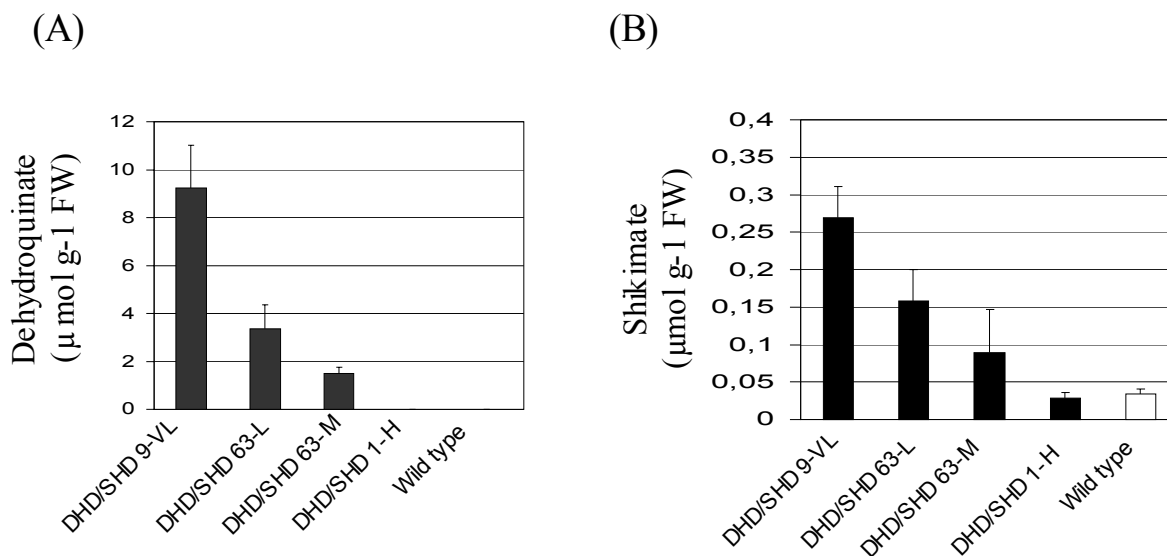


Figure 15. Dehydroquininate and shikimate accumulation in DHD/SHD RNAi plants. Shikimate and dehydroquininate were determined in transgenic plants by an enzymatic assay (see materials and methods section). (A), Dehydroquininate. (B), Shikimate. Metabolites were extracted from tobacco source leaves (6-weeks old) using a TCA method. Data are given as the mean of 4 replicates of each independent transgenic plants \pm SE.

3.2.9 Shikimate feeding experiment

One possible explanation for the accumulation of shikimate in DHD/SHD RNAi plants is that the silencing of DHD/SHD resulted in a reduced turnover of downstream reactions, and therefore shikimate could not be further metabolized. To check this hypothesis, a shikimate feeding experiment was performed. Tobacco leaf discs (about 40 mg) were floated on 50 mM HEPES solution (pH7.0) containing 20 mM shikimate at room temperature for 16 hours. As a control, leaf discs were floated on 50 mM HEPES solution without shikimate under the same conditions. Afterwards, leaf discs were washed 3 times with millipore water, dried with filter paper. Amino acids content was determined in all samples. As shown in Table 5, similar amounts of phenylalanine (118% - 79% of wild type plants) and tyrosine (122% - 84% of wild type plants) accumulated in leaf discs of transgenic plants after feeding (A.F.) with 50 mM shikimate, although less phenylalanine and tyrosine were detected in leaves of DHD/SHD RNAi plants before feeding (B.F.) experiment. This result indicates that silencing of DHD/SHD did not impair downstream enzymes of the shikimate pathway in transgenic plants.

Table 5. Effects of reduced DHD/SHD activity on the biosynthesis of aromatic amino acids in shikimate feeding experiment

		Wild type	DHD/SHD 1-H	DHD/SHD 63-M	DHD/SHD 63-L	DHD/SHD 9-VL
Phe (nmol g ⁻¹ FW)	B.F.	189.97±43.91	176.83±24.72	101.65±24.72	90.33±31.09	48.66±37.77
	Ratio to WT	100%	93 %	53%	48%	26%
	A.F.	2305.14±132.96	2679.51±699.85	2210.76±90.78	1828.24±510.77	1722.01±506.27
	Accumulation to WT	100.0%	118%	96%	82%	79%
Tyr (nmol g ⁻¹ FW)	B.F.	21.05±4.66	18.94±2.12	16.48±8.46	15.10±8.29	16.00±5.79
	Ratio to WT	100%	90%	78%	71%	76%
	A.F.	165.41±26.46	194.70±62.03	164.11±6.44	136.86±8.55	160.58±26.37
	Accumulation to WT	100%	122%	102%	84%	100%

Amino acids were measured in leaf materials of 6-week old plants. B.F. means before feeding experiment, A.F. means after feeding experiment. Wild type control is indicated as WT. Each value represents the mean of 4 different plants ± SE.

3.3 Inducible silencing of Nt-DHD/SHD-1 in transgenic tobacco

Due to the high efficiency of silencing, constitutive RNAi is not suitable to study gene products, which are required for basic cell functions or development. Constitutive silencing of Nt-DHD/SHD-1 led to many pleiotropic effects on primary and secondary metabolism, which might mask the real function of this enzyme. Therefore, to investigate the real-time response of plants, to trace the kinetics of pathway intermediates, and to distinguish between primary and secondary effects of gene silencing, a more flexible gene silencing system under the control of an ethanol inducible promoter (*alc A*) was established. The ethanol inducible gene switch (*alc*) is based on a regulon derived from the filamentous fungus *Aspergillus nidulans* (Caddick et al., 1998; Roslan et al., 2001; Chen et al., 2003). In plants, the system basically consists of two modules: the AlcR transcriptional regulator expressed from the cauliflowers mosaic virus (CaMV) 35S promoter and a modified *alcA* promoter in front of the gene of interest. In the presence of ethanol, AlcR binds to the modified *alcA* promoter and drives expression of the target gene. Using the *alc* system, Chen et al., (2003) achieved temporal and spatial control of gene silencing in tobacco by expressing dsRNA expression (RNAi). As summarized, the *alc*-RNAi system offers an enormous flexibility with respect to time point of induction, expression level, spatial control, and duration of expression, and is applicable to a variety of plant species.

3.3.1 Plasmid construction and plant transformation

To create the ethanol inducible RNAi construct, the entire cassette containing a double-stranded RNA (dsRNA) and the first intron of the GA20, which was used for constitutive silencing construct, was excised from vector pBin-DHD/SHD-RNAi by *Pst*I restriction digestion. The *Pst*I fragment was linked to the *alcA* promoter in downstream orientation and the entire cassette was subsequently cloned into p35S: *alcR*, resulting in the construct *Alc*-DHD/SHD RNAi (Figure 16) (Chen et al., 2003). The binary vector was transformed into *Agrobacterium tumefaciens* strain C58C1 (pGV2260). Following *Agrobacterium* mediated gene transfer, 80 kanamycin resistant tobacco plantlets were generated for further analysis and transferred to the greenhouse.

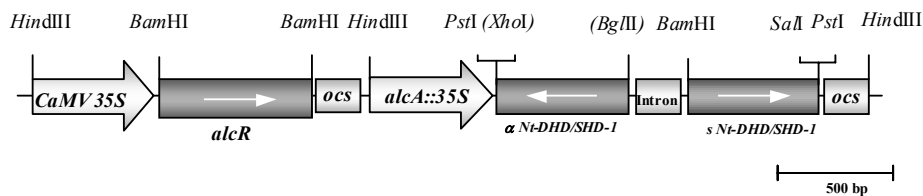


Figure 16. Schematic drawing of the *Alc*-DHD/SHD-RNAi. The construct was created by inserting the fragment DHD/SHD-RNAi (from the construct pBinDHD/SHD-RNAi) into the binary vector p35S: *alcR*, between *alcA*::35S promoter and the *ocs* terminator.

3.3.2 Screening the transgenic plants

To screen the primary transformants, the regenerated plants were transferred to the greenhouse. Plants (42 days old) cultivated in the greenhouse were induced with 100 ml 1% (v/v) ethanol solution via root drenching. Young leaves, being approximately 10 cm at the time point of induction, were followed over the time course of the experiment. Samples for enzyme analysis were taken at various time points. Before induction, similar levels of DHD/SHD activity were detected in all transgenic and wild type plants (data not shown), suggesting that the transcription of dsRNA is under strict control by the *AlcR* cassette.

DHD/SHD activity decreased dramatically 3 days after ethanol induction. Based on enzyme activity, 5 independent transgenic lines with a residual activity of 15% to 40% after induction were selected for detailed analysis in the T1 generation (Figure 17). In contrast to the dwarfed and lethal phenotypes of 35S-DHD/SHD-RNAi plants, the induced degradation of DHD/SHD

RNA resulted in only very weak phenotypic changes of leaves, such as wrinkling. In addition, the growth parameters of transgenic plants were not influenced (data not shown).

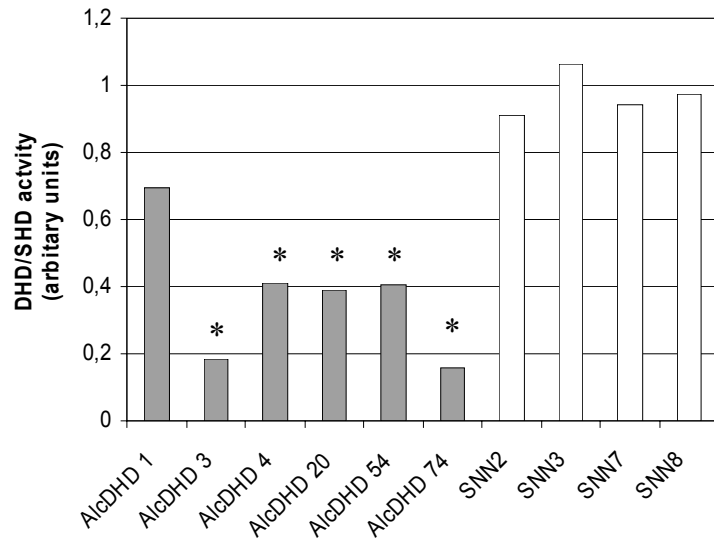


Figure 17. DHD/SHD activity was determined in *alc*-DHD/SHD-RNAi plants 3 days after ethanol induction via root drenching. Transgenic plants marked with an asterisk were selected to produce progenies. DHD/SHD activity was calculated based on soluble protein concentration.

3.3.3 Molecular characterization of *Alc*-DHD/SHD-RNAi plants

To analyze *Alc*-DHD/SHD-RNAi T1 plants, seeds of the transgenic plants were germinated on MS medium containing 50 mg L⁻¹ kanamycin. Resistant seedlings were transferred to the greenhouse for detailed analyses. T1 plants (42 days old) were induced by 1% ethanol via root drenching, and DHD/SHD transcripts and enzyme activity was analyzed. As shown in Figure 18A, the application of ethanol activated the transcription of dsRNA, led to a specific degradation of DHD/SHD RNA, and a reduction of DHD/SHD activity in T1 plants (Figure 18B).

To investigate the dynamic alteration of DHD/SHD transcripts, total RNA was prepared at various time points and analyzed by Northern blot hybridization. Northern blot hybridization revealed that the DHD/SHD mRNA started to decrease as early as 12 hours after induction. Transcript levels kept on decreasing until 60 hours after induction. At this time point, DHD/SHD signal can be hardly detectable.

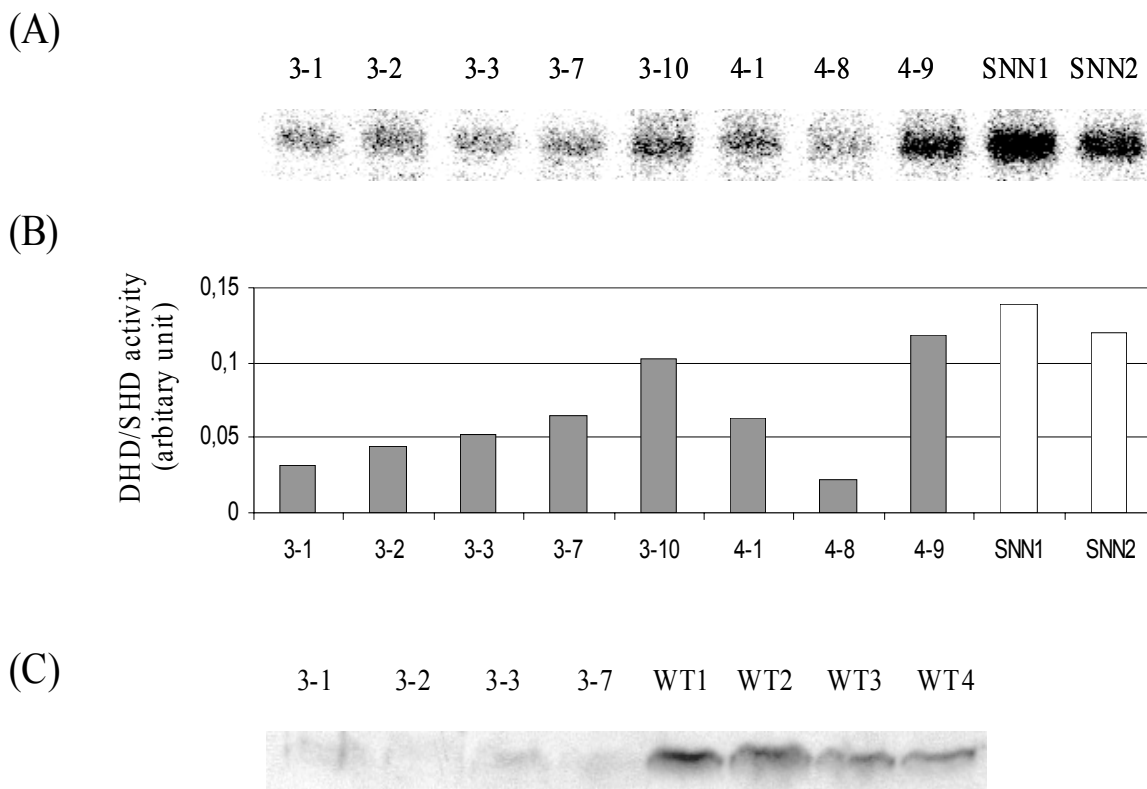


Figure 18. Molecular characterization of *alc*-DHD/SHD-RNAi plants. (A), Northern blot analysis of DHD/SHD transcripts in *alc*-DHD/SHD-RNAi plants 12 hours after ethanol induction. 30 μ g total RNA from tobacco source leaves were separated on a 1.5% agarose gel, blotted and hybridized. (B), DHD/SHD activity in transgenic plants 72 hours after ethanol induction. Enzyme activity was calculated based on total soluble protein. (C), Immuno-blot analysis of DHD/SHD protein in *alc*-DHD/SHD-RNAi mature leaves 72 hours after ethanol induction. Protein was prepared from tobacco source leaves 72 hours after induction. 20 μ g total soluble protein was separated on a 12.5% PAGE gel, blotted and hybridized.

In order to quantify the silencing of DHD/SHD, enzyme activity was determined from tobacco leaf materials harvested at various time points after ethanol induction. In contrast to the rapid reduction of RNA (12 hours after induction), the reduction of DHD/SHD activity lagged behind. Transgenic plants maintained wild-type level of DHD/SHD activity until 48 hours after induction. Significant decrease of DHD/SHD activity can be detected 60-72 hours after ethanol induction, which drop dramatically to 20% of wild type level (Figure 19).

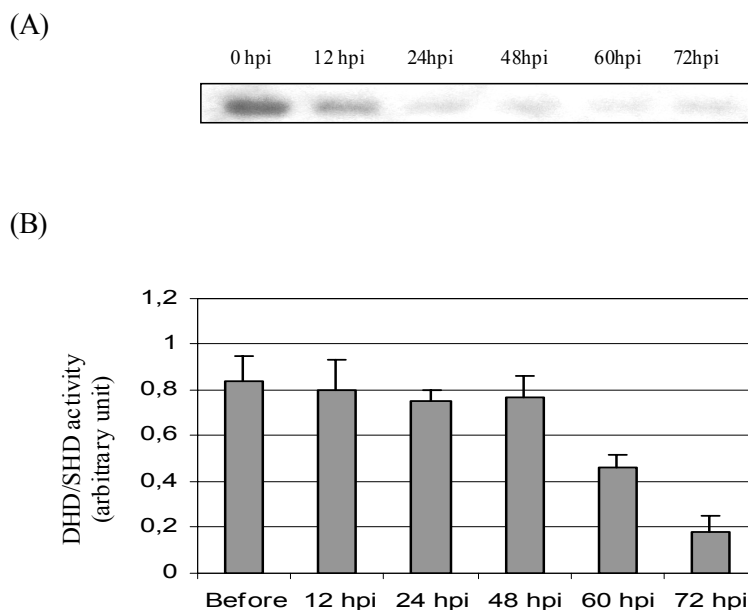


Figure 19. Dynamic analysis of DHD/SHD transcripts and activity in *alc*-DHD/SHD-RNAi 4-8 line after ethanol induction. (A), Northern blot analysis of DHD/SHD transcripts in plants. 30 μ g total RNA from tobacco source leaves were separated on a 1,5% agarose gel, blotted and hybridized. Samples were taken at various time points as indicated. (B), DHD/SHD activity in transgenic plants. DHD/SHD activity was determined based on total soluble protein concentration. Data are given as the mean of 4 replicates of transgenic plants \pm SE.

3.3.4 Kinetic analysis of the shikimate pathway intermediates

The ethanol gene switch enables a real time analysis of the metabolites during the silencing of DHD/SHD enzyme. 40 T1 plants (42 days cultivated in the greenhouse), twenty each from *alc*-DHD/SHD-RNAi line 3 and line 4, were induced and analyzed (see materials and methods). Samples for enzyme activity and metabolites were taken at various time points. Based on the DHD/SHD activity, 8 plants with a residual activity of 15% - 30% (5 plants from line 3 and 3 plants from line 4) were selected for the determination of the shikimate pathway intermediates. As indicated, dehydroquinate cannot be detected in all transgenic and wild type plants before ethanol induction. This metabolite started to accumulate 2 to 3 days after ethanol induction in the plants 3-1 and 4-8, and the accumulation was correlated with the silencing of DHD/SHD enzyme. Shikimate started to accumulate 1 or 2 day later than dehydroquinate (Figure 20), suggesting that the accumulation of dehydroquinate was a direct consequence of the blockage of DHD/SHD, whereas the buildup of shikimate derived from some side effects.

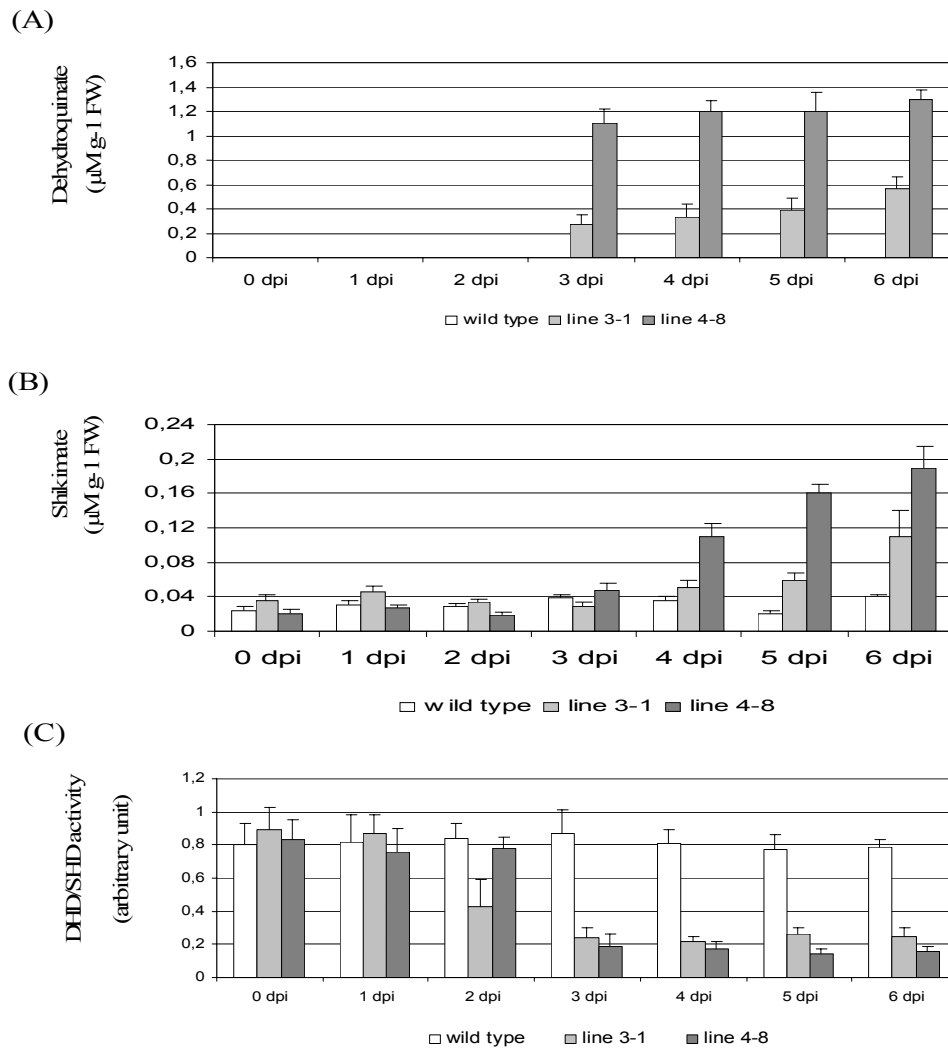


Figure 20. Kinetic analyses of the shikimate pathway intermediates in *alc*-DHD/SHD-RNAi plants after ethanol induction. Metabolites and enzyme activity were taken at various time points indicated in the pictures. was measured in leaf materials of 6-week old plants. Dehydroquinate (A) and shikimate (B) were determined in transgenic plants by an enzymatic assay. DHD/SHD activity was determined based on total soluble protein.

3.3.5 Spatial silencing of Nt-DHD/SHD-1 in flowers resulted in male sterility

One application of the ethanol gene switch is to control gene expression at different developmental stages, which can overcome early detrimental effects of gene expression and provides an opportunity for a detailed analysis of gene function in different developmental windows (Deveaux et al., 2003). To investigate the roles of the shikimate pathway in flower development, silencing of DHD/SHD was induced at different flowering stages.

To induce DHD/SHD silencing at an early flowering stage, flower buds were exposed to ethanol in a bagging experiment as described by Sweetman et al. (2002). Floral organ of wild

type and transgenic plants was enclosed in a 25 cm x 20 cm transparent plastic bag with 3 ml of 4% (v/v) ethanol. The bag was removed 24 h later and phenotype development was followed daily. The nascent flowers of transgenic plants developed a pale phenotype as compared to wild type (Figure 21 B-D). The phenotypic changes were restricted to flowers, indicating that neither transport of ethanol into adjacent parts of the plants, nor spread of the silencing occurred. In addition to above fading phenotypes, the induction of DHD/SHD silencing in flowers perturbed the differentiation and growth of stamen, resulting in male sterility (Figure 21 B-D).



Figure 21. Spatial silencing of DHD/SHD in flower led to fading petals and male sterility. Pictures were taken 10 days after ethanol induction. (A), Wild type flower. (B)-(D), *alc*-DHD/SHD-RNAi nascent flowers.

DHD/SHD activity was determined in stamens, petals and leaves of the treated plants. As indicated in Figure 22, DHD/SHD activity decreased exclusively in the flowers of transgenic plants. A 65% to 91% reduction of enzyme activity was observed in stamens and a 59% to 82% reduction was determined in petals. In contrast, DHD/SHD activity did not change in the leaves of transgenic plants, suggesting that silencing was stringent controlled.

The induction of DHD/SHD silencing in the flowering plants resulted in a miscellaneous phenotype. For spatial induction, floral organ was enclosed in a 25 cm x 20 cm transparent plastic bag with 3 ml of 4% (v/v) ethanol as described previously by Sweetman et al. (2002). The bag was removed 24 h after ethanol induction, and phenotype development was followed daily.

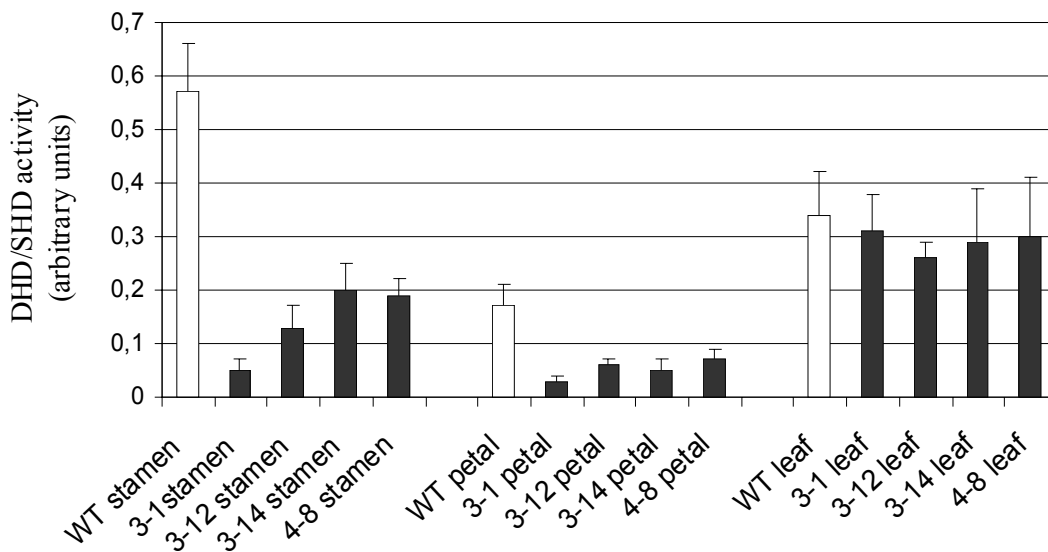


Figure 22. DHD/SHD activity in the leaves and nascent floral organs of alc-DHD-SHD-RNAi plants 10 days after ethanol induction. DHD/SHD activity was calculated based on total soluble protein. Values were given as mean of 4 replicates of each independent transgenic plants \pm SE.

The open flowers at the time point of induction exhibited a wild type like phenotype, whereas flower buds developed into open flowers and formed a pale phenotype. (Figure 23 B-D).

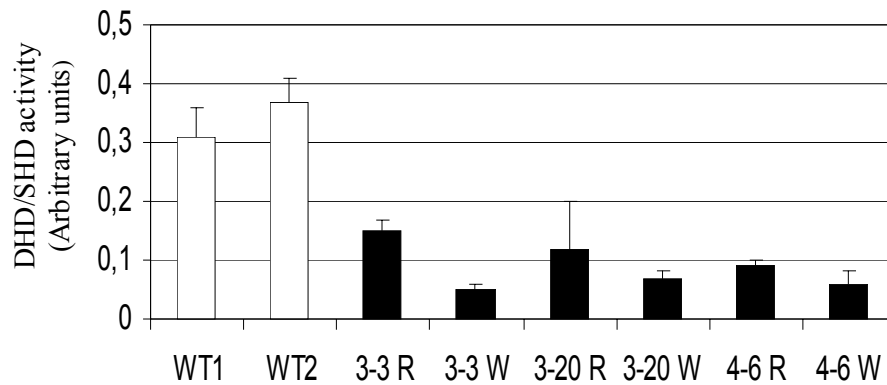


Figure 23. Spatial silencing of DHD/SHD at the flowering stage resulted in a miscellaneous phenotype. The fully blown flowers remained red after ethanol treatment, whereas the nascent flowers developed pale petals. (A), Wild type flowers. (B)-(D), transgenic flowers. Pictures were taken 7 days after induction.

DHD/SHD activity was determined in transgenic tobacco flowers. As shown in Figure 24A, DHD/SHD activity decreased dramatically in both red and pale flowers in transgenic plants,

whereas in wild type plants, DHD/SHD activity did not decrease after ethanol treatment. DHD/SHD transcripts were investigated by Northern blot hybridization. As shown in Figure 24B, the degradation of DHD/SHD mRNA correlated with the reduction of enzyme activity in transgenic plants. As a control, the transcript of EPSPS was probed in above samples. A similar amount of EPSPS transcripts was detected in all samples, indicating that the degradation of DHD/SHD in the flowers of transgenic plants is specific.

(A)



(B)

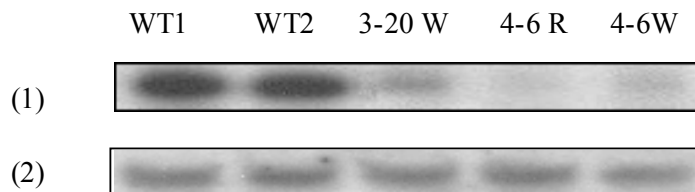


Figure 24. Spatial induction of DHD/SHD silencing leads to a decrease of DHD/SHD activity and transcripts in flowers (A) DHD/SHD activity was measured in total flowers of wild type flowers and the transgenic plants 7 days after ethanol induction, DHD/SHD activity was calculated based on total soluble protein; Data are given as the mean of 4 replicates of each independent transgenic plants \pm SE. (B1) Northern blot analysis of DHD/SHD transcripts in flowers (B2) Northern blot analysis of EPSPS transcripts in flowers. Red flowers are indicated as R and pale flowers as W. Data are given as the mean of 4 replicates of each independent transgenic plants \pm SE.

The shikimate pathway provides the precursors for the biosynthesis of anthocyanin and flavonoid. Thus the induction of DHD/SHD silencing in floral organs might reveal the kinetics of anthocyanin synthesis during flower development. The senescent flowers of transgenic plants exhibited wild type like phenotype, whereas the nascent flowers exhibited pale phenotypes. The abundance of anthocyanin in whole flowers was determined according to Martin et al. (2002).

As shown in Figure 25, anthocyanin content increased slightly in red flowers (senescent flowers) and decreased dramatically in the pale flowers (nascent flowers).

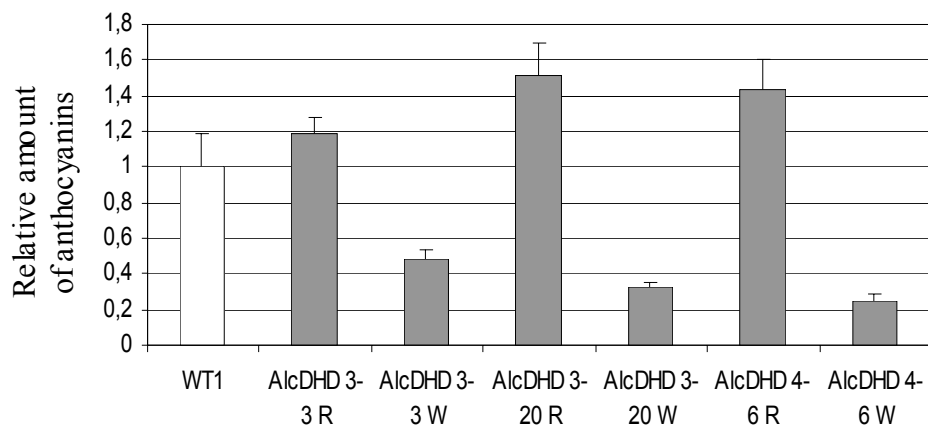


Figure 25. Spatial silencing of DHD/SHD in transgenic flowers result in a remarkable decrease of anthocyanins in nascent flowers. Anthocyanin content in wild type flowers was set as 1. The anthocyanins content in transgenic flowers is given in relation to the wild type flowers. Red flowers are indicated as R, and pale flowers as W.

3.4 Cloning a cytosolic DHD/SHD (Nt-DHD/SHD-2) from tobacco

In higher plants, the shikimate pathway is present in plastids and has also been proposed to exist in the cytoplasm (Jensen et al., 1989). The major function of the shikimate pathway in chloroplasts is to produce aromatic amino acids for protein synthesis, while the role of the proposed cytosolic pathway is not well understood (Hrazdina and Jensen, 1992). The existence for a dual shikimate pathway is further supported by isozyme analysis in subcellular fractions. Putative cytosolic isozymes have been described for DAHP synthase (Ganson et al., 1986), DHD/SHD (Mousdale et al., 1987), EPSP synthase (Mousdale and Coggins, 1985) and chorismate mutase (d'Amato, 1984).

It was observed that silencing of DHD/SHD resulted in an accumulation of shikimate in leaves of transgenic plants (Figure 15). Although speculative, the obvious contradiction between the reduced DHD/SHD activity and elevated shikimate led to a prediction of the cytosolic DHD/SHD isozyme. According to the shuttle model (Figure 47), silencing of the plastidic DHD/SHD led to a high level accumulation of dehydroquinate, thus a certain amount of this metabolite would be exported from chloroplasts to the cytosol, and be converted to shikimate by a postulated cytosolic DHD/SHD enzyme.

3.4.1 Cloning a tobacco DHD/SHD isozyme (Nt-DHD/SHD-2)

To clone tobacco DHD/SHD isozyme, a 270 bp sequence encoding tobacco DHD/SHD homolog was retrieved from an EST database search. Based on this sequence, a 1.2 Kb fragment and a 0.7 Kb fragment have been amplified by 5'RACE and 3'RACE with the primers indicated in Table 1 (primer 12, 13), respectively. PCR products were cloned into the vector pCRblunt, sequenced and analyzed. The sequence of the 5'RACE fragment overlapped with that of 3'RACE fragment, and the cDNA encoding DHD/SHD homolog was assembled by the software VectorNTI (InforMax, Inc., USA), as shown in Figure 26. Upstream of the underlined ATG, a stop codon TGA (bolded) was located in frame with the coding sequence, indicating that the full-length cDNA was amplified. This sequence was designated as Nt-DHD/SHD-2 and submitted to GenBank (accession No. AY578143).

```

1   GAAATAGCTTAAAGTTCATTCTTTTCTTGATTCTTAATTCTTTAT
61  TCTTAATTCTTAATTCTTGATTCTTGATTCTTGATTCTTGATTCTTGATTCTTGATTCTT
      M G S V G L L K N P A M V C A
121 ATTTGGTTTGTGGAAATGGGTAGTGTGGATTGTTGAAGAATCCGCCATGGTTTGTGCT
      P L M A P S V D Q L V H G M L Q A K A Q
181 CCATTAATGGCCCCATCAGTGGACCAATTGGTTCATGGTATGCTTCAGGCAAAGCACAA
      G A D L V E I R L D G I H N F Q P Q K D
241 GGTGCTGATTTAGTTGAGATTAGGCTGGATGGTATCCACAACCTCCAACCCAGAAAGAT
      L Q V L L K N N P L P V L I V Y R P I W
301 CTTCAAGTCCTCCTAAAAAATAATCCACTTCTGTTCTCATTGTTTACAGGCCAATATGG
      E G N E F E E D D D H I H K Q L E V L R
361 GAAGGAAATGAGTTTGAAGAGGATGATGACCACATCCACAAGCAGTTGGAAGTCCTTCGG
      W A K E L G A D Y I E L D L K I A S D F
421 TGGGCTAAAGAATTGGGAGCTGATTATATTGAGTTGGACCTCAAGATAGCTAGTGACTTC
      T K K E K S R W S S G C K V I A S C F V
481 ACGAAAAAGAAAAGTCGAGGTGGAGTAGTGGTTGTAAAGTAATTGCATCATGCTTTGTG
      D N V T S K E D L S Q V V A H M Q S T G
541 GACAATGTGACCTCAAAGAAGACCTCAGCCAAGTTGTTGCACACATGCAATCTACTGGG
      A D I L K I V T N A N D I T E L E K M F
601 GCTGATATCCTCAAATTTGTTACAAATGCAATGACATTACAGAAGTACAGAAAATGTTT
      H L L S H C Q V P L I A Y S L G E R G L
661 CACTTGCTTTCACATTGCCAGGTACCACTTATTGCATACTCTCTTGGGAAAGAGGTCTC
      I S Q L L G P K F G S V L V Y G S L D C
721 ATAAGTCAGTTGTTGGGCCGAAATTTGGTAGTGTCTAGTATATGGATCTCTTGATTGT
      N A V P G L P T L G S L R Q A Y G V D F
781 AATGCTGTACCTGGTCTGCCTACTCTCGGCAGCCTTAGACAAGCCTATGGAGTTGATTTT
      M D T D T K V F G L I S K P V G H S K G
841 ATGGATACTGATACTAAAGTGTTTGGGCTCATCTCTAAACCAGTGGGTCATAGTAAAGGA
      P I L H N P T F R H V G Y N G I Y V P M
901 CCTATTTTGCATAATCCTACATTTAGACATGTGGGGTACAATGGAATTTATGTTCCAATG
      F V D D L K E F F R V Y S S P D F A G F
961 TTTGTCGATGATCTTAAGGAGTTCTTCAGGGTCTACTCAAGTCCTGACTTTGCTGGTTTC
      S V G I P Y K E A V V S F C D E V D P L
1021 AGTGTGGGATCCCTTACAAGGAAGCAGTGGTGTGATTTTGTGATGAAGTCGATCCTCTG
      A K S I G A G Q I L S Y R G L A T G K L
1081 GCTAAGTCTATAGGGCTGGTCAAATACTATCATAACAGAGGCCTTGGCAGGGAAAGCTA

```

```

1141 I G Y N X D C E A S I T A I E D A L K V
ATTGGTTATAACNCAGATTGTGAGGCTTCTATAACAGCCATTGAGGATGCTTTGAAAGTA
N G A A F L P S P L A G K L F V L V G A
1201 AATGGAGCAGCTTTTCTTCTTCTCCACTCGCGGGTAAACTGTTTGTGCTGGTGGGTGCT
G G A G R A L A F G A K S R R A Q I M I
1261 GGAGGTGCAGGAAGAGCTTTGGCATTTCGGAGCCAAAAGCAGGAGAGCTCAAATTATGATT
F D I D F D R A K A L A A A V S G E A L
1321 TTTGACATTGATTTTGATAGAGCAAAGGCTCTTGCTGCTGCAGTTTCTGGTGAAGCTCTG
P F E N L A S F Q P E K G A I L A N A T
1381 CCATTTGAGAATTTAGCTTCTTTTCAGCCTGAGAAAGGTGCAATCCTTGCCAATGCAACA
P I G M H P N K D R I P V S E A T L K D
1441 CCTATCGGAATGCATCCAAATAAAGATAGGATACCTGTTTCTGAGGCAACCTTGAAGGAT
Y L V V F D A V Y T P R K T T L L K D A
1501 TATCTAGTGGTCTTTGATGCTGTTTATACACCTAGAAAGACTACTCTGCTGAAAGACGCT
E A A G A I T V S G V E M F L R Q A I G
1561 GAGGCTGCTGGAGCAATCACTGTGAGTGGAGTTGAAATGTTTCTTAGACAGGCCATTGGC
Q F H L F T G S K A P E E F M R D I V M
1621 CAATTCCACCTTTTCACGGGAAGTAAAGCACCCGAAGAATTCATGCGCGACATCGTTATG
A K F *
1681 GCAAAATTCTAA
    
```

Figure 26. Nucleotide and deduced amino acid sequences of Nt-DHD/SHD-2 from *Nicotiana tabacum*. The translation start codon and stop codon are underlined.

To investigate the homology between Nt-DHD/SHD-1, Nt-DHD/SHD-2 and *Arabidopsis* DHD/SHD, amino acids sequences were aligned by the software Vector NTI (Informax Inc., USA). The alignment suggested that there are homologies between *Arabidopsis* DHD/SHD, Nt-DHD/SHD-1 and Nt-DHD/SHD-2. The homolog value between Nt-DHD/SHD-1 and *Arabidopsis* DHD/SHD is 63%; the value between Nt-DHD/SHD-1 and Nt-DHD/SHD-2 is 48%; the value between Nt-DHD/SHD-2 and *Arabidopsis* DHD/SHD is 51%; and the identity value between all three sequences is 39% (Figure 27).

		1	-----	50
Nt-DHD/SHD-2	(1)		-----	
<i>Arabidopsis</i> DHD/SHD	(1)	MAASSTNARL	TNPPRLLSKPRLSPTS	SVANLRFPAADFSTRFFADSSSPRL
Nt-DHD/SHD-1	(1)		-----	
		51	-----	100
Nt-DHD/SHD-2	(1)		-----	MGSVGLLKNPAMV
<i>Arabidopsis</i> DHD/SHD	(51)	RSVPFPVVFSDQRRRR	SMEPSNVYVASNSTEMEIGSHDIVKNPSLICAPV	CAPL
Nt-DHD/SHD-1	(1)		-----	MELVVD
		101	-----	150
Nt-DHD/SHD-2	(18)	MAPSV	DQLVHGMLQAKAQGADLVEIRLDGIHNFQPKDLQVLLKNNPLPV	
<i>Arabidopsis</i> DHD/SHD	(101)	MADSIDKMVIETSKAHEL	GADLVEIRLDWLKDFNPLEDLKTI	IKKSPLPT
Nt-DHD/SHD-1	(29)	MADTV	DQMLNLMQKAKISGADLVEVRLDSLKSFNPQSDIDTIIKQSPLPT	
		151	-----	200
Nt-DHD/SHD-2	(68)	LIVYRPIWEGNEFEE	DDHIHKQLEVLRWAKELGADYIELDLKI	ASDFUK
<i>Arabidopsis</i> DHD/SHD	(151)	LFTYRPKWEGGQYEGDEN	---ERRDVLRLAMELGADYIDVELQVASEFIK	
Nt-DHD/SHD-1	(79)	LFTYRPTWEGGQYAGDEV	---RLDALRVAMELGADYIDVELKAIDEFNT	
		201	-----	250
Nt-DHD/SHD-2	(118)	KEKSRWSSGCKVIASCF	-VDNVUSKEDLSQVVAHQ	SUGADILKIVUNAN
<i>Arabidopsis</i> DHD/SHD	(198)	SIDGKPKGFKFVIVSSHNYQNT	PSVEDLDGLVARIQQTGADIVKIATTAV	
Nt-DHD/SHD-1	(126)	ALHGNSAKCKVIVSSHNYDNT	PSSEELGNLVARIQASGADIVK	FATTAL

		251	300
Nt-DHD/SHD-2	(167)	DIUELEKMFHLLSHCQVPLIAYSLGERGLISQLLGPKFGSVLVYGS LD CN	
<i>Arabidopsis</i> DHD/SHD	(248)	DIADVARMFHITSKAQVPTIGLVMGERGLMSRILCSKFGGYLTFGTL DSS	
Nt-DHD/SHD-1	(176)	DIMDVARVFQITVHSQVPIIAMVMGEKGLMSRILCPKFGGYLTFGTL EVG	
		301	350
Nt-DHD/SHD-2	(217)	AV--PGLPULGSLRQAY G VDFM DUDUKVFGLISKPVGHSGKGPILHNP UFR	
<i>Arabidopsis</i> DHD/SHD	(298)	KVSAPGQPTIKDLLDLYNFRRI GPDTKVYGIIGKPVSHSKSPIVHN QAFK	
Nt-DHD/SHD-1	(226)	KVSAPGQPTIKDLLNIYNFRQLGPDTRI FGIIGKPVSHSKSP LLYNEAFR	
		351	400
Nt-DHD/SHD-2	(265)	HVGYNGIYVPMFVDDLKEFFRVYSSPDFAGF SVGIPYKEAVVSFCDE VDF	
<i>Arabidopsis</i> DHD/SHD	(348)	SVDFNQVYVHLLVDNLVSLQAYSSSDFAGF SC TIPHKEAALQCCDE VDP	
Nt-DHD/SHD-1	(276)	SVGFNGVYMPLLVDVANFR TYSSLD FAGSAVTIPHKEAIVDCCDE LNP	
		401	450
Nt-DHD/SHD-2	(315)	LAKSIGAGQILSYRGLAUGKLI GYNXDCEAS IUAIEDAL KVNGAAFLP--	
<i>Arabidopsis</i> DHD/SHD	(398)	LAKSIGAVNTILRRK-SDGKLLGYNTDC IGSISAIEDGLRSSGD PSSVPS	
Nt-DHD/SHD-1	(326)	TAKVIGAVNCVVSRL--DGKLF GCNTDYVGAISAIEEAL QSQPSMSG--	
		451	500
Nt-DHD/SHD-2	(363)	--SPLAGKLFVLV GAGGAGRALAF GAKSRRAQ IMIFDIDF RAKALAAV	
<i>Arabidopsis</i> DHD/SHD	(447)	SSSPLASKTVVVI GAGGAGKALAYGAKE KGAKVVIANR TYERALELAEAI	
Nt-DHD/SHD-1	(372)	--SPLAGKLFVVI GAGGAGKALAYGAKE KGARVVIANR TYERARELADV	
		501	550
Nt-DHD/SHD-2	(411)	SGEALPFENLAS FQPEKGA LANAUP IGMHPNK DRI PVSE AULKDYLV VF	
<i>Arabidopsis</i> DHD/SHD	(497)	GGKALS SLTDLDNY HPEDGM LANTTSMGM QPNVEET PISKD ALKHYAL VF	
Nt-DHD/SHD-1	(420)	GGQALS SLDELSNF HPENDMI LANTT SI GMQPKV DDTPI FKEAL RY SL VF	
		551	600
Nt-DHD/SHD-2	(461)	DAVYUP PRKUULLK DAEAGAI UVSG VEMFL RQAIG QFHLE UGSKA ----	
<i>Arabidopsis</i> DHD/SHD	(547)	DAVYTP PRITRLL REAEES GAI TVSG SEM FV RQAYE QFE I FTGL PA ----	
Nt-DHD/SHD-1	(470)	DAVYTP KITRLL REAHES GV KIVT GV EMF I QAYE QYER FTGL ASSK GT F	
		601	650
Nt-DHD/SHD-2	(506)	----- PEE FMRD I VMAK F -----	
<i>Arabidopsis</i> DHD/SHD	(592)	----- PKEL YWQ I MSKY -----	
Nt-DHD/SHD-1	(520)	QENY GWIL RARS LSL FNA ALL V T F PK SL H S C V I A M V L D S S A L P F V L R R N	

Figure 27. Sequence alignment of the two isoforms of tobacco DHD/SHD and *Arabidopsis* DHD/SHD (NC_003074). Transit peptides were indicated in bold. Conserved amino acids were indicated in red or blue. DHD and SHD of Nt-DHD/SHD-2 were indicated in box.

Conversed domain database (CDD, NCBI) search recognized both DHD and SHD domains from the deduced amino acid sequence of Nt-DHD/SHD-2. The DHD domain located at the N' terminus, from amino acids 13 to 230, whilst the SHD domain located at the C terminus, from amino acid 235 to 513, as shown in Figure 28.

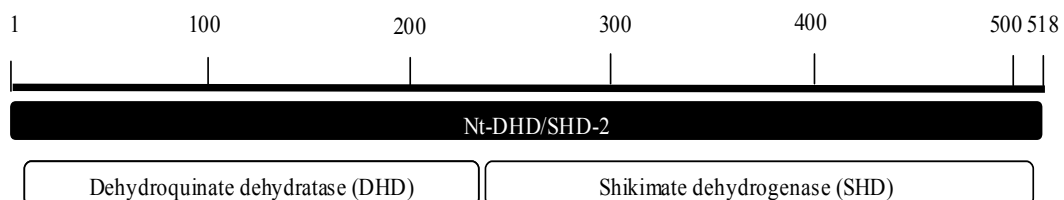


Figure 28. Both dehydroquinate dehydratase (from amino acids 13 to 230) and shikimate dehydrogenase (from amino acids 235 to 513) domains were recognized based on deduced amino acid sequence of Nt-DHD/SHD-2 by NCBI-CCD.

Unlike Nt-DHD/SHD-1, Nt-DHD/SHD-2 did not contain a typical chloroplast transit peptides and was predicted to be cytosolic by the software ChloroP (Emanuelsson et al., 1999).

3.4.2 Tissue specific expression of tobacco isoforms

Tissue specific expression of Nt-DHD/SHD-2 was investigated by Northern blot hybridization, as shown in Figure 29. Nt-DHD/SHD-1 was strongly expressed in petals, stigmas, ovaries, pollen, source leaves, and stems, and weakly expressed in sepals, sink leaves, petioles, and roots. In contrast to Nt-DHD/SHD-1, Nt-DHD/SHD-2 was specifically expressed in petals, source leaves, stems and roots.

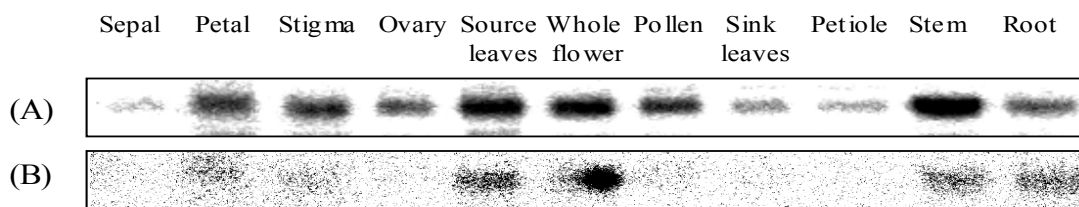


Figure 29. Tissue specific expression of tobacco Nt-DHD/SHD-2. RNA transcripts were investigated in different tissues by Northern blot hybridization. (A), Tissue specific expression patterns of Nt-DHD/SHD-1 gene. (B), Expression patterns of Nt-DHD/SHD-2 gene. 30 μ g total RNA from different tobacco tissues were separated on a 1,5% agarose gel, blotted and hybridized.

3.4.3 Enzymatic properties of Nt-DHD/SHD-2

To determine the enzymatic properties of Nt-DHD/SHD-2, coding sequence of this enzyme was amplified by RT-PCR, and cloned into expression vector pQE (refer to materials and methods).

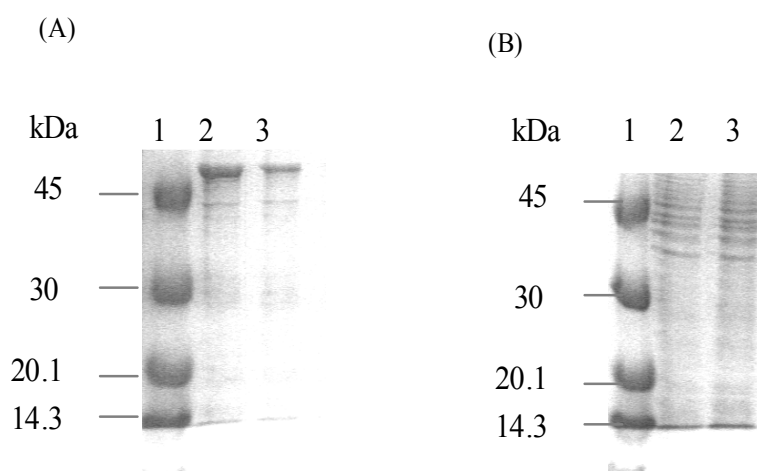


Figure 30. Overproduction of Nt-DHD/SHD-2 protein in *E.coli*. (A), Nt-DHD/SHD-2 protein (52 kDa) was purified under denaturing condition. (B), Nt-DHD/SHD-2 protein was purified under native condition. Lane 1, Molecular marker. Lane 2, 3, purified protein of Nt-DHD/SHD-2.

Protein was induced and purified under native and denaturing condition. In contrast to Nt-DHD/SHD-1, Nt-DHD/SHD-2 was completely insoluble when purified under native conditions (Figure 30), hindering further analysis of this protein.

Agrobacterium infiltration offers an opportunity to transiently express Nt-DHD/SHD-2 and determine its enzymatic property *in planta*. The coding sequence of Nt-DHD/SHD-2 was cloned into the binary vector pBinAR, between CaMV 35S promoter and *ocs* terminator, in sense orientation as shown in Figure 31A. *Agrobacterium* infiltration was performed according to the Bechtold and Pelletier (1998).

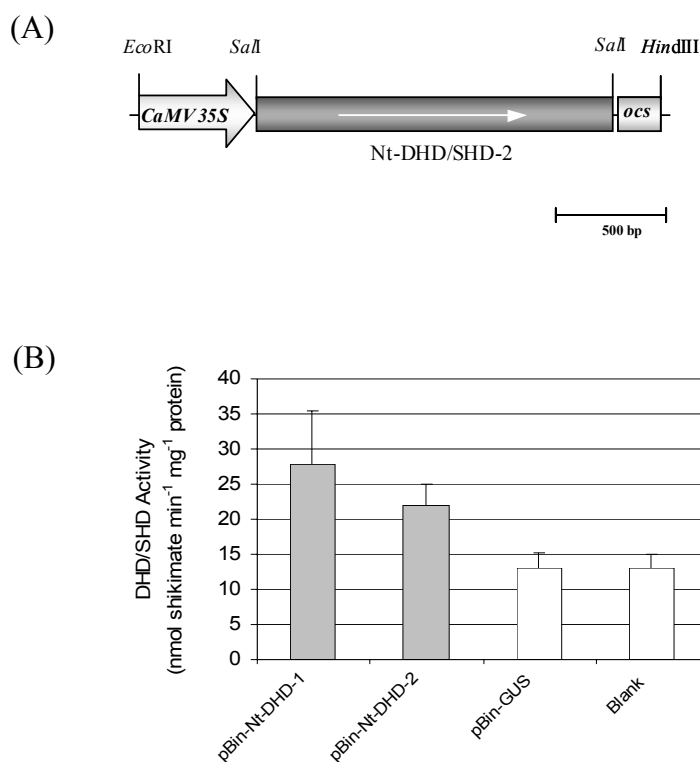


Figure 31. Overproducing tobacco DHD/SHD isoforms in *Nicotiana benthamiana* via *Agrobacterium* infiltration. (A), Schematic drawing of pBin-Nt-DHD/SHD-2 construct. This construct was created by inserting the coding sequence of Nt-DHD/SHD-2 into binary vector pBinAR between 35S promoter and *ocs* terminator. (B), DHD/SHD activity in plants 48 hours after *Agrobacterium* infiltration. Wild type control was indicated as WT, and treated plants were indicated as DHD/SHD. DHD/SHD activity was calculated based on total soluble protein. Data are given as the mean of 4 replicates of infiltrated plants \pm SE.

DHD/SHD activity was determined 48 hours after *Agro*-infiltration. The construct pBin-Nt-DHD/SHD-1 was used as positive control, and the construct pBin-GUS was served as a negative control. The measurement confirmed DHD/SHD activity of both Nt-DHD/SHD isoforms. Compared to pBin-GUS and blank control, DHD/SHD activities increase significantly in plants expressing Nt-DHD/SHD-1 and Nt-DHD/SHD-2 proteins Figure 31B.

3.4.4 Subcellular localization of tobacco DHD/SHD isoforms

To determine the subcellular localization, the coding sequences of tobacco DHD/SHD isoforms were fused to fluorescence proteins, GFP (YFP and CFP) respectively. The fusion proteins were

transiently expressed in tobacco epidermal cells by bombardment, and analyzed by confocal microscopy (Hofius et al., 2004).

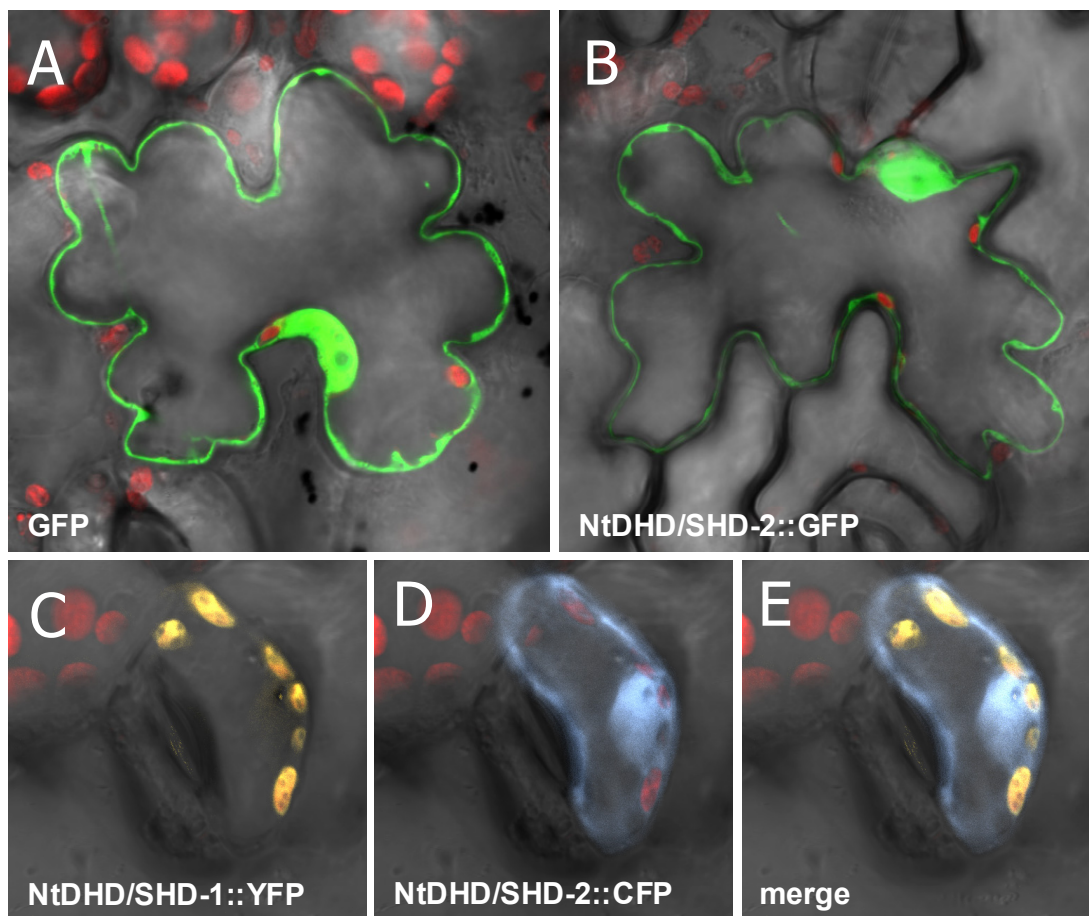


Figure 32. Subcellular localizations of tobacco DHD/SHD isoforms. (A), the intracellular localization of free GFP. (B), the intracellular localization of the Nt-DHD/SHD-2-GFP fusion protein. (C), the intracellular localization of Nt-DHD/SHD-1-YFP in stomata cells. (D), the cytosolic localization of Nt-DHD/SHD-2-CFP. (E), the merged images of picture (C) and (D).

As depicted in Figure 32B, Nt-DHD/SHD-2 appeared to be targeted into the cytosol, because the transient expression of Nt-DHD/SHD-2-GFP fusion protein resulted in a similar fluorescence pattern as free GFP (Figure 32A). In contrast, Nt-DHD/SHD-1 was targeted into chloroplasts, because it co-localized with the red fluorescence of chlorophyll in stoma cell (Figure 32C). The cytosolic localization of Nt-DHD/SHD-2 was confirmed in picture D. Picture E is the merged picture of picture C and D. From this picture we can see clearly the different subcellular localizations of tobacco DHD/SHD isoforms.

3.5 Constitutive silencing of EPSPS in transgenic tobacco

EPSPS is the sixth enzyme of the shikimate pathway. This enzyme is deeply analysed because it is the target of the broad-spectrum herbicide glyphosate (Steinrucken and Amrhein, 1980). As described in section 3.2, the constitutive silencing of DHD/SHD resulted in severe phenotypical changes and metabolite alterations in tobacco plants. This result suggested that DHD/SHD could be a second herbicide target in the shikimate pathway, and impelled to investigate the roles and the regulations of the pathway by exploring the similarity and difference between DHD/SHD and EPSPS silenced plants.

3.5.1 Plasmid construct and plant transformation

To achieve an efficient silencing of EPSPS, an EPSPS co-suppression construct was created. The partial coding region of tobacco EPSPS (GenBank: M61904) ranging from codon 116 to 1255 was amplified by PCR using the primers in Table 1 (primer 3, 4).

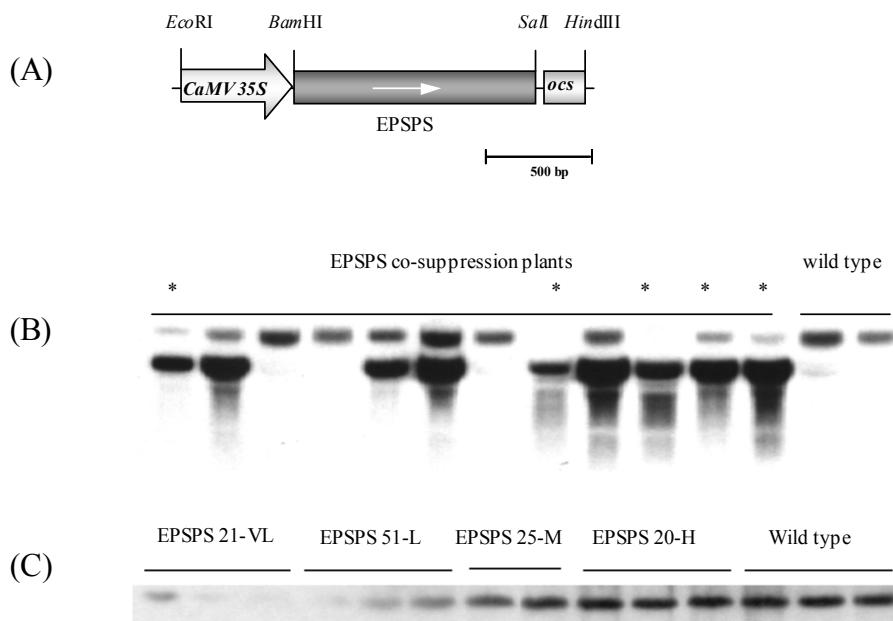


Figure 33. Silencing of EPSPS in tobacco plants. (A), Schematic drawing of pBin-EPSPS co-suppression construct. The construct was created by inserting the partial sequences of EPSPS into binary vector pBinAR, between the CaMV 35S promoter and the *ocs* terminator. (B), Northern analysis of EPSPS transcripts in transgenic plants. 30 μ g total RNA was prepared from tobacco source leaves, which was cultivated in greenhouse for 6 weeks. RNA was separated on a 1.5% agarose gel, blotted and hybridized. Transgenic plants with an asterisk were selected to produce progeny. (C), EPSPS protein in T1 progenies was detected by Western blot hybridization. Protein was prepared from tobacco source leaves. 20 μ g of soluble protein was separated on 12.5% PAGE gel, blotted and hybridized.

*Bam*HI sites were introduced to both ends of the PCR products. The amplified EPSPS fragment was sub-cloned into the binary vector pBinAR, between the CaMV 35S promoter and the *ocs* terminator, in sense orientation (Figure 33A). The binary vector was transformed into *Agrobacterium tumefaciens* strain C58C1 (pGV2260). Following *Agrobacterium* mediated gene transfer, 60 kanamycin resistant tobacco plants were selected for further analysis and transferred to the greenhouse.

3.5.2 Screening the transgenic plants

EPSPS co-suppression plants were screened by Northern blot hybridization. 5 independent transgenic plants were selected for detailed analysis in the T1 generation (Figure 33B). EPSPS protein was analyzed by immunoblotting. To prepare EPSPS antiserum, the cDNA encoding the predicted mature protein was PCR amplified with the primer listed in Table 1 (primer 20, 21), and cloned into the *E. coli* expression vector pQE (see materials and methods). Expression of the 6xHis tagged Nt-DHD/SHD-1 mature protein (60 kDa) was induced and purified under native conditions by a metal-chelated affinity chromatography (Ni-NTA, Qiagen). Antiserum against EPSPS was prepared by immunizing rabbits with the purified 6xHis-tagged EPSPS proteins. Based on the residual EPSPS protein, T1 progeny of selected EPSPS co-suppression lines were categorized into 4 classes: high (H, EPSPS protein 80-60 %); middle (M, EPSPS protein 60-40 %); low (L, EPSPS protein 40-20 %) and very low (VL, EPSPS protein 20-5 %) (Figure 33C).

3.5.3 Growth characterisation of EPSPS silenced plants

The silencing of EPSPS resulted in dramatic phenotypical changes in the transgenic plants, which were similar to those of DHD/SHD RNAi plants (Figure 10). A 20-40% reduction of EPSPS protein (EPSPS-H) resulted in wild type like phenotype. A 40-60% reduction of EPSPS protein (EPSPS-M) led to bleached phenotypes, and a further reduction (60-80%) resulted in a dwarfed phenotype. When the level of EPSPS protein dropped below 20% of the wild type value, transgenic plants (EPSPS-VL) stopped development and died in one to two weeks after transfer from tissue culture to the greenhouse.

To quantify the effects of the decreased EPSPS protein on biomass production, EPSPS co-suppression plants (T1 generation) were germinated in sand and fertilised with nutrient solution, as described in Geiger et al. (1999). Growth parameters were acquired by measuring the fresh

weight (FW), the dry weight (DW) and the plant height. As indicated in Table 6, the loss of EPSPS protein led to a consistent reduction of FW, DW and plant height.

Table 6. Growth parameters of EPSPS co-suppression plants.

	Plant height (cm)	Shoot FW (g)	Shoot DW (g)	FW/DW
EPSPS 20-H	13.9±2.2	7.31±1.18	0.37±0.12	19.76
EPSPS 25-M	9.4±1.1	5.47±0.39	0.34±0.08	16.09
EPSPS 51-L	8.2±1.9	4.33±0.81	0.26±0.05	16.67
EPSPS 21-VL	7.1±1.6	1.57±0.47	0.08±0.01	19.62
SNN	13.5±2.6	7.13±1.24	0.41±0.18	17.39

Growth parameters are determined in 6-week old plants in greenhouse Results are mean of 6 wild type plants and 6 T1 progenies of each independent transgenic lines ± SE.

3.5.4 Silencing of EPSPS leads to reduced chlorogenate, lignin, and aromatic amino acids content

The shikimate pathway converts Ery4P and PEP into aromatic amino acids that could be further metabolized into a large number of important phenolic compounds including alkaloids, phytoalexins, chlorogenate and lignin etc. To evaluate the silencing effect of EPSPS on secondary metabolism, content of aromatic amino acids, chlorogenate and lignin were determined in transgenic plants. Phe content decreased to 93%, 56% and 46% of wild-type level in the lines EPSPS 20-H, 25-M and 51-L, respectively. Unexpectedly, in transgenic lines with 20% or less EPSPS residual protein (EPSPS 21-VL), an accumulation of Phe was detected, which was two times higher than in wild type plants, and four times higher than in EPSPS 51-L lines (Table 7). The content of Tyr decreased in all EPSPS co-suppression plants, as observed in DHD/SHD inhibited plants (Table 5). Because Trp level was too low to be detected in all investigated samples, Phe and Tyr were summed up as the total aromatic amino acids. The reduction of total aromatic amino acids was consistent with the decrease in EPSPS protein.

As a consequence of the blockage of the shikimate pathway, a strong reduction of chlorogenate and lignin (Figure 34) was observed when EPSPS was efficiently inhibited. In EPSPS 20-H plants with more than 70% residual EPSPS protein, a slight decrease of chlorogenate and lignin was measured with values of 90% and 87% of wild type plants, respectively. A 40% to 60%

reduction of EPSPS protein led to a remarkable decrease of above aromatic compounds, in which the chlorogenate and lignin dropped to 61% and 69% of wild type values, respectively.

Table 7. Effects of reduced EPSPS protein on aromatic amino acids production in leaves of tobacco plants

	Wild type	EPSPS 20-H	EPSPS 25-M	EPSPS 51-L	EPSPS 21-VL	
Phe	nmol g ⁻¹ FW	189.97±43.91	175.94±43.13	106.59±21.68	88.40±47.17	364.23±60.88
	Ratio to WT	100%	93%	56%	46%	193%
Tyr	nmol g ⁻¹ FW	21.05±10.66	16.74±6.58	12.74±2.65	13.64±3.24	15.20±3.57
	Ratio to WT	100%	80%	61%	65%	72%

Amino acids were measured in leaf materials taken from 6-week old plants. Wild type control is indicated as WT. Each value represents the mean of 4 different plants ± SE.

An 80% or more reduction of EPSPS protein (EPSPS 21-VL) led to a further reduction of chlorogenate and lignin, to 36% and 32% of wild type value, respectively. The reduction of chlorogenate and lignin was paralleled with the reduction of EPSPS protein.

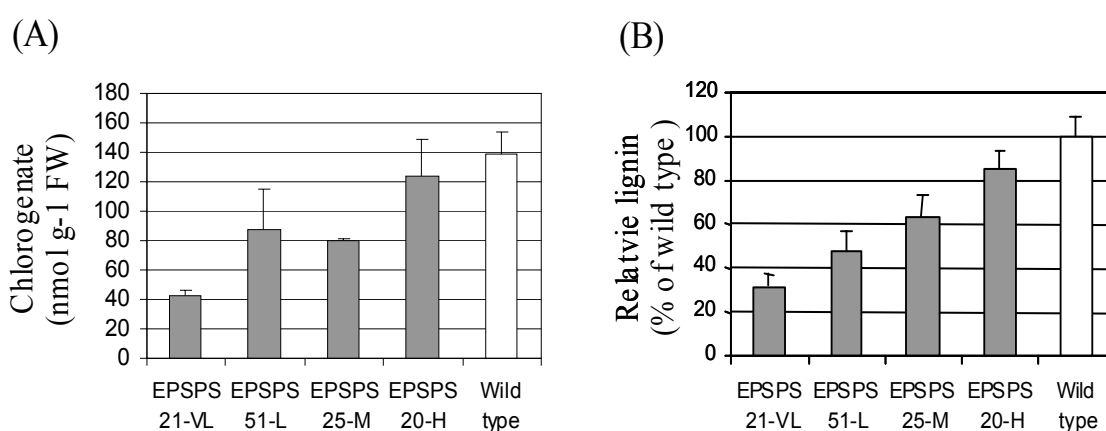


Figure 34. Chlorogenate and lignin content in DHD/SHD RNAi and EPSPS co-suppression plants. (A), Chlorogenate content in EPSPS inhibited plants. Chlorogenate was prepared from tobacco source leaves, which was cultivated in greenhouse for 6 weeks. The content was determined by HPLC. (B), Relative lignin content in EPSPS inhibited plants. Lignin was prepared from the midrib of tobacco source leaves according to Campbell and Ellis (1992). Data are given as the mean of 4 replicates of independent transgenic lines ± SE.

3.5.5 Carbohydrates and chlorophyll

To investigate whether the inhibition of the shikimate pathway may impair primary metabolism, carbohydrate and chlorophyll contents in EPSPS silenced plants were determined. As shown in

Table 8, similar amounts of carbohydrates were detected in all EPSPS silenced plants, suggesting that the silencing of EPSPS had no effect on primary metabolism. In contrast, chlorophyll contents decreased in EPSPS silenced plants.

Table 8. Influence of decreased EPSPS protein on the content of carbohydrates and chlorophyll in tobacco

	Glucose ($\mu\text{mol g}^{-1}$ FW)	Fructose ($\mu\text{mol g}^{-1}$ FW)	Sucrose ($\mu\text{mol g}^{-1}$ FW)	Chlorophyll (mg m^{-2})
EPSPS 21-VL	4.21 \pm 1.03	1.96 \pm 0.33	12.37 \pm 2.15	92.20 \pm 18.36
EPSPS 51-L	3.91 \pm 0.95	2.36 \pm 0.77	12.90 \pm 2.20	159.47 \pm 27.95
EPSPS 25-M	3.94 \pm 0.88	3.23 \pm 0.52	14.41 \pm 2.79	215.17 \pm 50.14
EPSPS 20-H	4.59 \pm 1.31	2.18 \pm 0.72	15.01 \pm 0.113	246.89 \pm 1.34
SNN	4.55 \pm 0.79	2.22 \pm 0.36	14.17 \pm 2.11	262.26 \pm 17.49

Carbohydrates and chlorophyll were measured in leaf materials taken from 6-week old plants. Each value represents the mean of 6 different plants \pm SE.

3.5.6 Silencing of EPSPS resulted in an accumulation of the pathway intermediates

Dehydroquinate and shikimate, the shikimate pathway intermediates were determined in EPSPS co-suppression plants using an enzymatic assay. Transgenic plants with an average of 70%, 50%, 30% and 10% EPSPS protein (EPSPS H, M, L and VL series) accumulated 3, 8, 20 and 30 times of shikimate respectively (Figure 35). In contrast to DHD/SHD RNAi plants, the silencing of EPSPS did not result in an accumulation of dehydroquinate (data not shown).

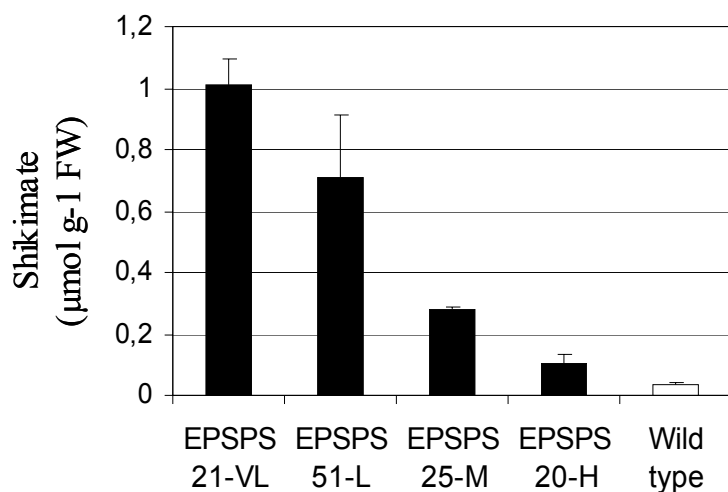


Figure 35. Accumulation of the shikimate in EPSPS co-suppression plants. Shikimate was extracted from tobacco source leaves, which was cultivated in greenhouse for 6 weeks. Shikimate content was determined by an enzymatic assay. Data are given as the mean of 4 replicates of each independent transgenic plants \pm SE.

3.5.7 Shikimate feeding experiment

To check whether the silencing of EPSPS would impair the metabolism of shikimate, a shikimate feeding experiment (section 3.2.9) was performed.

Metabolism of shikimate was evaluated by measuring the production of the aromatic amino acids. As indicated in Table 9, EPSPS silenced plants with an average of 70%, 50%, 30% EPSPS residual protein (EPSPS-H, M and L series, respectively) synthesized 78%, 63% and 49% Phe of wild type levels after feeding (A.F.). When EPSPS protein dropped below 20% of wild type (EPSPS 21-VL), no Phe was synthesized. In contrast, Try biosynthesis was activated in EPSPS silenced plants. More Tyr was synthesized from shikimate in plants with less EPSPS residual protein, suggesting a disturbed balance between Tyr and Phe biosynthesis. Trp could not be detected before or after shikimate feeding experiment.

Table 9. The effects of reduced EPSPS protein on the accumulations of aromatic amino acids in the shikimate feeding experiments

		Wild type	EPSPS 20-H	EPSPS 25-M	EPSPS 51-L	EPSPS 21-VL
Phe (nmol g ⁻¹ FW)	B.F.	189.97±43.91	175.94±43.13	106.59±21.68	88.40±47.17	364.23±60.88
	Ratio to WT	100%	93%	56%	46%	19%
	A.F.	2305.14±132.96	1843.62±84.36	1459.47±199.17	1134.23±240.05	329.52±65.70
	Accumulations to WT	100%	78%	63%	49%	-2%
Tyr (nmol g ⁻¹ FW)	B.F.	21.05±10.66	16.74±6.58	12.74±2.65	13.64±3.24	15.20±3.57
	Ratio to WT	100%	80%	61%	65%	72%
	A.F.	165.41±26.46	182.31±77.20	204.92±47.15	407.16±123.92	517.77±65.99
	Accumulations to WT	100%	115%	133%	273%	348%

Amino acids are determined in leaf materials of 6-week old plants. B.F. means before feeding experiment, A.F. means after feeding experiment. Wild type control is indicated as WT. Each value represents the mean of 4 different plants ± SE.

3.6 Introducing a PEP biosynthetic pathway into chloroplasts

The immediate carbon substrates for the shikimate pathway are Ery4P and PEP. Ery4P can be generated in plastids through the pentose phosphate pathway. Unlike Ery4P, PEP cannot be

generated in plastids. Because most plastids have little or no PGM (phosphoglycerate mutase) and enolase activity, glycolysis cannot proceed further than to 3-phosphoglycerate (Bagge and Larsson, 1986; Stitt, 1997). Plastids therefore rely on the supply with cytosolic PEP. The availability of PEP in chloroplasts was believed to be a limitation for secondary metabolism. To increase the plastidic PEP content and carbon flux to secondary metabolism, a plastidic PEP biosynthetic pathway was created by over-producing *E.coli* PGM and enolase in chloroplasts, which would convert plastidic 3-PGA to PEP.

3.6.1 Chloroplast targeting efficiency of tobacco transketolase transit peptide

Like most chloroplast proteins, transketolase is synthesized as a precursor protein containing a N-terminal amino acid sequence known as transit peptide, which directs the precursor protein to chloroplasts and facilitates its passage through the outer and inner envelope membranes. The construct, TK-TP-GFP was created to investigate chloroplasts targeting efficiency of the transketolase transit peptide.

(A)

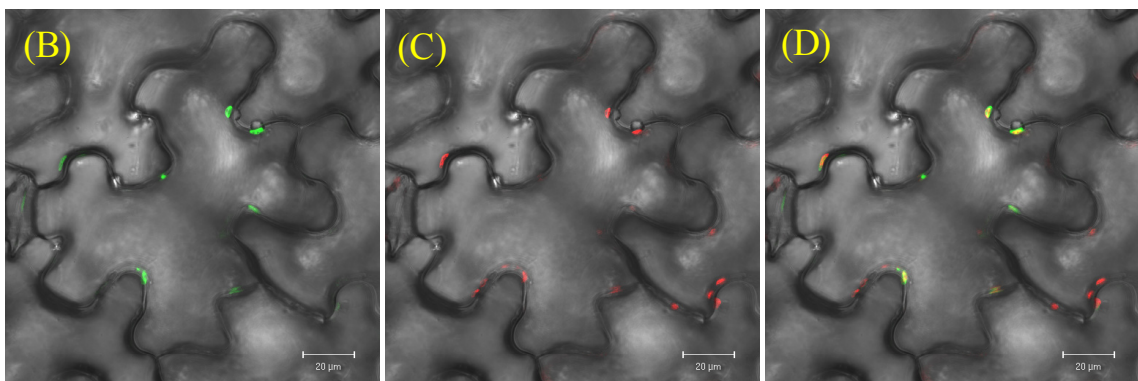
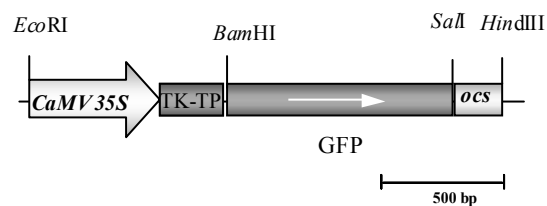


Figure 36. Chloroplast targeting of the transketolase transit peptide. (A), Schematic drawing of pBin-TK-TP-GFP construct. (B), GFP signals were detected in tobacco epidermal cells. (C), chlorophyll signals were detected in tobacco epidermal cells. (D), Co-localization of GFP and chlorophyll resulted in a yellow fluorescence (provided by Bernhard Claus).

The sequence encoding the transit peptide (from codon 1 to 245) of tobacco transketolase (Genbank: E13696) was introduced into the binary vector pBinAR, resulting in the plasmid TK-TP-pBinAR. The coding sequence of the green fluorescence protein (GFP) (Genbank: AF324408) (kindly provided by Dr. Daniel Hofius) was cloned into the binary vector TK-TP-pBinAR 9, between the 35S-TK-TP and the *ocs* terminator to give the construct TK-TP-GFP (Figure 36). Leaf material of *Nicotiana tabacum* L. cv. Samsun NN was transiently transformed by the construct TK-TP-GFP via *Agrobacteria* infiltration (Bechtold and Pelletier, 1998). Subsequently the GFP signal was checked after transient expression in epidermal cells of tobacco source leaves.

As depicted in Figure 36, TK-TP-GFP appeared to be targeted into chloroplasts since GFP signals (Figure 36B) co-localized with the red fluorescence of chlorophyll (Figure 36C) in the merged picture, producing a yellow fluorescence (Figure 36D). GFP localization indicates that TK-TP can efficiently target proteins into chloroplasts.

3.6.2 Introducing *E.coli* PGM and enolase into tobacco chloroplasts

3.6.2.1 Plasmid construction and plant transformation

To express *E. coli* phosphoglycerate mutase and enolase in tobacco plants, constructs TK-TP-PGM and TK-TP-enolase were created. The coding sequence of PGM (GenBank:AE000178) was amplified from genomic DNA of *E.coli* strain K-12 via PCR using primers listed in Table 1 (primer 7, 8). *Bam*HI and *Sal*I restriction sites were added to the 5' end and 3' end of PCR product, respectively. Likewise, the coding sequence of enolase (Genbank: AE000361) was amplified from K-12 attached with 5' *Bam*HI site and 3' *Sal*I site using primers listed in Table 1 (primer 5, 6).

PCR products were cloned into vector pCRBlunt and sequenced to ensure the accuracy of PCR amplification. PGM and enolase were excised from the vector by digestion with *Bam*HI and *Sal*I, and cloned into the binary vector TK-TP-pBinAR 9, between the CaMV 35S-TK-TP and the *ocs* terminator to give the constructs TK-TP-PGM and TK-TP-enolase construct, respectively (Figure 37).

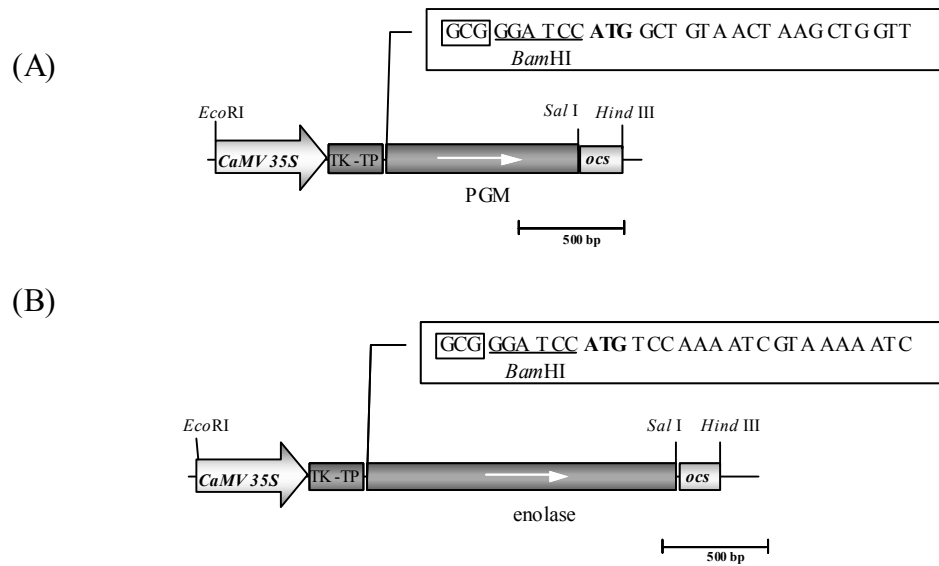


Figure 37. Schematic drawings of pBin-TK-TP-PGM and pBin-TK-TP-enolase construct. (A), pBin-TK-TP-PGM construct was created by inserting the coding sequence of PGM into the binary vector TK-TP-pBinAR, between 35S-TK-TP and *ocs* terminator. (B), pBin-TK-TP-enolase construct was created by inserting the coding sequence of enolase into the binary vector TK-TP-pBinAR, between 35S-TK-TP and *ocs* terminator. Reading frame as indicated in box. Translation start codon is indicated in bold.

The binary vector was transformed into *Agrobacterium tumefaciens* strain C58C1 (pGV2260). Following *Agrobacterium* mediated gene transfer, 80 independent primary transformants were obtained from each constructs. After two weeks in the greenhouse, plants were screened using enzyme assay for PGM or enolase activity (Figure 38).

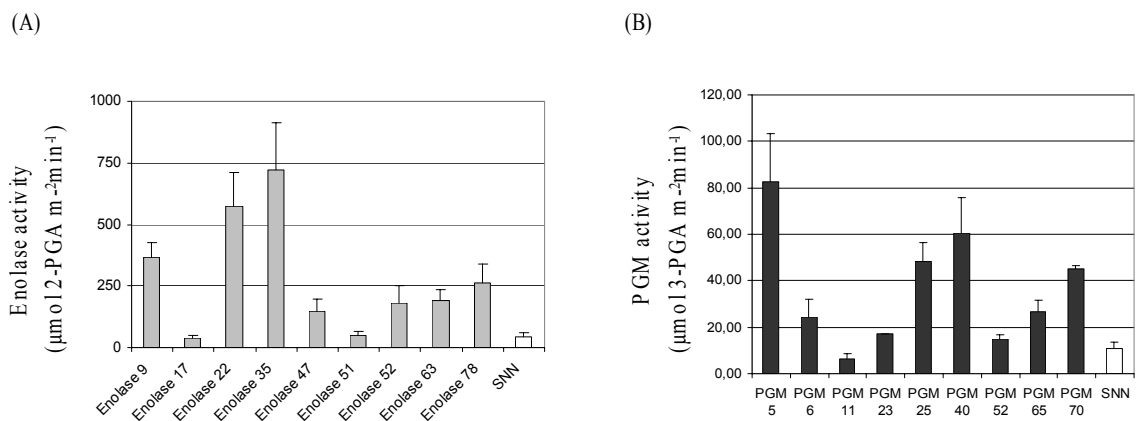


Figure 38. Enolase and PGM activity in TK-TP-enolase and TK-TP-PGM plants. Enolase activity in wild type plants was calculated to be $44.21 \pm 5.34 \mu\text{mol shikimate m}^{-2} \text{ min}^{-1}$. PGM activity in wild type plants was calculated to be $10.54 \pm 2.64 \mu\text{mol shikimate m}^{-2} \cdot \text{min}^{-1}$. Enzyme activity was measured in leaf materials taken from 6-week old plants. Data are given as the mean of 4 replicates of each independent transgenic plants \pm SE.

27 enolase positive lines and 33 PGM positive lines with different levels of corresponding enzyme activity was obtained. PGM and enolase activity was determined as described in materials and methods. Based on enzyme activity, 6 enolase positive lines and 6 PGM lines were selected for detailed analysis.

3.6.2.2 Growth characterization of transgenic plants

All of 27 TK-TP-enolase plants with an elevated enolase activity (1.2-16 times higher than wild type plants) developed wild type like phenotypes.

In contrast, TK-TP-PGM plants developed two apparently different phenotypes. 17 out of 33 TK-TP-PGM transgenic lines, with 1.6 to 6.7 folds increase in PGM activity, exhibited a bleached phenotype, with dark green paraveinal and light green interval regions (Figure 39B). The growth of the transgenic plants was slightly delayed, compared to the wild type plants (Figure 39C). Three PGM transgenic lines, with 2.5 to 4.3 times increase of PGM activity, exhibited a dwarfed phenotype (Figure 39D, E). In contrast to the bleached plants, the growth of these 3 plants was strongly inhibited. The fully extended major stems of these three plants were about 8- 15 cm high, which was only one tenth of wild type plants. Side shoots developed into secondary stems. The major stem developed 10-14 leaves, and each of the secondary stems developed 8-10 leaves (Figure 39F).

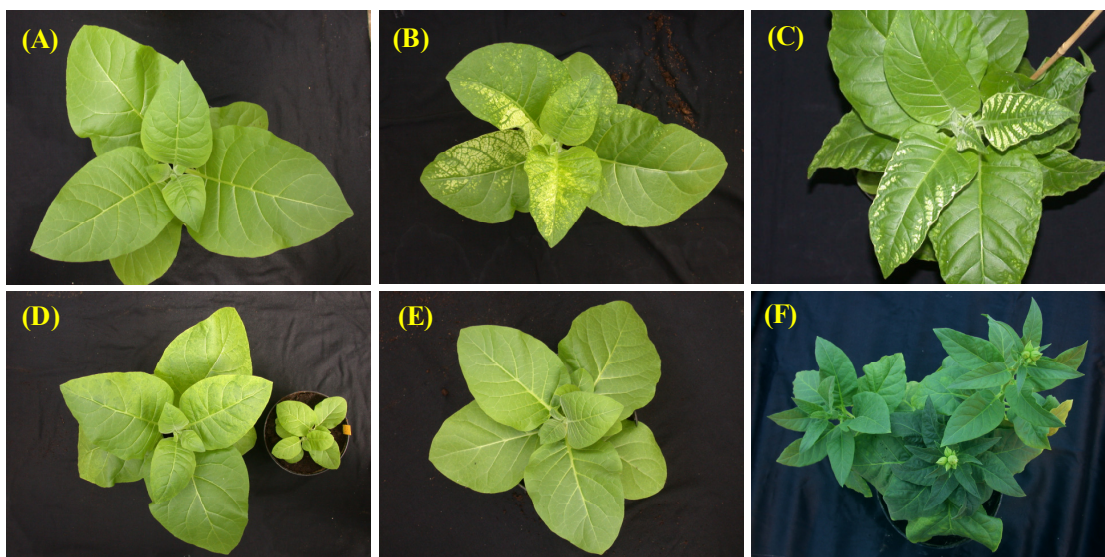


Figure 39. Phenotypes of TK-TP-PGM transgenic plants. (A), Wild type plants (4 weeks old). (B), transgenic plants with bleached phenotype (4 weeks old). (C), Transgenic plants with bleached phenotype (12 weeks old). (D), Comparison of transgenic plants showing bleached phenotypes and dwarfed phenotypes (4 weeks old). (E), TK-TP-PGM plants showing dwarfed phenotypes (4 weeks old). (F), Fully developed dwarfed plants (12 weeks old).

Bleached plants were able to produce a dwarfed progeny. For examples, PGM5 and PGM40, which exhibited a bleached phenotype in the T0 generation, produced 2 types of offspring, the bleached phenotype and the dwarfed phenotype, with the ratio of 7:3 and 8:2, respectively. In contrast, dwarfed PGM plants only produced dwarfed offspring.

Although PGM activity increased in all plants showing phenotypes, the elevation of PGM activity did not correlate with individual phenotypical changes. The dual-phenotype of PGM plants was quite puzzling. It could be postulated that one phenotype resulted from the elevation of PGM activity, and the other was a result of the silencing of transketolase or PGM in transgenic plants. However, this hypothesis was not supported by the expression analysis of corresponding genes. A similar amount of transketolase transcript was detected in all transgenic and wild type plants by Northern blot hybridization, suggesting that the co-suppression effect of TK-TP sequence is negligible in transgenic plants (Figure 40).

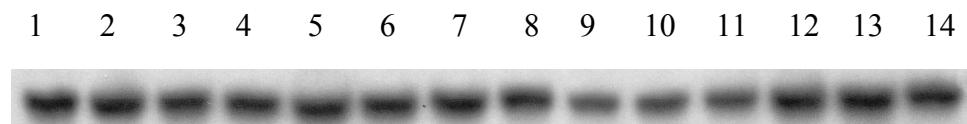


Figure 40. Northern blot analyses of transketolase transcripts in TK-TP-PGM transgenic plants. 30 μ g total RNA was prepared from tobacco source leaves, which was cultivated in greenhouse for 6 weeks. RNA was separated on a 1.5% agarose gel, blotted and hybridized using transketolase probe which were labeled with 32 P-dCTP. Lane 1-6: TK-TP-PGM transgenic plants showing bleached phenotype; Lane 7-12: TK-TP-PGM transgenic plants showing dwarfed phenotype. Lane 13-14 wild type plants.

In addition, TK-TP-enolase transformants did not develop any phenotypes, suggesting that the transketolase transit peptide cannot be responsible for the phenotypes. The silencing of endogenous of PGM homolog in tobacco can also be excluded as the possible reason of the dual-phenotype phenomenon, because PGM fragment did not hybridize with wild type tobacco mRNA (data not shown), indicating that no homolog of *E.coli* PGM exists in tobacco.

To characterize the effect of the increased PGM and enolase activity on biomass production, TK-TP-PGM and TK-TP-enolase plants were germinated from seeds (T1 generation) in sand and fertilised with nutrient solution, as described in Geiger et al. (1999). Wild type like growth parameters were measured in TK-TP-enolase plants (data not shown). In contrast, in TK-TP-PGM plants, a weak reduction and a strong reduction of growth parameters were measured in bleached plants and dwarfed plant, respectively, as shown in Table 10.

Table 10. Growth parameters of TK-TP-PGM transgenic plants

	PGM activity ($\mu\text{mol m}^{-2} \text{min}^{-1}$)	Shoot Numbers	Leaf numbers	Main Shoot FW (g)	Total Shoot FW (g)	Main Shoot DW (g)	Total Shoot DW (g)	Shoot Length (cm)
PGM 25	47.32±8.12	6.25±0.95	48.50±9.37	10.1±3.45	20.16±5.35	1.29±0.17	2.62±0.34	10.08±1.06
PGM 65	25.96±4.85	4.75±1.71	41.00±11.59	10.3±2.77	20.44±5.07	1.24±0.21	2.46±0.37	9.56±0.79
PGM 5	80.88±20.66	1	22.25±7.09	82.69±12.84	82.69±12.84	6.97±0.89	6.97±0.89	83.21±6.47
PGM 70	44.26±1.26	1	18.75±5.97	74.71±13.70	74.71±13.70	6.16±0.74	6.16±0.74	88.93±7.26
WT	10.54±2.64	1	22.25±8.59	95.55±14.65	95.55±14.65	10.35±1.20	10.35±1.20	103.31±11.82

Plant parameters were determined in plants, which was cultivated in greenhouse for 12 weeks. Each value represents the mean of 6 different plants \pm SE. Wild type control was indicated as WT. PGM25 and PGM 65 are dwarfed plants; PGM5 and PGM 70 are bleached plants.

3.6.2.3 PEP and 3-PGA content in transgenic plants

In the first step of the Calvin cycle, one molecule of CO_2 reacts with one molecule of ribulose 1.5-bis-phosphate (RuBP) to yield two molecules of 3-PGA. Under the catalysis of 3-phosphoglycerate kinase (PGK) and NADP: glyceraldehyde-3-phosphate dehydrogenase (GAPDH), 3-PGA is reduced to glyeraldehyde-3-phosphate (GAP) to participate in the regeneration of RuBP.

The elevation of PGM activity would disturb the biosynthesis of 3-PGA in transgenic plants. Although PGM catalyzed a reversible reaction, the high-level of 3-PGA vs. low-level of 2-PGA in chloroplasts facilitated the conversion of 3-PGA to 2-PGA. As shown in Figure 41, the increase of PGM activity in chloroplasts in the bleached plants led to a sharp decrease of 3-PGA (line PGM5, 6, 40, 52 and 70), whereas in the dwarfed plants, the elevation of PGM activity did not result in a pronounced decrease of 3-PGA (line PGM 11, 25 and 65).

The increases of enolase activity in chloroplasts did not lead to a decrease of 3-PGA content in TK-TP-enolase plants (Figure 42). 3-PGA is not a direct substrate for enolase. Although enolase activity increased substantially in TK-TP-enolase plants, the lack of PGM activity in chloroplasts hindered the metabolism of 3-PGA to PEP.

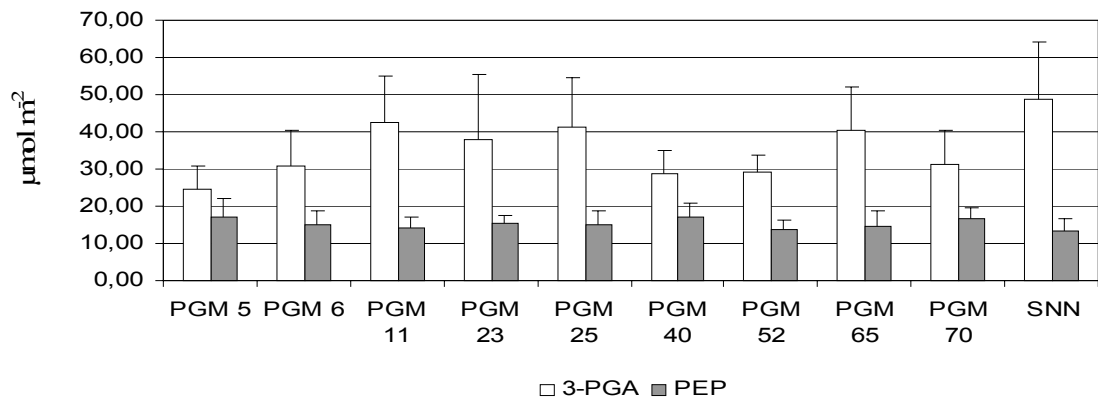


Figure 41. 3-PGA and PEP contents in TK-TP-PGM transgenic plants. 3-PGA and PEP were determined in leaf materials of 6-week old plants. Data are given as mean of 4 replicates of each independent transgenic plants \pm SE.

To convert 3-PGA to PEP, both enolase and PGM are required. Because the endogenous PGM and enolase is negligible in chloroplasts, an individual increase of either enzyme would not contribute to a significant increase of PEP content in this compartment. Thus a similar amount of PEP was measured in all transgenic plants and wild type plants.

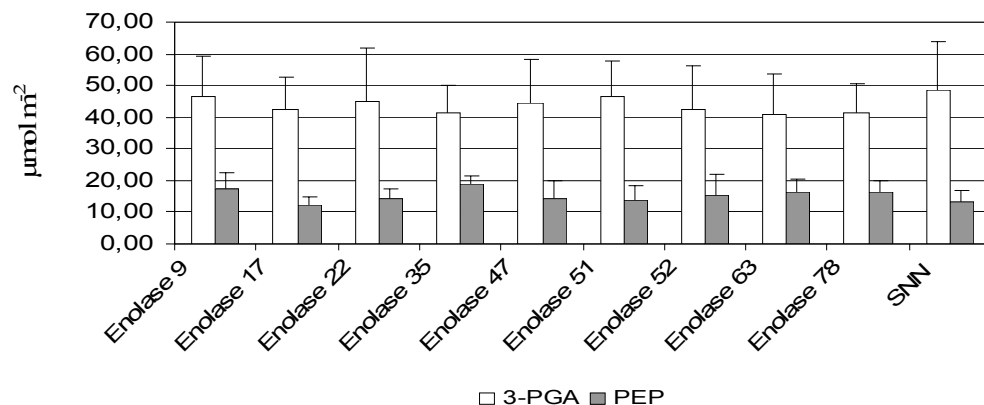


Figure 42. 3-PGA and PEP in TK-TP-enolase transgenic plants. 3-PGA and PEP were determined in leaf materials of 6-week old plants. Data were given as the mean of 4 replicates of each independent transgenic plants \pm SE.

3.6.2.4 Carbohydrates contents in transgenic plants

To investigate the impact of the elevated plastidic enolase or PGM activity on primary metabolism, carbohydrates were determined in transgenic plants. As shown in Table 11, soluble sugars and starch decreased dramatically in PGM bleached plants (PGM 5), and remained unchanged in PGM dwarfed plants (PGM 65) and enolase plants (enolase 22).

Table 11. Carbohydrates and chlorophyll in TK-TP-PGM and TK-TP-enolase plants

	PGM activity ($\mu\text{mol m}^{-2} \text{min}^{-1}$)	Enolase activity ($\mu\text{mol m}^{-2} \text{min}^{-1}$)	Glucose ($\mu\text{mol m}^{-2}$)	Fructose ($\mu\text{mol m}^{-2}$)	Sucrose ($\mu\text{mol m}^{-2}$)	Starch ($\mu\text{mol m}^{-2}$)
PGM 5	80.88±20.66	39.56±3.09	318.67±166.57	248.92±51.32	347.03±87.52	1005.87±113.56
PGM 65	25.96±4.85	56.37±7.08	642.03±116.06	414.45±49.94	645.63±97.52	2688.71±218.28
enolase 22	13.25±3.11	615.24±162.25	667.45±101.31	265.52±27.65	531.50±77.33	2567.10±292.12
Wild type	10.54±2.64	44.21±8.62	769.49±248.04	382.24±90.56	766.60±93.65	2737.39±387.81

Carbohydrates were measured in leaf materials of 6-week old plants. PGM 65 is a dwarfed plant. PGM5 is a bleached plant. Each value represents the mean of 6 different plants \pm SE.

In chloroplasts, 3-PGA is reduced to GAP, which joins in starch synthesis in chloroplasts and sucrose synthesis in the cytosol. The increase of PGM activity in bleached plants (PGM 5) depleted 3-PGA in chloroplasts, thus leading to a substantial reduction of sucrose and starch. In contrast, the increase of PGM activity in PGM dwarfed plants (line PGM 65) did not lead to a reduction of 3-PGA, and this did not impair the biosynthesis of sucrose and starch (Table 11). 2-PGA is the product of PGM and the substrate of enolase. In TK-TP-enolase plants, due to the lack of PGM activity, 2-PGA content is low in chloroplasts. An increase of enolase did not result in changes of PEP and 3-PGA contents in the transgenic plants. Thus, a similar amount of soluble sugars and starch was detected in TK-TP-enolase plants (line TK-TP-enolase 22) as compared to wild type plants.

3.6.2.5 Aromatic amino acids and total soluble phenolics in transgenic plants

Amino acids were determined by HPLC (Table 12). Total amino acid content increased in both TK-TP-PGM and TK-TP-enolase plants. In TK-TP-PGM bleached plants (line PGM5), the depletion of 3-PGA led to a reduction of 3-PGA derived amino acids (Ser, Gly and Cys). In TK-TP-enolase plants, the increase of enolase activity did not lead to a decrease of 3-PGA, and a similar amount of Ser and Gly were measured.

PEP and Ery4P concentration are believed to determine the carbon flux rate to secondary metabolism. The introduction of PGM or enolase alone into chloroplasts did not lead to an increase of PEP production. In addition, the enhanced conversion of 3-PGA to 2-PGA in chloroplasts strongly inhibited the Calvin cycle, which might lead to a decreased supply of Ery4P in PGM transgenic plants.

Table 12. Contents of amino acids of TK-TP-PGM and TK-TP-enolase transgenic plants

	PGM5	PGM65	Enolase 22	Wild type
Asp	73.15±17.25	88.17±14.57	46.21±3.18	32.07±5.09
Glu	145.60±28.82	188.68±17.07	124.02±39.27	76.70±12.01
Ser	104.89±15.25	219.75±10.66	148.31±7.96	182.35±26.87
Asn	8.62±1.68	17.76±2.25	26.51±3.79	36.65±8.35
Gly	166.30±27.70	206.86±1.90	204.24±1.78	205.33±1.94
Gln	34.29±8.23	29.33±2.35	35.74±2.52	26.61±3.82
His	46.47±11.73	1.78±0.42	2.20±0.63	22.56±14.51
Thr	450.84±22.32	179.87±5.51	217.82±13.64	177.69±18.01
Arg	12.13±1.99	10.25±0.79	13.70±0.75	38.10±8.52
Ala	134.71±13.53	207.18±6.51	208.85±15.96	160.19±17.59
Pro	153.76±18.48	185.77±7.57	154.53±16.80	120.59±12.76
Tyr	2.05±0.27	1.82±0.08	3.01±0.17	3.62±0.74
Cys	12.24±1.34	12.44±3.40	14.28±1.42	21.68±4.93
Val	12.57±0.69	13.86±0.66	12.97±0.89	17.08±1.92
Met	2.67±0.35	2.21±0.15	1.83±0.12	4.35±1.53
Ile	2.50±0.48	11.12±0.55	4.36±1.16	10.20±1.18
Lys	5.55±0.80	6.78±0.93	5.11±0.49	14.10±2.24
Leu	4.85±1.60	1.93±0.37	2.95±0.14	5.48±3.22
Phe	15.61±0.88	14.55±0.83	14.54±0.92	13.98±1.06
Total	1388.78±134.79	1400.13±27.01	1240.19±78.60	1169.33±58.07

Amino acids were measured from leaf materials, which was cultivated in the greenhouse for 6 weeks. PGM 65 is a dwarfed plant. PGM5 is a bleached plant. Each value represents the mean of 6 different plants ± SE.

Thus, the increase of enolase alone in chloroplasts would not help to increase carbon flux into secondary metabolism; whereas the increase of PGM alone might even lead to a reduced production of phenolic compounds.

3.6.3 Establishment of a plastidic PEP biosynthetic pathway

The aim this project was to increase plastidic PEP production by mobilizing the 3-PGA reservoir in chloroplasts, and therefore to increase the carbon flux into the shikimate pathway. To convert 3-PGA to PEP, both enolase and PGM are required. As shown in the previous section, an increase of either enzyme would not contribute to a significant increase of PEP production in chloroplasts. To create a plastidic PEP biosynthetic pathway, both PGM and enolase should be introduced into chloroplasts.

3.6.3.1 Plasmid construction and plant transformation

To create PGM-enolase construct, the 35S-TK-TP-Enolase-*ocs* fragment with *Hind*III sites on both 5' and 3' end was PCR-amplified from the plasmid TK-TP-enolase using 35S promoter and *ocs* terminator primers (Table 1 primer 9, 10). The fragment was cloned into the *Hind*III site of plasmid TK-TP-PGM to give the construct PGM-enolase (Figure 43). The binary vector was transformed into *Agrobacterium tumefaciens* strain C58C1 (pGV2260). Following *Agrobacterium*-mediated gene transfer, 60 independent kanamycin-resistant tobacco plants were regenerated and transferred to the greenhouse.

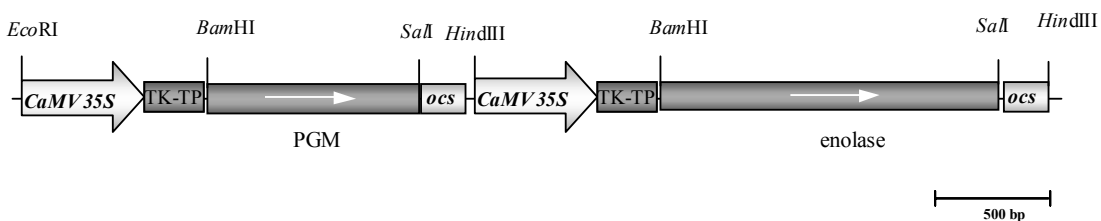


Figure 43. Schematic drawing of PGM -enolase construct. The PGM-enolase construct was created by inserting the fragment TK-TP-enolase-*ocs* into the *Hind*III site of the binary construct pBin-TK-TP-PGM.

11 transgenic plants were shown to express both PGM and enolase by enzyme activity screening. The overproduction of PGM and enolase together did not result in phenotypes other than phenotypes of TK-TP-PGM alone. Among 11 transgenic plants, 7 plants displayed the bleached phenotype, 2 displayed the dwarfed phenotype, and other 2 plants showed wild type like phenotype. The bleached phenotype was the major phenotype observed in PGM single positive plants, and it was correlated with the increase of PGM activity and decrease of 3-PGA. In contrast, the dwarfed phenotype was the minor phenotype, and the increase of PGM activity did not result in a decrease of 3-PGA and sugars content in these dwarfed plants. Thus, 2 wild type like plants and 4 bleached plants were selected for the detailed analyses.

3.6.3.2 Conversion efficiency of 3-PGA to PEP in transgenic plants

The coupling efficiency between PGM and enolase might determine the conversion of 3-PGA to PEP in transgenic plants. To determine the coupling efficiency, protein extracts of tobacco plants were incubated in enolase reaction buffer, the measurement was started by the substrate 3-PGA, instead of 2-PGA. Conversion of 3-PGA to PEP was determined by checking the production of PEP in the reaction mixture. As shown in Figure 44, PGM-enolase lines 1, 22, 47 and 53, gave high 3-PGA to PEP conversion velocities and were selected for further analyses.

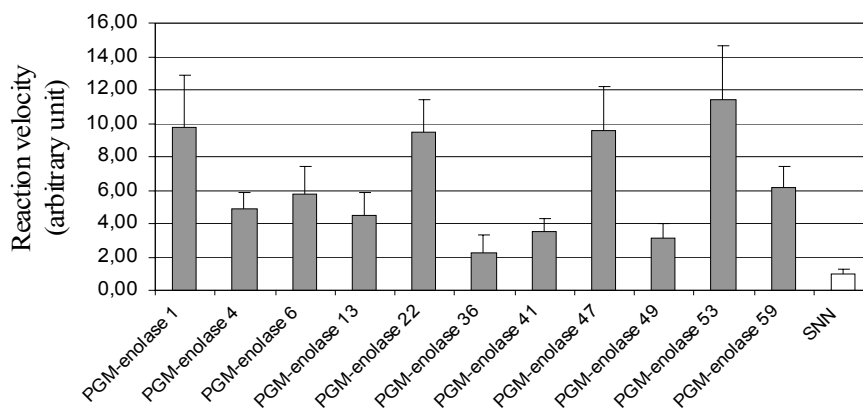


Figure 44. Conversion efficiency of 3-PGA to PEP in PGM-enolase transgenic plants. Data were given as the mean of 4 replicates of independent transgenic plants \pm SE.

3.6.3.3 PEP, pyruvate and 3-PGA content in transgenic plants

In chloroplasts, 2-PGA is converted to PEP under the catalysis of enolase, thus both enolase activity and 2-PGA are prerequisites for the production of PEP. In PGM-enolase plants, the first requirement was fulfilled directly by introducing enolase into chloroplasts, whereas the second was accomplished by elevating PGM activity, which would produce 2-PGA from the 3-PGA pool in chloroplasts.

As shown in Figure 45, the coupling of PGM and enolase in chloroplasts led to an increased PEP production. PGM-enolase lines 1, 22, 47 and 53 with an optimum coupling between PGM and enolase gave the best result of PEP production. Pyruvate, which could be synthesized from PEP in a reaction catalyzed by pyruvate kinase, was also found to accumulate in PGM-enolase plants. In most cases, the buildup of pyruvate paralleled the PEP accumulation. In contrast to the increase of PEP content, 3-PGA decreased dramatically in PGM-enolase plants. The decrease of 3-PGA correlated with the increase of PEP and pyruvate.

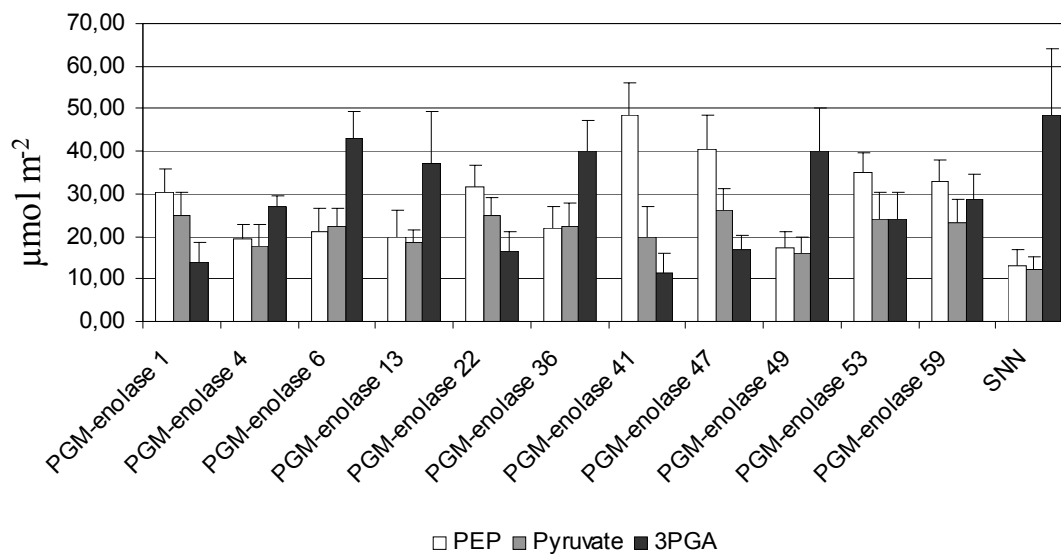


Figure 45. Contents of 3-PGA, PEP and pyruvate in PGM-enolase transgenic plants. 3-PGA, PEP and pyruvate were determined by an enzymatic assay. Metabolites were prepared from leaf materials of 6-week old plants grown in the greenhouse. Data were given as the mean of 4 replicates of each independent transgenic plants \pm SE.

Although the elevated PGM and enolase activity in chloroplasts disrupted the balance between 3-PGA, PEP and pyruvate, the total amount of these intermediates (3-PGA, PEP and pyruvate) were similar in all transgenic plants and wild type plants (Figure 45), suggesting that the PEP and pyruvate in chloroplasts of the transgenic plants might not be efficiently metabolized.

3.6.3.4 Carbohydrates content in transgenic plants

Plastidic 3-PGA play an essential role in carbohydrates biosynthesis. On one hand, 3-PGA participates the regeneration of RuBP in the dark reaction of photosynthesis, which regulates the carbon fixation efficiency. On the other hand, this metabolite can be reduced to GAP to join in starch synthesis in chloroplasts and sucrose synthesis in the cytosol.

The introduction of PGM and enolase into chloroplasts disrupted the balance between 3-PGA and PEP. Thus both primary and secondary metabolism would be affected. To evaluate carbon flux to primary metabolism, soluble sugars and starch were determined in plants with elevated PGM and enolase activity. As indicated in Table 13, soluble sugars and starch contents decreased dramatically in the PGM-enolase plants. The reduction of carbohydrates paralleled the decrease of 3-PGA (Figure 45).

Table 13. Carbohydrates content of PGM-enolase plants

	Glucose ($\mu\text{mol m}^{-2}$)	Fructose ($\mu\text{mol m}^{-2}$)	Sucrose ($\mu\text{mol m}^{-2}$)	Starch ($\mu\text{mol m}^{-2}$)
PGM-enolase 1	205.31 \pm 86.32	219.28 \pm 61.12	206.39 \pm 67.33	808.11 \pm 193.89
PGM-enolase 47	311.07 \pm 69.77	207.12 \pm 45.07	222.94 \pm 39.69	741.09 \pm 87.62
PGM-enolase 53	280.34 \pm 64.85	179.08 \pm 64.26	238.37 \pm 46.24	930.37 \pm 148.61
Wild type	769.49 \pm 248.04	382.24 \pm 190.56	766.60 \pm 93.65	2737.39 \pm 387.81

Carbohydrates were measured in leaf materials of 6-week old plants. The data are the mean \pm SD of 4 independent replicates.

3.6.3.5 Amino acids, chlorogenate and total soluble phenolic compounds

Under the catalysis of a series of seven enzymes of the shikimate pathway, 2 molecules of PEP and 1 molecule of Ery4P are converted to 1 molecule of chorismate. Thus PEP level is supposed to play a crucial role in determining the carbon partitioning between primary and secondary metabolism.

3-PGA, PEP and pyruvate participate in the biosynthesis of amino acids in plants (Figure 46). In PGM-Enolase plants, PEP and pyruvate content increased significantly, whereas 3-PGA content decreased dramatically. Therefore, amino acids content might change in transgenic plants accordingly.

Amino acids were determined in the transgenic plants by HPLC. As shown in Table 14, total amino acid content increased in PGM-enolase plants. This was mainly due to a big increase of Glu, Thr, Ala and Pro. Although pyruvate content increased in transgenic plants, Ala, Val and Leu, which are derived from pyruvate, did not increase accordingly. One possible reason is that these three amino acids are synthesized in the cytosol, whereas pyruvate increased in chloroplasts. In contrast to pyruvate, 3-PGA could be transported from chloroplasts to cytosol. The depletion of 3-PGA in chloroplasts might lead to a reduced 3-PGA content in the cytosol. Thus, 3-PGA derived amino acids (Ser, Gly and Cys) decreased dramatically in PGM-enolase plants.

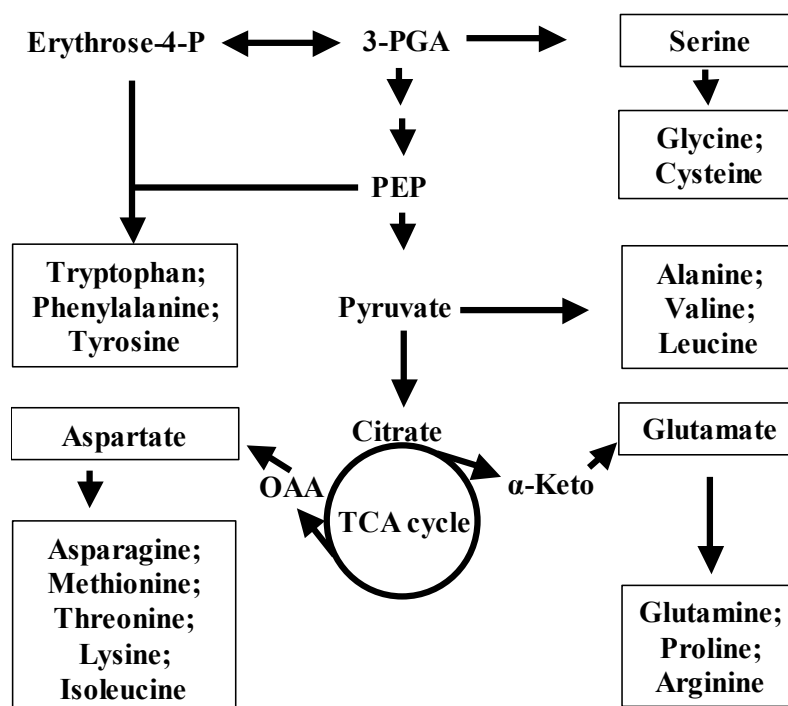


Figure 46. The biosynthesis of amino acids in plant.

The increase of PEP production influenced the biosynthesis of aromatic amino acids in PGM-enolase plants (Table 14). Phe increased 53% to 71% in PGM-enolase plants, whereas Tyr content decreased 18% to 37%. Trp content was beyond detection in both transgenic and wild type plants. Thus Phe and Tyr were summed up to give an estimation of total aromatic amino acids production. Total aromatic amino acids increased by 56% in PGM-enolase plants. The result suggested that the increase of plastidic PEP enhanced the biosynthesis of aromatic amino acids.

Table 14. Contents of amino acids in wild type plants and PGM-enolase plants

	Wild type	PGM-Enolase1	PGM-Enolase 47	PGM-Enolase 53
Asp	32.07±5.09	65.80±10.70	127.80±7.63	66,42±4,42
Glu	76.70±12.01	249.40±25.72	345.94±6.29	267,77±7,71
Ser	182.35±26.87	107.70±12.65	108.24±5.74	122,46±1,29
Asn	36.65±8.35	64.06±3.89	28.75±0.98	57,19±2,76
Gly	205.33±1.94	103.00±2.46	118.05±0.45	128,77±2,50
Gln	26.61±3.82	52.47±3.88	163.23±5.42	155,93±11,86
His	22.56±14.51	3.22±0.42	2.21±0.07	10,64±0,79

Thr	177.69±18.01	263.66±12.25	463.82±4.66	415,97±32,65
Arg	38.10±18.52	12.17±0.74	10.36±0.43	40,06±5,34
Ala	160.19±17.59	177.35±14.60	195.37±3.15	147,56±4,87
Pro	120.59±12.76	210.93±9.38	232.53±6.43	204,6±13,24
Tyr	3.62±0.74	2.95±0.25	3.02±0.08	2,28±0,14
Cys	21.68±4.93	11.81±2.13	10.78±0.63	10,17±1,21
Val	17.08±1.92	19.35±0.87	17.29±0.44	15,00±0,74
Met	4.35±1.53	2.60±0.17	2.75±0.09	5,30±0,27
Ile	10.20±1.18	21.06±0.27	7.88±0.06	13,22±0,35
Lys	14.10±2.24	11.03±1.62	2.83±0.12	8,19±0,37
Leu	5.48±3.22	7.31±0.37	5.10±0.01	7,91±2,40
Phe	13.98±1.06	23.98±1.09	24.58±0.56	21,38±0,81
Total	1169.33±58.07	1452.85±79.40	1772.51±27.97	1703,91±91,31

Amino acids were measured from leaf materials, which was cultivated in the greenhouse for 6 weeks. The amount of amino acids is given as $\mu\text{mol m}^{-2}$. The data are the mean \pm SD of 4 independent replicates.

Chlorogenate is the major soluble phenylpropanoid in tobacco and a preformed protectant against fungal attack (Maher et al., 1994). Although not pronouncedly, the increase of plastidic PEP led to an elevated production of chlorogenate in transgenic plants (Table 15).

Table 15. Chlorogenate and total soluble phenolics in PGM-enolase plants

	Chlorogenate ($\mu\text{mol m}^{-2}$)	Total soluble Phenolics (mmol m^{-2})
PGM-enolase 1	197.65±26.54	1.06±0.17
PGM-enolase 47	207.62±42.32	0.97±0.11
PGM-enolase 53	224.14±52.61	0.95±0.08
Wild type	169.25±31.48	0,84±0.05

Chlorogenate and total soluble phenolics were measured from leaf materials, which was cultivated in the greenhouse for 6 weeks. The data are the mean \pm SD of 4 independent replicates.

In addition, total soluble phenolic compounds were measured in transgenic plants by Folin-Ciocalteu reagent (Díaz and Merino, 1998). As indicated in Table 15, total soluble phenolics increased by 13%-26% in PGM-enolase plants, suggesting that the increase of PEP production

enhanced the phenolic compounds production in transgenic plants. However, when compared with the increase of PEP in transgenic plants, which given a value of 153%-242% (Figure 45), the increase of secondary metabolites production was not significant.

4 Discussion

4.1 Constitutive silencing of Nt-DHD/SHD-1 in tobacco

The shikimate pathway links primary and secondary metabolisms. Under normal growth conditions about 20% of fixed carbon runs through this pathway to secondary metabolites (Haslam, 1993). Thus this pathway was believed to be a pivot, which regulate carbon partitioning between primary and secondary metabolism. Researches on this pathway mainly focus on two subjects: 1. The regulation mechanism of the pathway; and 2. The Identification of targets for herbicide or drug. Most of information was acquired from DAHPS (Entus et al., 2002), the first enzyme of the pathway and EPSPS (Hollaender-Czytko and Amrhein, 1983; Jensen, 1985; Steinrucken et al., 1986; Pline et al., 2002), the enzyme target of glyphosate. Little is know about other enzymes of this pathway, e.g. DHD/SHD. To investigate the physiological roles and the regulation mechanisms of the pathway, RNAi (RNA interference) technique was applied to silence the expression of corresponding genes.

4.1.1 Silencing of Nt-DHD/SHD-1 led to a reduced biosynthesis of secondary metabolites

dsRNA triggered the silencing of Nt-DHD/SHD-1 in tobacco, and led to severe phenotypic and metabolic alterations (Chapter 3.2.3, Figure 10). A 50% reduction of DHD/SHD activity (DHD/SHD-M plants) resulted in bleached leaves, and a further reduction of DHD/SHD activity to 40% of wild type value led to strong decreases of growth parameters, highlighting the importance of DHD/SHD for plant development. Further reduction of endogenous DHD/SHD activity (DHD/SHD-VL plants) led to a lethal phenotype, in which case transgenic plants were stunted, and died 2-3 weeks after being transferred to the greenhouse. The approximately linear correlation between DHD/SHD residual activity and the amounts of phenolic compounds indicates the crucial role of the shikimate pathway enzymes in controlling carbon flux towards secondary metabolism.

4.1.2 Silencing of Nt-DHD/SHD-1 activated the transcription of DAHPS

The demand for phenolic metabolites varies during plant development or under environmental stress such as wounding or pathogen attack. Therefore, mechanisms that regulate carbon flow towards the shikimate pathway must perceive and respond accordingly. Expressions of

shikimate pathway enzymes were probed in DHD/SHD RNAi plants, to investigate the regulation mechanism. Among seven shikimate pathway enzymes, DAHPS was the only one found to be regulated on the transcriptional level in DHD/SHD silenced plants. As shown in Figure 11 (Chapter 3.2.4), four times more DAHPS RNA was detected in plants with 20 % or lower DHD/SHD residual activity. The Northern blot hybridization was supported by cDNA macroarray, which detected the activation of secondary metabolism genes, including DAHPS, PAL, and PPT, in DHD/SHD silenced plants (Chapter 3.2.5, Figure 12). In addition to the transcript analysis, activities of the downstream enzymes were determined by shikimate feeding to leaf disks. Leaves of transgenic and wild type plants synthesized a similar level of phenylalanine and tyrosine shortly after being fed with shikimate. Even when DHD/SHD activity dropped to very low level, still 79 % of phenylalanine and tyrosine was produced as compared to wild type plants (Chapter 3.2.9, Table 5), suggesting that the silencing of DHD/SHD did not lead to a regulation of the downstream enzymes. The activation of DAHPS transcription was previously described, when plants were challenged by abiotic stresses such as mechanical wounding (Dyer et al., 1989) and glyphosate (Pinto et al., 1988), indicating DAHP synthase represents a target for controlling carbon flow through the shikimate pathway. A regulation mechanism can be figured out that low level of phenolic compounds may signal, or initiate a certain signal to activate the expression of DAHPS, and as a result, to direct more carbon flux to the shikimate pathway.

DHD/SHD RNAi plants accumulated a high level of dehydroquinic acid and shikimate. To check if these chemicals were responsible for the activation of DAHP synthase, tobacco leaves were treated with both compounds via *in vitro* feeding and *in vivo* injection. Similar amounts of DAHPS mRNA were detected in all treated samples and control plants 48 hours after the treatment (data not shown), indicating that shikimate and dehydroquinic acid could not activate the expression of DAHP synthase.

4.1.3 Silencing of Nt-DHD/SHD-1 led to an accumulation of shikimate and dehydroquinic acid

Silencing of an enzyme usually results in a reduction of its product. Unexpectedly, the silencing of DHD/SHD gave contradictory data. In DHD/SHD RNAi plants, the silencing of DHD/SHD enzyme resulted in a buildup of dehydroquinic acid and shikimate, which were the substrate and product of this enzyme, respectively (Chapter 3.2.8, Figure 15). The accumulation of dehydroquinic acid and shikimate was correlated with DHD/SHD residual activity in transgenic

plants: the less DHD/SHD activity, the more dehydroquinate and shikimate. The obvious contradiction of the decreased DHD/SHD activity and the accumulation of shikimate could not be explained by the downregulation of the downstream reactions, because the feeding experiment indicated that shikimate can be metabolized at a similar efficiency in transgenic plants as in wild type plants (Chapter 3.4.9, Table 5). The accumulation of pathway intermediates was kinetically analyzed in ethanol inducible gene silencing system (Chapter 4.2.1). Based on the results, a metabolite shuttle model (Chapter 4.2.2, Figure 47) was established to interpret the accumulation of shikimate in DHD/SHD silenced plants.

4.1.4 Nt-DHD/SHD-1 might be regulated by light

The chemiosmotic theory of energy transduction across the chloroplast thylakoid membrane postulated that a pH gradient between the stroma and the thylakoid lumen developed under illumination (Carmeli, 1970). The light induced stromal alkalization is quickly reversed in the dark as protons passively diffuse across the membrane from the thylakoid lumen. Thus the stromal environment changed from neutral (pH7.0) to alkaline (pH8.0) periodically through the dark/light period (Hauser et al., 1995; Song et al., 2004). DHD/SHD enzyme is located in the stroma of chloroplast (Bischoff et al., 2001), and is pH sensitive, therefore this enzyme might be regulated by light. The optimum pH for the anabolic and catabolic reaction were determined *in vitro*, which gave the value of 6.8-7.2 and 9.0-9.4 respectively (Chapter 3.1.3, Figure 4). This result hints that the anabolic reaction would be predominant at night (pH7.0), and partially suppressed in the day, whereas the catabolic reaction would be almost inactive at night, and partially active in the day.

Other shikimate pathway enzymes may also be regulated by light. For example, DAHPS was found to be regulated by light at enzymatic level (Dyer et al., 1989; Henstrand et al., 1992; Entus et al., 2002), however, in a different manner. This enzyme is regulated by reduced thioredoxin, which is available only during active electron flow through the photosystems, i.e. exposure to light. This finding suggests that light might replace the aromatic amino acids as the main regulator in higher plants during evolution.

The immediate substrates for the shikimate pathway are erythrose 4-phosphate (Ery4P) and phosphoenolpyruvate (PEP). Both metabolites are derived from the branch pathways of photosynthesis. Excessive depletion of these metabolites by the shikimate pathway might impair photosynthesis. The physiological significance of the light (pH) regulation of DHD/SHD

enzyme might be that as a result, the shikimate pathway can be tuned precisely to ensure the circulation of photosynthesis, which is mostly active in the day, and less active at night.

4.1.5 Nt-DHD/SHD-1 was identified as a potential herbicide target

As shown in Chapter 3.5.3, gene silencing of EPSPS nicely mimicked the inhibition of EPSPS activity by glyphosate in transgenic tobacco plants. Gene silencing of EPSPS resulted in an accumulation of shikimate (Chapter 3.5.6, Figure 35) and the decreased biosynthesis of phenolic compounds (Chapter 3.5.4, Figure 34). Moreover, the inhibition of EPSPS enzyme led to similar phenotypic changes as observed in glyphosate-treated plants (Ye et al., 2001). The results indicate that gene silencing is capable of providing reliable data in identifying herbicide / drug target in the metabolic pathway. The silencing of Nt-DHD/SHD-1 led to comparable phenotypic alterations as in EPSPS inhibited plants (Chapter 3.2.3, Figure 10). The impairment of growth characters of transgenic plants correlated with the silencing levels of DHD/SHD, highlighting the possibility of Nt-DHD/SHD-1 as an herbicide target in the shikimate pathway. Production, and purification of Nt-DHD/SHD-1 protein facilitated the study of enzyme properties, 3-D structure, regulation mechanism and the identification of potent enzyme inhibitors as well (Chapter 3.1.3, Figure 4) ([US2003145348](#)).

4.2 Inducible silencing of Nt-DHD/SHD-1 in tobacco

Constitutive silencing often entails pleiotropic effects on growth and development of the transgenic plants, which complicate the interpretation of the phenotypes and might mask the real gene function. Furthermore, if the expression of the target gene is essential for early growth or regeneration during tissue culture, vital plants might not be recovered. Ethanol-inducible silencing of the target genes caused strong but transient phenotypical alterations (Chen et al., 2003). Therefore the inducible system offers a powerful tool in analyzing a real-time response of plants, tracing the kinetics of pathway intermediates during the induction of a specific gene, and distinguishing primary and secondary effects of gene silencing.

4.2.1 Silencing of Nt-DHD/SHD-1 triggered transient changes of the pathway intermediates

As described in Chapter 4.1.3, the constitutive silencing of DHD/SHD enzyme led to a high-level accumulation of dehydroquinate (substrate), and a moderate accumulation of shikimate

(enzyme product) in the transgenic plants. The kinetics of transcript abundance, enzyme activity, and pathway intermediates were investigated in *alc*-DHD/SHD-RNAi plants, following the ethanol induction. As shown in Figure 19 (Chapter 3.3.3), the degradation of DHD/SHD mRNA started as early as 12 hours after ethanol treatment, and reached the peak level in another 12 hours. As a result, DHD/SHD polypeptides would be synthesized at a decreased velocity immediately after RNA degradation. However ethanol did not induce an instant decrease of DHD/SHD activity. DHD/SHD activity started to drop, and reach the bottom level 60 to 72 hours after induction. The duration between RNA degradation and decrease of DHD/SHD activity revealed *in vivo* stability of DHD/SHD enzyme. Dehydroquinate started to accumulate 3 days after induction (Chapter 3.3.4, Figure 20). The accumulation of dehydroquinate was concurrent to the decrease of DHD/SHD activity, suggesting that the buildup of dehydroquinate was a direct consequence of DHD/SHD silencing. In contrast, the accumulation of shikimate was not concurrent to the decrease of DHD/SHD enzyme activity. It started to accumulate 1 day after, suggesting that the accumulation of shikimate resulted from side effects. This timeline supports the shuttle model (Chapter 4.2.2, Figure 47) to interpret the accumulation of shikimate in DHD/SHD RNAi plants.

4.2.2 A shuttle to interpret the accumulation of shikimate in DHD/SHD silenced plants

A shuttle model was put forward based on the following facts: 1. The silencing of DHD/SHD in chloroplast would definitely impair synthesis of shikimate *in situ*. 2. A high level of dehydroquinate and a moderate level of shikimate were accumulated in DHD/SHD silenced plants (Chapter 3.2.8, Figure 15). 3. Shikimate could be normally metabolized into phenolic compounds in chloroplast of DHD/SHD silenced plants (Chapter 3.4.9, Table 5). Taken together, it is logical to predict that shikimate may not be accumulated in chloroplast, but in the cytosol.

According to this model, the silencing of Nt-DHD/SHD-1 led to a high-level accumulation of dehydroquinate in chloroplasts. A certain amount of this metabolite could be transported from chloroplasts to the cytosol and be converted to shikimate by a cytosolic DHD/SHD isozyme. The cytosolic shikimate most likely was not efficiently re-imported into chloroplasts, or metabolized by the downstream shikimate pathway enzymes in the cytosol. Thus an accumulation of shikimate could be expected in transgenic plants (Figure 47). This model predicts an early accumulation of dehydroquinate and a subsequent accumulation of shikimate as a result of DHD/SHD silencing. As shown in Figure 20 (Chapter 3.3.4), this prediction was

confirmed by the analysis of the pathway intermediates in *alc*-DHD/SHD-RNAi plants, and give a support to the metabolites shuttle model vice versa.

The cloning and enzymatic analysis of a cytosolic DHD/SHD isozyme (Nt-DHD/SHD-2), gave a second support to this shuttle model. There is still argument about the existence of shikimate pathway in cytosol. Although putative cytosolic isozymes have been described for DAHP synthase (Ganson et al., 1986), DHD/SHD (Mousdale et al., 1987), EPSP synthase (Mousdale and Coggins, 1985) and chorismate mutase (d'Amato, 1984), no molecular evidence was published up to now. Nt-DDH/SHD-2 might be a component of cytosolic shikimate pathway. If so, the cDNA of Nt-DDH/SHD-2 would be the first molecular evidence for a cytosolic shikimate pathway.

However, it is also possible that Nt-DDH/SHD-2 is not a component of the cytosolic shikimate pathway, but because of its high homolog to the plastidic DHD/SHD enzyme, it can catalyze the conversion of dehydroquinate to shikimate in the cytosol.

4.2.3 Spatial silencing of Nt-DHD/SHD-1 led to a reduced biosynthesis of anthocyanins

The shikimate pathway provides the precursors for the biosynthesis of aromatic amino acids, auxins, lignin, anthocyanins and flavonoids (Herrmann, 1995). The induced silencing of DHD/SHD in flower buds resulted in a dramatic decrease of anthocyanins, and thus led to a pale phenotype (Chapter 3.3.5 Figure 21). In contrast, the induced silencing of DHD/SHD in the flowering plants resulted in a miscellaneous phenotype (Chapter 3.3.5, Figure 23). The open flowers at the time point of induction did not develop a visible phenotype, whereas the flower buds developed a pale phenotype.

The biosynthesis of anthocyanins is likely more active in flower buds to encounter the requirement of pigments during flower development. The silencing of DHD/SHD in flower buds deprived the precursors of anthocyanins, thus developed a pale phenotype. Whereas in an open flower, the biosynthesis of anthocyanins is less active and an essential storage of anthocyanins has been established. Therefore, the silencing of DHD/SHD resulted in rather weak phenotypical changes in mature flower.

In *alc*-DHD/SHD-RNAi flowers, the residual DHD/SHD dropped below 10% of wild type value. This level of silencing in flowers could not be achieved using constitutive expression,

since plants with less than 20% DHD/SHD activity did not produce flowers. Thus, no pale phenotypes were observed in the constitutive DHD/SHD silenced flowers.

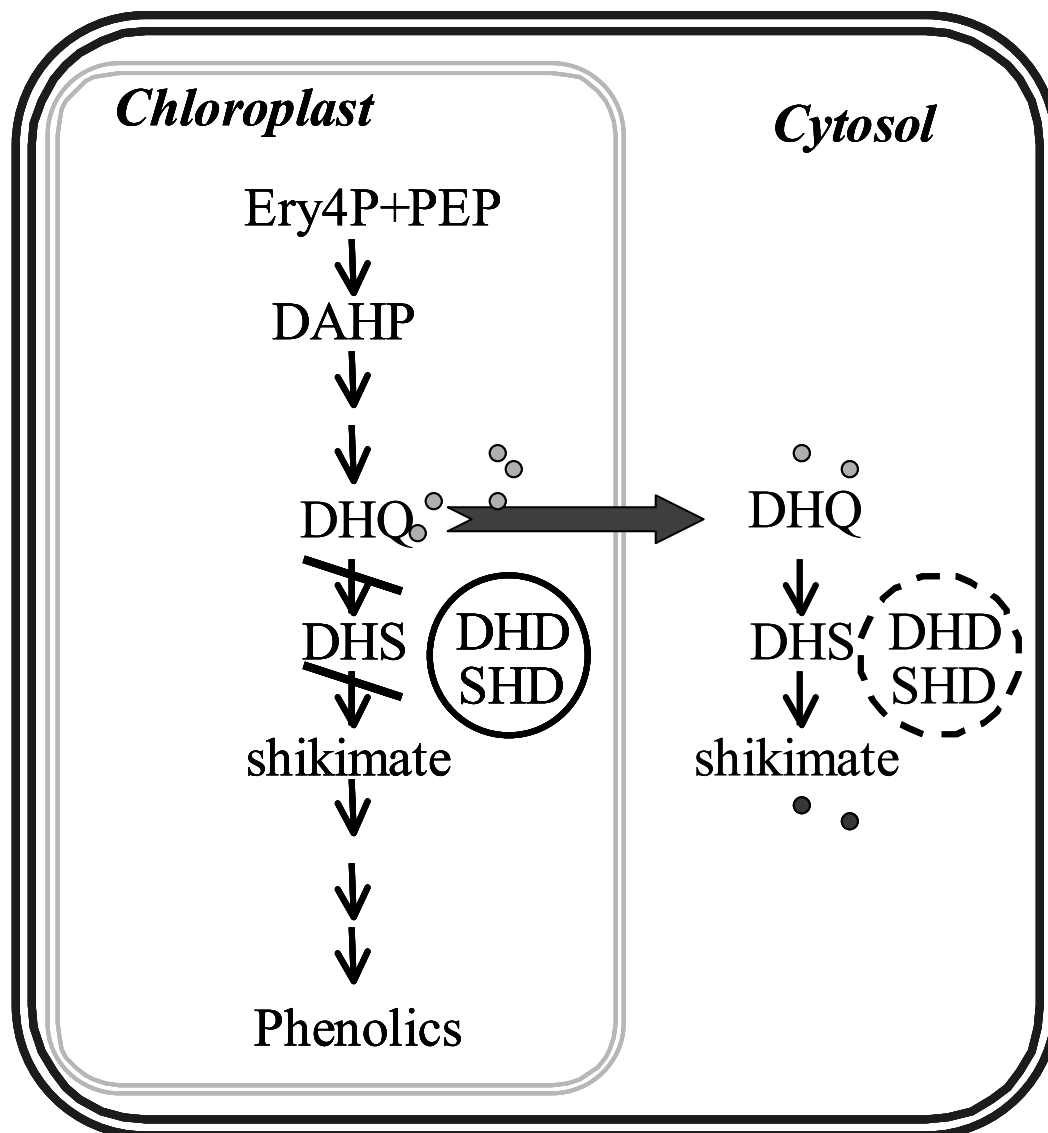


Figure 47. A model to interpret the accumulation of shikimate in DHD/SHD silenced plants. A partial or complete shikimate pathway was assumed in the cytosol, which might be responsible for the biosynthesis of phenylpropanoid. Under normal physiological condition, PEP an Ery4P can be smoothly metabolized to chorismate and phenolic compounds through the shikimate pathway, and no pathway intermediates were accumulated. The silencing of DHD/SHD resulted in a high level accumulation of dehydroquinone in plastids. This pathway intermediate might be transported into the cytosol, and catalyzed to shikimate by the cytosolic DHD/SHD isoform. The cytosolic shikimate is most likely not efficiently re-imported into chloroplasts, or metabolized *in situ*, thus resulting an accumulation in the cytosol.

4.2.4 Spatial silencing of Nt-DHD/SHD-1 in floral organ led to male sterility

Because male sterility is a prerequisite for the development of hybrid seed systems, the generation of this trait by metabolite engineering is an important goal. Flavonoids are required for pollen germination. In maize and petunia, the loss of chalcone synthase (CHS) activity, the first enzyme in flavonoids biosynthesis, results in a male-sterile phenotype (van der Meer et al., 1992). In tobacco plants, the overexpression of a stilbene synthase (STS) gene, which competes with the endogenous CHS for common substrates, causes male sterility in addition to altered flower pigmentation. The male fertility and flower colour can be restored by the treatment of flavonol or 4-coumarate, indicating that flavonoids play an essential role in the development of the male gametophyte (Fischer et al., 1997b).

The spatial silencing of DHD/SHD in tobacco flowers led to a dramatic reduction of anthocyanin and male sterility. Although not measured, flavonoids were expected to decrease in transgenic flowers, because they shared the same precursors with anthocyanins (Lo and Nicholson, 1998). This male sterility was likely resulted from the reduced biosynthesis of flavonoids in floral organ.

To induce male sterility, *alc*-DHD/SHD-RNAi plants should be treated at the transition point from vegetative to reproductive phase. A later induction at flowering stage did not result in a male sterility, suggesting that flavonoids influence male fertility at an early stage of pollen development. This finding is consistent with the previous publication (Fischer et al., 1997b), which indicated that the depletion of flavonoids during the differentiation of the tapetal cells (early stage) was required for an effective disruption of pollen development.

Ethanol inducible male sterility is particularly useful for hybrid seed production since the male sterile plants can easily be manipulated. In the absence of ethanol, *Alc*-DHD/SHD-RNAi plants are fully fertile, and male fertility can be easily maintained by self-pollination. When treated with ethanol, ethanol inducible promoter is activated and the transgenic plants showed to be male fertile. Compared with the conventional hybrid breeding system (3 lines system) (Khush, 2001), ethanol inducible male sterility has the following advantages: 1. No maintainer and restorer lines are required. 2. The system can be imposed on all breeding lines or cultivars without the need for extensive backcrossing and disruption of established inbred lines, leading to the rapid production of male sterile lines with well-characterized and superior agronomic performance.

4.3 Silencing of EPSPS in tobacco plants

4.3.1 Silencing of EPSPS led to a marked reduction of secondary metabolism

In fully sensitive plants, glyphosate induces severe stunting, chlorosis of newly emerged leaves and meristem tissues (Ye et al., 2001). In EPSPS co-suppression plants, the inhibition of EPSPS led to consistent phenotypic and metabolic changes as in glyphosate-treated plants. A 50% or more reduction of EPSPS protein led to bleached leaves. A 60%-80% reduction of EPSPS protein resulted in dwarfed phenotypes. Further reduction (90% or more) led to a lethal phenotype (Chapter 3.5.3, Table 6). The inhibition of the shikimate pathway genes resulted in dramatic decrease of aromatic amino acids, chlorogenate and lignin. The reduction of above phenolic compounds correlated with the decrease of EPSPS protein (Chapter 3.5.4, Figure 34), highlighting the important role of EPSPS in the shikimate pathway. In addition to above phenotypic and metabolic changes, silencing of EPSPS activates DAHPS in EPSPS silenced plants, in a similar manner as observed in DHD/SHD silenced plants (Chapter 4.1.2).

4.3.2 Differences between DHD/SHD and EPSPS silenced plants

Although silencing of either DHD/SHD or EPSPS led to similar phenotypic and physiological changes, including reduction of chlorophyll and secondary metabolites, EPSPS inhibited plants differed from DHD/SHD inhibited plants in two aspects.

First, DHD/SHD silenced plants accumulated a high level of dehydroquinate (substrate) and a moderate level of shikimate (product) (Chapter 3.2.8, Figure 15). In contrast, EPSPS silenced plants only accumulated shikimate (Chapter 3.5.6, Figure 35). The accumulation of shikimate in EPSPS silenced plants correlated with the reduction of EPSPS protein. The accumulation of shikimate was previously observed in glyphosate treated plants. Hollaender-Czytko and Amrhein (1983) presented a model to explain the accumulation of shikimate in glyphosate-treated plants. According to this model, the inhibition of EPSPS by glyphosate blocked the shikimate pathway, and resulted in a big accumulation of shikimate 3-phosphate (the immediate substrate of EPSPS) in plants. This compound was not stable and likely to be degraded by a phosphatase, yielding shikimate.

Second, EPSPS silenced plants differed from DHD/SHD silenced plants in shikimate feeding experiments. In shikimate feeding experiment, DHD/SHD RNAi plants produced a high level of phenylalanine and tyrosine from shikimate. The production of aromatic amino acids was not

restrained by the loss of DHD/SHD activity. Even when DHD/SHD activity dropped below 20% of wild type level, still 70% of phenylalanine and tyrosine could be synthesized as compared to wild type plants (Chapter 3.2.9, Table 5). In EPSPS silenced plants, the synthesis of aromatic amino acids from shikimate was in an approximately linear correlation with EPSPS residual protein (Chapter 3.5.7, Table 9). This result is not surprising because the metabolism of shikimate to aromatic amino acids needs the enzyme activities from shikimate kinase to chorismate synthase in the pathway (Chapter 1.2.1, Figure 1).

4.4 Introducing a PEP biosynthetic-pathway into tobacco chloroplasts

There is increasing evidence to suggest that flavonoids, in particular flavonols (such as kaempferol and quercetin), are potentially health-protecting components in the human diet, as a result of their high antioxidant capacity (Rice Evans et al., 1997) and their ability to induce human protective enzyme systems *in vitro* (Choi et al., 1999). These studies suggest that a systematic increase in the daily intake of certain flavonoids could lead to a 30 to 40% reduction in death by coronary heart diseases.

Recent advances in concerning pathway regulation and the biochemistry of specific enzymes and enzyme complexes have opened up several potential pathway modification strategies to enhance the plant's ability to synthesize flavonoid bioactive products. Muir, et al., (2001) up-regulated flavonol biosynthesis in tomato by expressing the *petunia* chalcone isomerase, and obtained an increase of up to 78 fold in fruit peel flavonols. However, the increase of flavonol is limited to peel, which only constitutes 5% of the total fruit weight. There was no significant accumulation of flavonoids in the fruit flesh, suggesting that the flavonoids biosynthesis pathway is less active in fruit flesh. To activate the flavonoid biosynthesis in the fruit flesh, Bovy et al. (2002) expressed the transcription factor genes (*MYB-C1* and *MYC-LC*) specifically in the fruit of transgenic tomatoes, and achieved a strong accumulation of flavonol and falconine in the tomato flesh.

Plastidic PEP is believed to be a limiting factor controlling carbon flux through the shikimate pathway to flavonoids, because this pathway intermediate could not be generated in plastids (Bagge and Larsson, 1986; Stitt, 1997). To interpret the access of PEP in chloroplast, Fischer et al. (1997a) figured out a metabolites shuttle model. According to this model, 3-PGA is exported from plastid to the cytosol by the chloroplast triose phosphate translocator (cTPT), and then converted to PEP by the cytosolic PGM and enolase. Cytosolic PEP needs to be imported into

chloroplasts by a specific PEP/phosphate translocator (PPT) to join the shikimate pathway. Thus, an extra of two-step translocations are required. By introducing PGM and enolase into chloroplast, a PEP biosynthetic pathway was established, which would convert 3-PGA to 2-PGA, and then to PEP in two successive reactions *in situ*. This pathway modification was expected to elevate PEP content in chloroplast, and improve the biosynthesis of secondary metabolites.

4.4.1 Increase of PEP content did not result in a significant increase of secondary metabolites

To evaluate the plastidic PEP biosynthetic pathway on secondary metabolism, pathway intermediates (3-PGA, PEP and pyruvate) and phenolic compounds were determined in transgenic tobaccos. PEP and pyruvate content increased 153%-242% and respectively, whereas 3-PGA decreased dramatically to 23%-50% of wild type value in transgenic tobacco plants (Chapter 3.6.3.3, Figure 45). Unexpectedly, the increase of PEP did not lead to a significant increase of phenolic compounds in transgenic plants accordingly. For examples, chlorogenate increased 17%-22% and total soluble phenolic compounds increased 13%-28% in PGM-enolase plants (Chapter 3.6.3.5, Table 15). The increase of phenolic compounds production lagged far behind the increase of PEP in transgenic plants (Chapter 3.6.3.3, Figure 45), suggesting that plastidic PEP might not be a limiting factor for secondary metabolism.

Recent publication on the research of *Arabidopsis* mutant gives a consistent result. In *Arabidopsis*, a *cue1* mutant exhibiting a reticulate leaf phenotype was recognized as a deficiency of plastidic PEP/phosphate translocator (PPT) (Knappe et al., 2003). In this mutant, less aromatic metabolites are synthesized as a result of decreased abundance of PEP in chloroplast. The *cue1* phenotypes could be rescued by constitutive expression of a PPDK (pyruvate, orthophosphate dikinase), which catalyzes the ATP-dependent conversion of pyruvate to PEP in chloroplast (Voll et al., 2003). The introduction of PPDK into chloroplast led to an elevation of PEP (up to sevenfold above wild type plants) during photoperiod. Although the biosynthesis of phenolic compounds (phenylpropanoids and anthocyanins) was mostly rescued in the *cue1*/PPDK lines, total phenolic compounds level did not increase above wild type value, in accordance with the increase of plastidic PEP.

4.4.2 3-PGA pool in the chloroplast of photosynthetic tissues is not an ideal carbon source for the secondary metabolism

An important property of the Calvin cycle is that it can increase its turnover by increasing the concentration of its intermediates (Taiz and Zeiger, 2002). As the initial product of photosynthesis, a balanced level of 3-PGA is crucial to ensure the circulation of photosynthesis. Under normal physiological condition, the production, metabolism and transport of 3-PGA are deliberately regulated (Foyer and Quick, 1997). The introduction of PGM into chloroplast consumed 3-PGA, and led to many detrimental consequences in transgenic plants, including retarded growth (Chapter 3.6.2.2, Figure 39), repressed photosynthesis and reduced production of carbohydrates (Chapter 3.6.2.4, Table 11). It is likely that these detrimental consequences are resulted from the depletion of plastidic 3-PGA. In chloroplast of source tissues, the increase of PEP was achieved with the price of a reduced fixation of carbon dioxide, suggesting that plastidic 3-PGA of photosynthetic tissues was not an ideal carbon source for secondary metabolism.

This conclusion is drawn from the study of tobacco source tissues, and it might not be applicable to sink tissues, for example, fruit flesh. On one hand, sink tissue is non-photosynthetic tissue (Gilbert et al., 1998), the conversion of 3-PGA to PEP in sink tissues would not impair primary metabolism. On the other hand, sink tissues and source tissues have different metabolite contents and regulation mechanisms, and the metabolites pool sizes in sink tissues change during development (Roessner-Tunali et al., 2003). Therefore the establishment of PEP biosynthetic pathway in sink tissues might result differently on secondary metabolism.

5. Summary

Within the shikimate pathway the bifunctional enzyme 3-dehydroquinate dehydratase / shikimate dehydrogenase (DHD/SHD) catalyzes the reversible conversion of dehydroquinate into shikimate. Despite its central function within the shikimate pathway, little is known about its biochemical characteristics or its *in planta* importance.

To determine the kinetic properties of DHD/SHD, the enzyme was expressed in *E.coli*, purified to homogeneity and characterized *in vitro*. The pH optimum for the anabolic reaction was found to be approx. pH 7.0, whereas the catabolic reaction reached its maximum at approx. pH 9.0, suggesting that the enzyme might be regulated by light. The SHD reaction exhibited Michaelis-Menten kinetics. The apparent Michaelis constant (K_m) values for its substrate shikimate and NADP were $130 \pm 15 \mu\text{M}$ and $31 \pm 7 \mu\text{M}$, respectively.

To elucidate the *in planta* function of DHD/SHD enzyme, enzyme activity was strongly decreased by RNAi (RNA interference) in transgenic tobacco. Plants with suppressed DHD/SHD activity below 40 % of the wild type level displayed severe growth retardation. Further reduction in DHD/SHD activity below 20 % resulted in non-viable plants under greenhouse condition. Secondary metabolites (chlorogenic acid and lignin) and aromatic amino acids decreased in transgenic plants. Surprisingly, silencing of DHD/SHD enzyme resulted in an accumulation of dehydroquinate (substrate) and shikimate (product) in transgenic plants. This product accumulation cannot be explained by the impairment of downstream metabolism. When provided with shikimate, leaf discs of transgenic plants accumulated a similar amount of aromatic amino acids as wild type plants, suggesting that the inhibition of DHD/SHD did not impair the activity of downstream enzymes. This assumption is further strengthened by the observation that with the exception of DAHPS similar transcript levels of shikimate pathway genes were detected in transgenic and wild type plants. DAHPS mRNA levels increased four-fold as compared to wild type controls, suggesting that DAHPS is subject to feedback regulation.

To investigate kinetics of shikimate and dehydroquinate during the silencing of DHD/SHD, an ethanol inducible silencing construct *alc*-DHD/SHD-RNAi was created. The induced silencing of DHD/SHD led to an early accumulation of dehydroquinate and a late accumulation of shikimate in the leaves of transgenic plants. This result strongly suggested that the accumulation

of dehydroquinate is a direct consequence of the silencing of DHD/SHD, whereas the buildup of shikimate is derived from secondary effects. This leads us to put forward a model to interpret the buildup of shikimate in transgenic plants. We assume that a certain amount of dehydroquinate would be transported from chloroplasts to the cytosol, and be converted to shikimate by a cytosolic isoform of DHD/SHD. The cytosolic shikimate most likely is not efficiently re-imported into chloroplasts, thus further metabolism is impaired. The isolation of a full-size cDNA encoding a putative DHD/SHD isozyme (Nt-DHD/SHD-2) supports this hypothesis. Lacking a typical chloroplast transit peptides, Nt-DHD/SHD-2 was judged to be a cytosolic enzyme. Transient expression using *Agrobacterium* infiltration confirmed the enzyme activity and cytosolic localization of Nt-DHD/SHD-2.

The ethanol-inducible gene switch enables a spatial control of gene silencing in specific organs. Spatial silencing of DHD/SHD in flowers resulted in a pale phenotype and male sterility. In these flowers, DHD/SHD activity dropped below 10% of wild type value. This level of silencing in flowers could not be achieved using constitutive expression, since plants with less than 20% DHD/SHD activity did not produce flowers.

5-enolpyruvylshikimate-3-phosphate synthase (EPSPS) catalyzes the reversible formation of 5-enolpyruvylshikimate-3-phosphate (EPSP) from shikimate 3-phosphate and phosphoenolpyruvate (PEP). This enzyme is well analyzed because of the interest in it as the target of the broad-spectrum herbicide glyphosate. To investigate the physiological importance of EPSPS, enzyme activity was strongly decreased by co-suppression technique in transgenic tobacco. The inhibition of EPSPS expression led to comparable phenotypic and metabolic changes as shown for the DHD/SHD enzyme in transgenic plants. A 60 % or more reduction of this enzyme led to growth retardation. Further reduction to below 10 % resulted in non-viable plants. EPSPS co-suppression plants differed from DHD/SHD RNAi plants in two aspects. Firstly, EPSPS co-suppression plants only accumulate high levels of shikimate, whereas DHD/SHD RNAi plants accumulated both shikimate and dehydroquinate. Secondly, when provided with shikimate, DHD/SHD RNAi plants built up a high level of phenylalanine and tyrosine, and the accumulation of aromatic amino acids was not restrained by the loss of DHD/SHD activity. In contrast, the shikimate feeding of EPSPS silenced tobacco plants did not restore the synthesis of aromatic amino acids.

Because most plastids have little or no PGM (phosphoglycerate mutase) and enolase activity, 3-phosphoglycerate (3-PGA) cannot be metabolized to PEP in plastids. Plastids therefore rely on

the supply of cytosolic PEP via a shuttle mechanism. By introducing PGM and enolase into chloroplasts, we created a plastic PEP biosynthetic pathway. Under the subsequent catalyses of the above enzymes, plastidic 3-PGA was converted to PEP *in situ*. As a result, PEP and pyruvate content increased substantially, whereas 3-PGA levels decreased dramatically in leaves of transgenic tobacco plants. This genetic manipulation led to many detrimental consequences in transgenic plants, including retarded growth, repressed photosynthesis and reduced production of carbohydrates. Unexpectedly, the elevated supply of PEP to plastids did not significantly enhance carbon flux into the shikimate pathway and secondary metabolism.

6. Zusammenfassung

Innerhalb des Shikimatstoffwechsels katalysiert das bifunktionelle Enzym 3-Dehydroquinat-Dehydratase / Shikimat-Dehydrogenase (DHD/SHD) die reversible Überführung von Dehydroquinat in Shikimat. Ungeachtet der zentralen Rolle des Enzyms ist wenig über die biochemischen Eigenschaften bzw. die *in planta* Funktion des Enzyms bekannt.

Zur Bestimmung der biochemischen Eigenschaften des Enzyms wurde die DHD/SHD Kodierregion aus *N. tabacum* kloniert, in *E. coli* exprimiert, das Protein zur Homogenität gereinigt und *in vitro* charakterisiert. Als pH-Optimum für die Enzymreaktion konnte pH 7.0 (anabolisch) bzw. pH 9.0 (katabolisch) bestimmt werden. Die unterschiedlichen pH-Optima deuten auf eine Licht-/Dunkelregulation der Enzymreaktion hin. Die Reaktion der SHD folgt einer Michaelis-Menten Kinetik mit einem K_m von $130 \pm 15 \mu\text{M}$ für Shikimat bzw. $31 \pm 7 \mu\text{M}$ für NADP.

Um die *in planta* Funktion des Enzyms aufzuklären, wurde die Enzymaktivität mittels RNAi-Strategie in transgenen Tabakpflanzen gehemmt und die Konsequenz verminderter DHD/SHD Aktivität auf den Pflanzenstoffwechsel und den Pflanzenwuchs ermittelt. Erhebliche Wachstumseinbußen der transgenen Pflanzen traten bei einer 60%igen Hemmung der Enzymaktivität auf. Bei einer weiteren Inhibierung (80% Verminderung bezogen auf die untransformierte Kontrolle) der Enzymaktivität waren die resultierenden Pflanzen unter Gewächshausbedingungen nicht lebensfähig. Als Folge des inhibierten Shikimatstoffwechsels konnte eine verminderte Akkumulation von sekundären Pflanzeninhaltsstoffen (z.B. Lignin, Chlorogensäure) und aromatischen Aminosäuren in den transgenen Pflanzen beobachtet werden.

Überraschenderweise kam es in den transgenen Pflanzen neben einer Akkumulation des Substrates (Dehydroquinat) auch zu einem Anstieg des Produktes (Shikimat) der Enzymreaktion. Durch den Einsatz induzierbarer RNAi konnte nahegelegt werden, dass zunächst der Dehydroquinatgehalt und anschließend der Shikimatgehalt ansteigt. Dieser unerwartete Anstieg könnte durch eine Hemmung des weiteren Shikimatstoffwechsels oder eine Shikimat Synthese außerhalb der Plastiden erklärt werden. Um diese Hypothesen zu überprüfen wurden (i) Shikimatfütterungsversuche, (ii) eine detaillierte Expressionsanalyse sowie die (iii) Klonierung einer möglichen cytosolischen DHD/SHD Isoform durchgeführt. Basierend auf den

erhaltenen Ergebnissen kann die Hemmung der Shikimatverwertung ausgeschlossen werden, da Shikimatfütterung zu einem Anstieg aromatischer Aminosäuren sowohl in der untransformierten Kontrolle, als auch in den transgenen Pflanzen führte. Die Analyse der Expression von Genen, die Shikimatenzyme kodieren, ergab darüber hinaus keine Hinweise auf eine verminderte Expression. Im Gegenteil, die Expression des ersten Enzyms des Shikimatstoffwechsels, die 3-Deoxy-D-Arabino-Heptulosonate 7-Phosphat Synthase (DAHPS), war in den transgenen Pflanzen deutlich gesteigert, was auf eine Produktregulation des Enzyms hinweist. Unter der Annahme, dass Dehydroquinat aus den Plastiden transportiert werden und anschließend durch ein cytosolisches DHD/SHD Isoenzym in Shikimat überführt werden könnte, wurde nach weiteren DHD/SHD kodierenden cDNAs gesucht. Basierend auf Datenbankvergleichen und der Klonierung einer weiteren DHD/SDH kodierenden cDNA konnten erste Hinweise auf die Existenz einer cytosolischen DHD/SHD Isoform erhalten werden. Die Kodierregion der als NtDHD/SHD-2 bezeichneten Isoform verfügt über kein plastidäres Transitpeptid und führt nach transienter Expression in Tabakblättern zu einer starken Erhöhung der cytosolischen DHD/SHD Aktivität.

Als interessantes Nebenergebnis der induzierbaren Hemmung der DHD/SHD Aktivität konnte eine Hemmung der Anthocyanbiosynthese in Blütenblättern und ein männlich-steriler Phänotyp nach Induktion beobachtet werden. Da hierfür eine Hemmung der Enzymaktivität um mehr als 80% in den Blütenorganen erforderlich war, konnte dieser Phänotyp nicht mit konstitutiver Expression erreicht werden, da entsprechend gehemmte Pflanzen im Gewächshaus nicht lebensfähig gewesen wären.

Neben der detaillierten Analyse der DHD/SHD Aktivität wurden transgene Pflanzen mit verminderter 5-Enolpyruvylshikimat-3-Phosphat Synthase (EPSPS) hergestellt und biochemisch charakterisiert. Die EPSPS katalysiert die reversible Bildung von EPSP aus Shikimat-3-Phosphat und Phosphoenolpyruvat (PEP) und gilt als das zentrale Enzym des Shikimatstoffwechsels. Ähnlich wie bei der DHD/SHD führte eine Hemmung des Enzyms zu drastischen Einbußen des Pflanzenwachstums und zu einem Verlust der Lebensfähigkeit bei einer Hemmung um mehr als 90%. Erwartungsgemäß konnte der biochemische Defekt nicht durch Shikimatfütterung aufgehoben werden.

In einem weiteren Ansatz wurde versucht zu ermitteln, ob die Verfügbarkeit von PEP in Plastiden die Synthese phenolischer Inhaltsstoffe limitiert. Zu diesem Zweck wurden die Kodierregionen der *E. coli* Enzyme PGM (Phosphoglyceromutase) and Enolase mit einer

plastidären Transportsequenz fusioniert und in transgenen Tabakpflanzen exprimiert. Durch die Koexpression beider Enzyme sollte plastidäres 3-Phosphoglycerinsäure (3PGA) in zwei Schritten in PEP überführt werden. Subzelluläre Fraktionierung erbrachte den Nachweis, dass beide Enzymaktivitäten in die Plastiden transportiert wurden. Als Folge der ektopischen Expression konnte erwartungsgemäß eine Verminderung der 3PGA und eine Steigerung der PEP Gehalte beobachtet werden. Dies führte nicht zu einer Erhöhung phenolischer Inhaltsstoffe, aber zu einer Hemmung der Photosynthese und einem verminderten Wuchs der resultierenden Pflanzen.

7. Abbreviations

cDNA	complementary dna
DEPC	diethylpyrocarbonate
DNA	deoxyribonucleic acid
DTT	dithiothreitol
EDTA	ethylenediamine tetraacetic acid
GFP	green fluorescent protein
HPLC	high performance liquid chromatography
HEPES	<i>n</i> -2-hydroxyethylpiperazine- <i>n</i> '-2-ethane-sulfonic acid
IPTG	β -d-isopropyl-thiogalactopyranoside
kb	kilobase
kDa	kilodalton
<i>K</i> _m	michaelis constant
MES	2-(<i>n</i> -morpholino)ethanesulfonic acid
m	milli-
min	minute
MOPS	3-(<i>n</i> -morpholino)propanesulfonic acid
mRNA	messenger rna
MS	murashige-skoog medium
NAD	nicotinamide adenine dinucleotide
NADH	nicotinamide adenine dinucleotide, reduced
NADP	nicotinamide adenine dinucleotidephosphate
NADPH	nicotinamide adenine dinucleotidephosphate, reduced
<i>ocs</i>	octopin synthase
OD	optical density
ORF	open reading frame
PAGE	polyacrylamid electrophoresis
PCR	polymerase chain reaction
pH	hydrogen ion concentration
SDS	sodium dodecyl sulfate
RNA	ribonucleic acid
RNAi	rna interference
RT-PCR	reverse transcription pcr
Tris	tris(hydroxymethyl)aminomethane
u	unit
μ	micro-
(v/v)	volume:volume ratio
(w/v)	weight:volume ratio
WT	wild type

8. References

- Amasino, R. M.** (1986) Acceleration of nucleic acid hybridisation rate by polyethylene glycol. *Anal.Biochem.* **152**: 304-307.
- Amrhein, N., Deus, B., Gehrke, P., and Seinrucken, H. C.** (1980) The site of the inhibition of the shikimate pathway by glyphosate. II. Interference of glyphosate with chorismate formation *in vivo* and *in vitro*. *Plant Physiol.* **66**: 830-834.
- Anton, I. A. and Coggins, J. R.** (1988) Sequencing and overexpression of the Escherichia coli aroE gene encoding shikimate dehydrogenase. *Biochem.J* **249**: 319-326.
- Bagge, P. and Larsson, C.** (1986) Biosynthesis of aromatic amino acids by highly purified spinach chloroplast - Compartmentation and regulation of the reactions. *Physiol.Plant* **68**: 641-647.
- Bate, N. J., Orr, J., Ni, W., Meromi, A., Nadler-Hassar, T., Doerner, P. W., Dixon, R. A., Lamb, C. J., and Elkind, Y.** (1994) Quantitative relationship between phenylalanine ammonia-lyase levels and phenylpropanoid accumulation in transgenic tobacco identifies a rate-determining step in natural product synthesis. *Proc Natl Acad Sci U.S.A* **91**: 7608-7612.
- Beaudoin-Eagan, L. D. and Thorpe, T. A.** (1984) Turnover of shikimate pathway metabolites during shoot initiation in tobacco callus cultures. *Plant Cell Physiol.* **25**: 913-921.
- Bechtold, N. and Pelletier, G.** (1998) In planta Agrobacterium-mediated transformation of adult Arabidopsis thaliana plants by vacuum infiltration. *Methods Mol.Biol.* **82**: 259-266.
- Bender, S. L., Mehdi, S., and Knowles, J. R.** (1989) Dehydroquinate synthase: the role of divalent metal cations and of nicotinamide adenine dinucleotide in catalysis. *Biochemistry* **28**: 7555-7560.
- Bickel, H., Plame, L., and Schultz, G.** (1978) Incorporation of shikimate and other precursors into aromatic amino acids and prenylquinones of isolated spinach chloroplasts. *phytochemistry* **17**: 119-124.
- Bischoff, M., Schaller, A., Bieri, F., Kessler, F., Amrhein, N., and Schmid, J.** (2001) Molecular characterization of tomato 3-dehydroquinate dehydratase-shikimate:NADP oxidoreductase. *Plant Physiol* **125**: 1891-1900.
- Bonner, C. A. and Jensen, R. A.** (1994) Cloning of cDNA encoding the bifunctional dehydroquinase.shikimate dehydrogenase of aromatic-amino-acid biosynthesis in Nicotiana tabacum. *Biochem.J.* **302 (Pt 1)**: 11-14.
- Bovy, A., de Vos, R., Kemper, M., Schijlen, E., Almenar, Pertejo M., Muir, S., Collins, G., Robinson, S., Verhoeyen, M., Hughes, S., Santos-Buelga, C., and van Tunen, A.** (2002)

High-flavonol tomatoes resulting from the heterologous expression of the maize transcription factor genes LC and C1. *Plant Cell* **14**: 2509-2526.

Bradford, M. M. (1976) A rapid and sensitive method for the quantitation of microgram quantities of protein utilizing the principle of protein-dye binding. *Anal. Biochem.* **72**: 248-254.

Buchholz, B., Reupke, B., Bickel, H., and Schultz, G. (1979) Reconstruction of amino acid synthesis by combining spinach chloroplasts with other leaf organelles. *phytochemistry* **18**: 1109-1111.

Caddick, M. X., Greenland, A. J., Jepson, I., Krause, K. P., Qu, N., Riddell, K. V., Salter, M. G., Schuch, W., Sonnewald, U., and Tomsett, A. B. (1998) An ethanol inducible gene switch for plants used to manipulate carbon metabolism. *Nat. Biotechnol.* **16**: 177-180.

Campbell, M. M. and Ellis, B. E. (1992) Fungal Elicitor-Mediated Responses in Pine Cell-Cultures .1. Induction of Phenylpropanoid Metabolism. *planta* **186**: 409-417.

Carmeli, C. (1970) Proton translocation induced by ATPase activity in chloroplasts. *FEBS lett.* **7**: 297-300.

Chen, S., Hofius, D., Sonnewald, U., and Bornke, F. (2003) Temporal and spatial control of gene silencing in transgenic plants by inducible expression of double-stranded RNA. *Plant J* **36**: 731-740.

Chin, C. C., Brewer, J. M., and Wold, F. (1981) The amino acid sequence of yeast enolase. *J Biol. Chem.* **256**: 1377-1384.

Choi, S. U., Ryu, S. Y., Yoon, S. K., Jung, N. P., Park, S. H., Kim, K. H., Choi, E. J., and Lee, C. O. (1999) Effects of flavonoids on the growth and cell cycle of cancer cells. *Anticancer Res.* **19**: 5229-5233.

d'Amato, T. A. (1984) Subcellular localization of chorismate-mutase isoenzymes in protoplasts from mesophyll and suspension-cultured cells of *Nicotiana glauca*.

Deka, R. K., Anton, I. A., Dunbar, B., and Coggins, J. R. (1994) The characterization of the shikimate pathway enzyme dehydroquinase from *pisum sativum*. *FEBS lett.* **349**: 397-402.

Della-Cioppa, G., Bauer, S. C., Klein, B. K., Shah, D. M., Fraley, R. T., and Kishore, G. M. (1986) Translocation of the precursor of 5-enolpyruvylshikimate 3-phosphate synthase into chloroplasts of higher plants *in vitro*. *Proc. Natl. Acad. Sci.* **83**: 6873-6877.

Deveaux, Y., Peaucelle, A., Roberts, G. R., Coen, E., Simon, R., Mizukami, Y., Traas, J., Murray, J. A., Doonan, J. H., and Laufs, P. (2003) The ethanol switch: a tool for tissue-specific gene induction during plant development. *Plant J* **36**: 918-930.

- Ding, L., Sonnewald, U., and FREUND, A.** (2003) Dehydroquinate dehydrase/shikimate dehydrogenase as a herbicide target . [US2003145348](#)
- Domachowske, J. B., Bonville, C. A., and Rosenberg, H. F.** (2001) Gene expression in epithelial cells in response to pneumovirus infection. *Respir.Res.* **2**: 225-233.
- Dyer, W. E., Henstrand, J. M., Handa, A. K., and Herrmann, K. M.** (1989) Wounding induces the first enzyme of the shikimate pathway in Solanaceae. *Proc Natl Acad Sci* **86**: 7370-7373.
- Elkind, Y., Edwards, R., Mavandad, M., Hedrick, S. A., Ribak, O., Dixon, R. A., and Lamb, C. J.** (1990) Abnormal plant development and down-regulation of phenylpropanoid biosynthesis in transgenic tobacco containing a heterologous phenylalanine ammonia-lyase gene. *Proc Natl Acad Sci U.S.A* **87**: 9057-9061.
- Emanuelsson, O., Nielsen, H., and von Heijne, G.** (1999) ChloroP, a neural network-based method for predicting chloroplast transit peptides and their cleavage sites. *Protein Science* **8**: 978-984.
- Entus, R., Poling, M., and Herrmann, K. M.** (2002) Redox regulation of Arabidopsis 3-deoxy-D-arabino-heptulosonate 7-phosphate synthase. *Plant Physiol* **129**: 1866-1871.
- Fiedler, E. and Schultz, G.** (1985) Localization, purification and characterization of shikimate oxidoreductase-dehydroquinate hydrolyase from stroma of spinach chloroplasts. *Plant Physiol.* **79**: 212-218.
- Fire, A., Xu, S., Montgomery, M. K., Kostas, S. A., Driver, S. E., and Mello, C. C.** (1998) Potent and specific genetic interference by double-stranded RNA in *Caenorhabditis elegans*. *Nature* **391**: 806-811.
- Fischer, K., Kammerer, B., Gutensohn, M., Arbinger, B., Weber, A., Hausler, R. E., and Flügge, U. I.** (1997a) A new class of plastidic phosphate translocators: a putative link between primary and secondary metabolism by the phosphoenolpyruvate/phosphate antiporter. *Plant Cell* **9**: 453-462.
- Fischer, R., Budde, I., and Hain, R.** (1997b) Stilbene synthase gene expression causes changes in flower colour and male sterility in tobacco. *Plant J* **11**: 489-498.
- Flügge, U. I., Fischer, K., Gross, A., Sebald, W., Lottspeich, F., and Eckerskorn, C.** (1989) The triose phosphate-3-phosphoglycerate-phosphate translocator from spinach chloroplasts: nucleotide sequence of a full-length cDNA clone and import of the in vitro synthesized precursor protein into chloroplasts. *EMBO J* **8**: 39-46.
- Fothergill-Gilmore, L. A. and Watson, H. C.** (1989) The phosphoglycerate mutases. *Adv Enzymol Relat Areas Mol Biol* **62**: 227-313.

- Foyer, C. H. and Quick, W. P.**, A molecular approach to primary metabolism in higher plants, Taylor & Francis Ltd, Foyer, C. H. and Quick, W. P.1997.
- Fraser, H. I., Kvaratskhelia, M., and White, M. F.** (1999) The two analogous phosphoglycerate mutases of *Escherichia coli*. *FEBS Lett* **455**: 344-348.
- Ganson, R. J., d'Amato, T. A., and Jensen, R. A.** (1986) The two-isozyme system of 3-Deoxy-D-arabino-Heptulosonate 7-Phosphate synthase in *Nicotiana glauca* and other higher plants. *Plant Physiol* **82**: 203-210.
- Garner, C. C. and Herrmann, K. M.** (1985) Operator mutations of the *Escherichia coli* *aroF* gene. *J Biol Chem.* **260**: 3820-3825.
- Gasser, C. S., Winter, J. A., Hironaka, C. M., and Shah, D. M.** (1988) Structure, expression, and evolution of the 5-enolpyruvylshikimate-3-phosphate synthase genes of petunia and tomato. *J.Biol.Chem.* **263**: 4280-4287.
- Gavel, Y. and von Heijne, G.** (1990) A conserved cleavage-site motif in chloroplast transit peptides. *FEBS lett.* **261**: 455-458.
- Geiger, M., Haake, V., Ludewig, F., Sonnewald, U., and Stitt, M.** (1999) The nitrate and ammonium nitrate supply have a major influence on the response of photosynthesis, carbon metabolism, nitrogen metabolism and growth to elevated carbon dioxide in tobacco. *Plant Cell Environ.* **22**: 1177-1199.
- Gilbert, G. A., Gadush, M. V., Wilson, C., and Madore, M. A.** (1998) Amino acid accumulation in sink and source tissues of *Coleus blumei* Benth. during salinity stress. *Journal of Experimental Botany*, **49**: 107-114.
- Giles, N. H., Case, M. E., Baum, J., Geever, R., Hulet, L., Patel, V., and Tyler, B.** (1985) Gene organization and regulation in the *qa* (quinic acid) gene cluster of *Neurospora crassa*. *Microbiol.Rev.* **49**: 338-358.
- Gorlach, J., Schmid, J., and Amrhein, N.** (1994) Abundance of transcripts specific for genes encoding enzymes of the prechorismate pathway in different organs of tomato (*Lycopersicon esculentum* L.) plants. *Planta* **193**: 216-223.
- Hajirezaei, M. R., Peisker, M., Tschiersch, H., Palatnik, J. F., Valle, E. M., Carrillo, N., and Sonnewald, U.** (2002) Small changes in the activity of chloroplastic NADP(+)-dependent ferredoxin oxidoreductase lead to impaired plant growth and restrict photosynthetic activity of transgenic tobacco plants. *Plant J* **29**: 281-293.
- Hannaert, V., Brinkmann, H., Nowitzki, U., Lee, J. A., Albert, M. A., Sensen, C. W., Gaasterland, T., Muller, M., Michels, P., and Martin, W.** (2000) Enolase from *Trypanosoma brucei*, from the amitochondriate protist *Mastigamoeba balamuthi*, and from the chloroplast and cytosol of *Euglena gracilis*: pieces in the evolutionary puzzle of the eukaryotic glycolytic pathway. *Mol Biol Evol.* **17**: 989-1000.

- Harris, J., Kleanthous, C., Coggins, J. R., Hawkins, A. R., and Abell, C.** (1993) Different mechanistic and stereochemical courses for the reactions catalyzed by type I and type II dehydroquinases. *J.Chem.Soc.Chem.Commun* , 1080-1081.
- Hartmann, M., Heinrich, G., and Braus, G. H.** (2001) Regulative fine-tuning of the two novel DAHP isoenzymes aroFp and aroGp of the filamentous fungus *Aspergillus nidulans*. *Arch.Microbiol.* **175**: 112-121.
- Haslam, E.**, Shikimic acid: Metabolism and Metabolites, John Wiley and Sons Chichester New York, 1993.
- Hauser, M., Eichelmann, H., Oja, V., Heber, U., and Laisk, A.** (1995) Stimulation by Light of Rapid pH Regulation in the Chloroplast Stroma in Vivo as Indicated by CO₂ Solubilization in Leaves. *Plant Physiol* **108**: 1059-1066.
- Henkes, S., Sonnewald, U., Badur, R., Flachmann, R., and Stitt, M.** (2001) A small decrease of plastid transketolase activity in antisense tobacco transformants has dramatic effects on photosynthesis and phenylpropanoid metabolism. *Plant Cell* **13**: 535-551.
- Henstrand, J. M., McCue, K. F., Brink, K., Handa, A. K., Herrmann, K. M., and Conn, E. E.** (1992) Light and fungal elicitor induce 3-deoxy-arabino-heptulosonate 7-phosphate synthase mRNA in suspension cultured cells of parsley (*Petroselinum crispum* L.). *Plant Physiol* **98**: 761-763.
- Henstrand, J. M., Schmid, J., and Amrhein, N.** (1995) Only the Mature Form of the Plastidic Chorismate Synthase Is Enzymatically Active. *Plant Physiol* **108**: 1127-1132.
- Herrmann, K. M.** (1995) The Shikimate Pathway: Early Steps in the Biosynthesis of Aromatic Compounds. *Plant Cell* **7**: 907-919.
- Herrmann, K. M. and Weaver, L. M.** (1999) The shikimate pathway. *Annu.Rev.Plant Physiol Plant Mol.Biol.* **50**: 473-503.
- Hofius, D., Hajirezaei, M. R., Geiger, M., Tschiersch, H., Melzer, M., and Sonnewald, U.** (2004) RNAi-mediated tocopherol deficiency impairs photoassimilate export in transgenic potato plants. *Plant Physiol* **135**: 1256-1268.
- Hollaender-Czytko, H. and Amrhein, N.** (1983) Subcellular compartmentation of shikimic acid and phenylalanine in buckwheat cell suspension cultures grown in the presence of shikimate pathway inhibitors. *Plant Sci.Lett* **29**: 89-96.
- Hrazdina, G. and Jensen, R. A.** (1992) Spatial organization of enzymes in plants metabolic pathway. *Annu.Rev.Plant Physiol Plant Mol.Biol.*

- Jelitto, T., Sonnewald, U., Willmitzer, L., Hajirezeai, M., and Stitt, M.** (1992) Inorganic pyrophosphate content and metabolites in potato and tobacco plants expressing *E. coli* pyrophosphatase in their cytosol. *planta* **188**: 238-244.
- Jensen, R. A.** (1985) The shikimate / arogenate pathway: link between carbohydrate metabolism and secondary metabolism. *Physio.Plant* **66**: 164-168.
- Jensen, R. A., Morris, P., Bonner, C. A., and Zamir, L. O.** (1989) Biochemical Interface Between Aromatic Amino Acid Biosynthesis and Secondary Metabolism. 89-107. Washington DC USA, American Chemical Society.
- Keegstra, K., Olson, L. J., and Theg, S. M.** (1989) Chloroplastic precursors and their transport across the envelope membranes. *Annu.Rev.Plant Physiol Plant Mol.Biol.* **40**: 471-501.
- Khush, G. S.** (2001) Green revolution: the way forward. *Nat.Rev.Genet.* **2**: 815-822.
- Kishore, G. M. and Shah, D. M.** (1988) Amino acid biosynthesis inhibitors as herbicides. *Annu.Rev.Biochem.* **57**: 627-663.
- Klee, H. J., Muskopf, Y. M., and Gasser, C. S.** (1987) Cloning of an Arabidopsis thaliana gene encoding 5-enolpyruvylshikimate-3-phosphate synthase: sequence analysis and manipulation to obtain glyphosate-tolerant plants. *Mol.Gen.Genet.* **210**: 437-442.
- Klig, L. S., Carey, J., and Yanofsky, C.** (1988) trp repressor interactions with the trp aroH and trpR operators. Comparison of repressor binding in vitro and repression in vivo. *J Mol Biol* **202**: 769-777.
- Knappe, S., Lottgert, T., Schneider, A., Voll, L., Flügge, U. I., and Fischer, K.** (2003) Characterization of two functional phosphoenolpyruvate/phosphate translocator (PPT) genes in Arabidopsis-AtPPT1 may be involved in the provision of signals for correct mesophyll development. *Plant J* **36**: 411-420.
- Leuschner, C. and Schultz, G.** (1991) Uptake of shikimate pathway intermediates by intact chloroplasts. *Phytochemistry* **30**: 2203-2207.
- Lichtenthaler, H. K.** (1987) Chlorophylls and carotenoides: pigments of photosynthetic biomembranes. *Meth.Enzymol.* **148**: 350-382.
- Lo, S. C. and Nicholson, R. L.** (1998) Reduction of light-induced anthocyanin accumulation in inoculated sorghum mesocotyls. Implications for a compensatory role in the defense response. *Plant Physiol* **116**: 979-989.
- Logemann, J., Schell, J., and Willmitzer, L.** (1987) Improved method for the preparation of RNA from plant tissues. *Anal.Biochem.* **163**: 16-20.

- Maher, E. A., Bate, N. J., Ni, W., Elkind, Y., Dixon, R. A., and Lamb, C. J.** (1994) Increased disease susceptibility of transgenic tobacco plants with suppressed levels of preformed phenylpropanoid products. *Proc Natl Acad Sci U.S.A* **91**: 7802-7806.
- Martin, T., Oswald, O., and Graham, I. A.** (2002) Arabidopsis Seedling Growth, Storage Lipid Mobilization, and Photosynthetic Gene Expression Are Regulated by Carbon:Nitrogen Availability. *Plant Physiol.* **128**: 472-481.
- Mousdale, D. M., Campbell, M. S., and Coggins, J. R.** (1987) Purification and characterization of bifunctional dehydroquinase-shikimate:NADP oxidoreductase from pea seedlings. *phytochemistry* **26**: 2665-2670.
- Mousdale, D. M. and Coggins, J. R.** (1985) Subcellular localization of the common shikimate-pathway enzymes in *Pisum Sativum* L. *Planta* **163**: 241-249.
- Muday, G. K., Johnson, D. I., Somerville, R. L., and Herrmann, K. M.** (1991) The tyrosine repressor negatively regulates *aroH* expression in *Escherichia coli*. *J Bacteriol.* **173**: 3930-3932.
- Muir, S. R., Collins, G. J., Robinson, S., Hughes, S., Bovy, A., Ric, De, V, van Tunen, A. J., and Verhoeyen, M. E.** (2001) Overexpression of petunia chalcone isomerase in tomato results in fruit containing increased levels of flavonols. *Nat.Biotechnol.* **19**: 470-474.
- Mujer C.V., Fox T.C., Williams A.S., Andrews D.L., and Kennedy R.A.** (1995) Purification, properties and phosphorylation of anaerobically induced enolase in *Echinochloa phyllopogon* and *E. crus-pavonis*. *Plant Cell Physiol.* **36**: 1459-1470.
- O'Callaghan, D., Maskell, D., Liew, F. Y., Easmon, C. S., and Dougan, G.** (1988) Characterization of aromatic- and purin-dependent *Salmonella typhimurium*: attenuation, persistence and ability to induce protective immunity in BALB/c mice. *Infect.Immun.* **56**: 419-423.
- Pinto, J. E. B. P., Dyer, W. E., Weller, S. C., and Herrmann, K. M.** (1988) Glyphosate induces 3-deoxy-o-arabino-heptulosonate 7-phosphate synthase in potato (*Solanum tuberosum* L.) cells grown in suspension culture. *Plant Physiol* **87**: 891-893.
- Pline, W. A., Wilcut, J. W., Duke, S. O., Edmisten, K. L., and Wells, R.** (2002) Tolerance and accumulation of shikimic acid in response to glyphosate applications in glyphosate-resistant and nonglyphosate-resistant cotton (*Gossypium hirsutum* L.). *J.Agric.Food Chem.* **50**: 506-512.
- Redman, R. S., Freeman, S., Clifton, D. R., Morrel, J., Brown, G., and Rodriguez, R. J.** (1999) Biochemical Analysis of Plant Protection Afforded by a Nonpathogenic Endophytic Mutant of *Colletotrichum magna*. *Plant Physiol* **119**: 795-804.
- Rice Evans, C. A., Miller, N. J., Paganga, G., and Miller, N.** (1997) Antioxidant properties of phenolic compounds: The polyphenolic content of fruit and vegetables and their antioxidant activities. What does a serving constitute? *Trends Plant Sci.* **2**: 152-159.

Roessner-Tunali, U., Hegemann, B., Lytovchenko, A., Carrari, F., Bruedigam, C., Granot, D., and Fernie, A. R. (2003) Metabolic profiling of transgenic tomato plants overexpressing hexokinase reveals that the influence of hexose phosphorylation diminishes during fruit development. *Plant Physiol* **133**: 84-99.

Rosahl, S., Schmidt, R., Schell, J., and Willmitzer, L. (1987) Expression of a tuber specific protein in transgenic tobacco plants: demonstration of an esterase activity. *EMBO J.* **6**: 1155-1159.

Roslan, H. A., Salter, M. G., Wood, C. D., White, M. R., Croft, K. P., Robson, F., Coupland, G., Doonan, J., Laufs, P., Tomsett, A. B., and Caddick, M. X. (2001) Characterization of the ethanol-inducible alc gene-expression system in *Arabidopsis thaliana*. *Plant J* **28**: 225-235.

Rubin, J. L. and Jensen, R. A. (1985) Differentially regulated isozymes of 3-deoxy-D-arabino-heptulosonate 7-phosphate synthase from seedlings of *Vigna radiata L.* *Plant Physiol* **79**: 711-718.

Sambrook, J., Fritsch E.F., and Maniatis, T., Molecular cloning: a laboratory manual., Cold Spring Harbor Laboratory Press, Cold Spring harbor, NY, 1989.

Schmid, J. and Amrhein, N. (1995) Molecular organization of the shikimate pathway in higher plants. *Phytochemistry* **39**: 737-749.

Schmid, J., Schaller, A., Leibinger, U., Boll, W., and Amrhein, N. (1992) The in-vitro synthesized tomato shikimate kinase precursor is enzymatically active and is imported and processed to the mature enzyme by chloroplasts. *Plant J* **2**: 375-383.

Schmidt, C. L., Danneel, H. J., Schultz, G., and Buchanan, B. B. (1990) Shikimate kinase from spinach chloroplasts. Purification, characterization and regulatory function in aromatic amino acids biosynthesis. *Plant Physiol* **138**: 51-56.

Schulze, A. and Downward, J. (2001) Navigating gene expression using microarrays--a technology review. *Nat. Cell Biol* **3**: E190-E195.

Shah, D. M., Horsch, R. B., Klee, H. J., Kishore, G. M., Winter, J. A., Tumer, N. E., Hironaka, C. M., Sanders, P. R., Gasser, C. S., Aykent, S., Siegel, N. R., Rogers, S. G., and Fraley, R. T. (1986) Engineering herbicide tolerance in transgenic plants. *Science* **233**: 478-481.

Sinha, S. and Brewer, J. M. (1984) Purification and comparative characterization of an enolase from spinach. *Plant Physiol* **74**: 834-840.

Song, C. P., Guo, Y., Qiu, Q., Lambert, G., Galbraith, D. W., Jagendorf, A., and Zhu, J. K. (2004) A probable Na⁺(K⁺)/H⁺ exchanger on the chloroplast envelope functions in pH homeostasis and chloroplast development in *Arabidopsis thaliana*. *Proc.Natl.Acad.Sci.U.S.A* **101**: 10211-10216.

- Sonnewald, U., Brauer, M., von Schaewen, A., Stitt, M., and Willmitzer, L.** (1991) Transgenic tobacco plants expressing yeast-derived invertase in either the cytosol, vacuole or apoplast: a powerful tool for studying sucrose metabolism and sink/source interactions. *Plant J* **1**: 95-106.
- Steinrucken, H. C. and Amrhein, N.** (1980) The herbicide glyphosate is a potent inhibitor of 5-enolpyruvyl-shikimic acid-3-phosphate synthase. *Biochem.Biophys.Res.Communic.* **94**: 1207-1212.
- Steinrucken, H. C., Schulz, A., Amrhein, N., Porter, C. A., and Fraley, R. T.** (1986) Overproduction of 5-enolpyruvylshikimate-3-phosphate synthase in a glyphosate-tolerant *Petunia hybrida* cell line. *Arch.Biochem.Biophys.* **244**: 169-178.
- Stephens, C. M. and Bauerle, R.** (1992) Essential cysteines in 3-deoxy-D-arabino-heptulosonate-7-phosphate synthase from *Escherichia coli*. Analysis by chemical modification and site-directed mutagenesis of the phenylalanine-sensitive isozyme. *J Biol.Chem.* **267**: 5762-5767.
- Stitt, M.** (1997) The flux of carbon between the chloroplast and cytosol. 382-400. Longman Singapore Publishers.
- Suzich, J. A., Dean, J. F. D., and Herrmann K.M.** (1985) 3-Deoxy-D-arabino-heptulosonate 7-phosphate synthase from carrot root (*Daucus carota*) is a hysteretic enzyme. *Plant Physiol* **79**: 765-770.
- Sweetman, J. P., Chu, C., Qu, N., Greenland, A. J., Sonnewald, U., and Jepson, I.** (2002) Ethanol vapor is an efficient inducer of the alc gene expression system in model and crop plant species. *Plant Physiol* **129**: 943-948.
- Taiz, L. and Zeiger, E.**, Plant physiology, Sinauer Associates, Inc.,2002.
- van der Meer, I., Stam, M. E., van Tunen, A. J., Mol, J. N., and Stuitje, A. R.** (1992) Antisense inhibition of flavonoid biosynthesis in petunia anthers results in male sterility. *Plant Cell* **4**: 253-262.
- Van der Straeten, D., Rodrigues-Pousada, R. A., Goodman, H. M., and Van Montagu, M.** (1991) Plant enolase: gene structure, expression, and evolution. *Plant Cell* **3**: 719-735.
- Voll, L., Hausler, R. E., Hecker, R., Weber, A., Weissenbock, G., Fiene, G., Waffenschmidt, S., and Flügge, U. I.** (2003) The phenotype of the *Arabidopsis cue1* mutant is not simply caused by a general restriction of the shikimate pathway. *Plant J* **36**: 301-317.
- Wang, Y. X., Jones, J. D., Weller, S. C., and Goldsbrough, P. B.** (1991) Expression and stability of amplified genes encoding 5-enolpyruvylshikimate-3-phosphate synthase in glyphosate-tolerant tobacco cells. *Plant Mol.Biol.* **17**: 1127-1138.

Weng, M., Makaroff, C. A., and Zalkin, H. (1986) Nucleotide sequence of *Escherichia coli* pyrG encoding CTP synthetase. *J Biol.Chem.* **261**: 5568-5574.

Yao, K., De, Luca, V, and Brisson, N. (1995) Creation of a Metabolic Sink for Tryptophan Alters the Phenylpropanoid Pathway and the Susceptibility of Potato to *Phytophthora infestans*. *Plant Cell* **7**: 1787-1799.

Ye, G. N., Hajdukiewicz, P. T., Broyles, D., Rodriguez, D., Xu, C. W., Nehra, N., and Staub, J. M. (2001) Plastid-expressed 5-enolpyruvylshikimate-3-phosphate synthase genes provide high level glyphosate tolerance in tobacco. *Plant J.* **25**: 261-270.

Publication Lists

Silencing of DHD/SHD results in decreased biosynthesis of phenolic compounds, dramatic growth retardation and lethal phenotypes in tobacco plants (manuscript preparation). Li Ding, Mohammad-Reza Hajirezaei and Uwe Sonnewald

Patent:

Dehydroquinate dehydratase / shikimate dehydrogenase as an herbicide target
(US2003145348)

Curriculum vitae

Name: Li DING

Sex: male

Date & Place of Birth: August 3, 1972. Heilongjiang Province, China, P.R.

Nationality: Chinese

Family Status: Married

Education:

1979-1984 Primary school, Heilongjiang, China, P.R

1984-1990 Secondary school, Heilongjiang, China, P.R

1990-1994 Study in the biology department, Wuhan University, Hubei, China, P.R.

1994 Bachelor degree of science from Wuhan University

1994-1997 Study in Institute of Genetics, Chinese Academy of Science, Beijing, China, P.R.

1997 Master degree of Science from Institute of Genetics, Chinese Academy of Science

1999-2004 Ph.D student in Institute of Plant Genetics and Crop Plant Research (IPK), Gatersleben, Germany.

Acknowledgements

I would like to express my sincere gratitude to my Ph.D. supervisor, Prof. Dr. Uwe Sonnewald for giving me the opportunity to work in his group with this interesting project. I highly appreciate his great guidance through the project with valuable advice and creative suggestions in the experimental design and analysis, as well as his strong support in writing this dissertation.

I would like to express my special thanks to Drs. Daniel Hofius and Eric Glickman for their critical reviewing of this manuscript.

My work expanded to several areas. Therefore I extended my thanks to Drs. Mohammad Hajirezaei and Hans-Peter Mock (Biochemistry), Dr. Frederik Börnke (Molecular Networks), Mr. Bernhard Claus and Dr. Michael Melzer (Structural Cell Biology), Dr. Sophia Biemelt (Molecular Developmental Physiology), Dr. Henning Tschiersch (Photosynthesis), and Prof. Dr. Gotthard Kunze (Yeast Genetics). I appreciated valuable discussions with my colleagues, Drs. Mohammad Hajirezaei, Frederik Börnke, Eric Glickman and Daniel Hofius, Mr. Jens Giese and Mr. Shuai Chen.

My appreciation is extended to the technical staffs of my lab, Ms. Heike Deppner, Ms. Ulrike Schlereth, Ms. Melanie Ruff, Ms. Christiane Börnke, Ms. Andrea Knospe and Ms. Sibylle Freist for their excellent technical support.

Last but not least, I owe great gratitude to my wife, Chao Wang. I am grateful to her strong support during my PhD study. Without her support and contribution, this work would not be possible. I am also grateful to my pretty daughter, Jessica Ding, for bringing so much pleasure to my life.

Erklärung

Hiermit erkläre ich, dass ich die hier vorliegende wissenschaftliche Arbeit selbständig und ohne fremde Hilfe verfasst, nur die von mir angegebenen Quellen und Hilfsmittel benutzt und die den benutzten Werken wörtlich oder inhaltlich entnommenen Stellen als solche kenntlich gemacht habe. Darüber hinaus erkläre ich, dass ich den Doktorgrad nicht besitze und mich auch früher nicht um den Doktorgrad beworben habe.

Gatersleben, im Sept.

Li Ding